Age-Associated Changes in Voltage-Gated Sodium Channels Within the Right Atrium Predispose the Elderly to Atrial Fibrillation

Dr Emmanuel Salib Isaac MBCHB

MD by Thesis Doctorate of Medicine

The University of Hull and the University of York

Hull York Medical School

November 2022

Abstract

Atrial Fibrillation (AF) is the most common cardiac arrhythmia worldwide with sufferers of the condition facing significant morbidity and mortality. Ageing alone is identified as the most significant risk factor for developing the arrhythmia. As such, an ageing global population has, and will continue to give rise to a marked prevalence of AF, placing enormous pressure on healthcare systems around the world. Ionic remodelling of sodium channels has been observed in animal studies with regards to the ageing process which drive the arrhythmogenic pathology, with parallel observations made with regards to AF. This study will examine, and potentially unify, the narratives of ionic remodelling in AF and ageing, focusing specifically on the expression of two voltage-gated sodium channel (VGSC) isoforms within the human heart; $Na_v1.5$ & $Na_v1.8$. The former being the native cardiac isoform and principal driver for phase 0 of the action potential, and the latter a neuronal isoform implicated in pathological late currents which predispose the cardiomyocyte to electrical instability. This study involved sampling human right atrial appendage from patients undergoing routine cardiac surgery at Castle Hill Hospital.

With increasing age, expression of $Na_v1.5$ declined with a Pearson's correlation co-efficient of -0.25. Comparing the extremes in age of these samples, protein expression was decreased by 18.8% in the older group (P=0.18). The inverse trend was noted with regards to $Na_v1.8$ with a positive correlation of +0.259. When comparing the extremes of age an increase of 32% was observed (P=0.039). These results suggest that the ageing process remodels the human heart in a manner which diminishes the capacity for sodium ion influx critical for conduction during action potential upstroke, meanwhile

upregulating ion channels which enhance the aberrant late currents. To investigate the ionic landscape of cardiac tissue in AF, patients with the arrhythmia were matched on age with patients in sinus rhythm. AF patients were found to have significantly reduced expression of $Na_v1.5$ (P=<0.05). These results suggest that the loss of native cardiac sodium channels may be a key step in the pathophysiology of cardiac arrhythmia in humans, and a process in which the ageing heart undergoes which underpins development of AF.

In order to investigate the precise mechanics modulating the ionic redistribution observed, this study examined the role JNK may have as a potential regulator of sodium channel expression in the human heart. JNK has been suggested as having a strong influence in the expression of other ion channel proteins-specifically Cx43. Total expression of JNK was found to be 56 % greater in the oldest population compared to younger patients (P=0.05). Examination of the direct role increased levels of JNK may have on VGSC expression was investigated using pharmacological manipulation of this pathway through Anisomycin (JNK activator) and SP600125 (JNK inhibitor). Subjectively, it has been noted that inhibition of JNK markedly reduced the expression of $Na_v1.8$, whereas upregulation of this protein seemed to increase the density of expression of the neuronal isoform.

Publications & presentations

Abstracts:

- Emmanuel Isaac, Stephanie Cooper, Matthew K Lancaster, Mahmoud Loubani, Sandra A Jones.

  An age-associated reduction in $Na_v1.5$ protein expression correlates with an increase in $Na_v1.8$ protein expression in the right atrial appendage of the human heart. Circulation Research. 2020;127:A493

  https://www.ahajournals.org/doi/abs/10.1161/res.127.suppl_1.493

- E Isaac, M Lancaster, M Loubani and S Jones.

  Does a reduction in Nav1.5 protein expression within the right atria increase an elderly patient's susceptibility to atrial fibrillation? Proc Physiol Soc 48 (2021) PC026

  https://www.physoc.org/abstracts/does-a-reduction-in-nav1-5-protein-expression-within-the-right-atria-increase-an-elderly-patients-susceptibility-to-atrial-fibrillation/

Peer-reviewed manuscripts:

- Isaac E, Cooper SM, Jones SA, Loubani M. Do age-associated changes of voltage-gated sodium channel isoforms expressed in the mammalian heart predispose the elderly to atrial fibrillation? World J Cardiol. 2020 Apr 26;12(4):123-135.

  https://www.ncbi.nlm.nih.gov/pmc/articles/PMC7215965/

Oral Presentations:

- Expression of the voltage-gated sodium channel isoform $Na_v1.5$ is significantly reduced in the atrial tissue of patients with atrial fibrillation. (Society of Cardiothoracic Surgeons Annual Meeting 2020)

List of contents

List of figures

List of tables

Acknowledgements

Firstly, I must offer my deepest gratitude to my supervisors Professor Mahmoud Loubani & Dr Sandra Jones. Thank you, Prof. for recognising and nurturing my interest in cardiac disease, as a bright eyed, bushy tailed junior doctor on the cardiothoracics ward. I am eternally grateful for your enthusiastic and kind professional mentorship. My time attached to the department will remain as some of the most captivating and clinically satisfying work of my career. Thank you, Sandra, for keeping me motivated to manoeuvre through the many hurdles this degree has presented, and for having the patience to calm me down when experiments failed! Thank you for your support during the many turbulent personal twists and turns I've faced during this process, and for consistently pushing me to sharpen my skills and work to a higher standard. Taking on research degree immediately after foundation training is an extraordinary challenge for a young doctor; my appreciation for the tutelage of both of you cannot be overstated.

A special thank you goes out to Kathleen Bulmer for teaching me all about the dark art of western blotting-without whom this data would not exist. Her technical support has been outstanding as well as a friendly character to chat to in an otherwise solitary laboratory. Thank you to Dr Cordula Kemp, who dedicated much time advising me on the fascinating science of confocal microscopy. My thanks also goes to Dr Matthew Lancaster, for allowing me to visit his laboratory at the University of Leeds, setting up the electrophysiology rig, and for fixing the vibratome. WD-40 really is a miracle cure!

I gratefully acknowledge Hull University Teaching Hospitals for this research fellowship, without which the academic achievements I've been fortunate to attain would not have been possible. I must also thank Mr Chaudhry as my clinical supervisor during my

cardiothoracics rotation as a foundation year doctor, and for donating tissue from his case lists. My first time in cardiac theatres was with him-a remarkable experience and a pivotal moment of my career.

An enormous, humble thank you goes to all the patients who consented to participate in this research by literally offering us a piece of their hearts. Whilst facing the most major, life changing surgery, to have the foresight and altruism to donate their tissue is a remarkable thing indeed. You are the reason I love my vocation of clinical medicine.

Most importantly, thank you to my family and friends. True friendship makes life worth living and I am constantly amazed how lucky I am to have all of you. Words fall short of my appreciation for my brother Mina, who has always believed in me since I was an infant. For supporting my career not only financially, but with a genuine desire to see me succeed. My most gracious acknowledgement goes to my parents Salib & Mary. Thank you for your bravery to leave your home and move to this country. Thank you for instilling in me the value of education and hard work. Thank you for your unconditional love and support. Without your sacrifices I would not be blessed with this incredible life.

Author's declaration

I confirm that this work is original and that if any passage(s) or diagram(s) have been copied from academic papers, books, the internet or any other sources these are clearly identified by the use of quotation marks and the reference(s) is fully cited.

I certify that, other than where indicated, this is my own work and does not breach the regulations of HYMS, the University of Hull or the University of York regarding plagiarism or academic conduct in examinations.

I have read the HYMS Code of Practice on Academic Misconduct, and state that this piece of work is my own and does not contain any unacknowledged work from any other sources.

I confirm that any patient information obtained to produce this piece of work has been appropriately anonymised.

Chapter 1

Introduction & background

Chapter 1 Introduction & background

1.1 General introduction

The mammalian heart is a vital organ required for life by all mammals. Its pivotal function is to pump blood simultaneously to both the lungs, and rest of the body including the blood supply to itself. This allows the removal of metabolic waste, and supply much needed nutrients and oxygen, without crossover of these vascular pathways within the system due to the valve system within the circulation network. Blood supply is driven through the circulatory system every time a contraction of the heart occurs, that is when the organ is stimulated spontaneously under regulation by the nervous system. This study focuses on the electrical activity of the heart responsible for contraction. This can become unbalanced and cause arrhythmic events leading to irregular or ceased cardiac function.

1.2 Physiological background

1.2.1 Structure of the heart

The heart is located centrally in the thoracic cavity directly behind the sternum, between the lungs and above the diaphragm. The adult human heart is around the size of a clenched fist, and in healthy individuals weighs 233 - 383g in men and 148 - 296g in women (Molina & DiMaio, 2015). The mammalian heart structure consists of four chambers; right atrium (RA), right ventricle (RV), left atrium (LA) and left ventricle (LV).

The heart is a muscle, whose chambers differ in structure and function Figure 1.2.1. The superior chambers of the heart (the atria) are thin walled, expandable structures, which receive circulating blood back to the heart. The inferior chambers (the ventricles) are thicker more muscular walls which pump blood at high pressures out of the heart into the pulmonary and systemic vasculature. The atria and ventricles are separated by a tough ring of connective tissue called the annulus fibrosus. This acts as the heart's skeleton, encircling the atrio-ventricular, aortic and pulmonary valves, electrically insulating the ventricles from the atria. The annulus fibrosus also acts as a fulcrum; a fixed, non-mobile structure to which the connective tissue of the myocardium can attach for contraction to occur (Davidson, 2010).

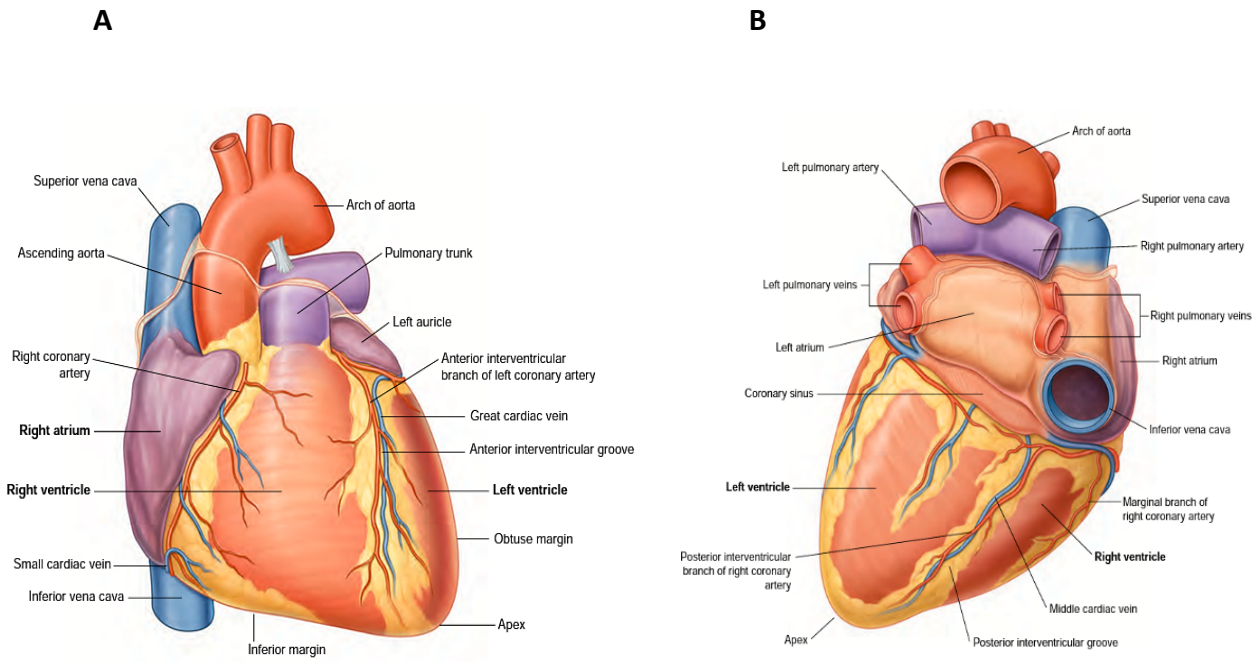

Figure 1.2.1 The mammalian heart

Anterior view (Panel A) and posterior view (Panel B) of the heart. Reproduced from (Drake, 2014).

1.2.2 The cardiomyocyte & contraction

There are important distinctions to note between ventricular and atrial myocytes which will be explored in detail later in this chapter. Typically adult human cardiomyocytes are roughly cylindrical in shape with a length of 50-100µm and 20-35 µm in width (Gillet et al., 2014). Each myocyte interdigitates with other adjacent myocytes at intercalated discs (ID) at the ends of each cylinder and additional side branches, forming an intercellular connected network. This organisation of cardiomyocytes provides both structural support via the mechanical linking of desmosomes, as well as electrical connections via gap junctions which allow an impulse to propagate from cell to cell. Gap junctions are formed through pore-forming transmembrane protein complexes called connexins, which allow the current to spread from cell to cell (Söhl & Willecke, 2004). The energy expenditure required for cardiac muscle, which is made-up of these cardiomyocytes, is provided by the large number of mitochondria that constitute ~ 35% of the myocyte overall volume (Stride et al., 2013).

Cardiac myofibrils form the contractile body of the cell with repeating sarcomeres, which are roughly 2 µm long and are arranged in a reiterating manner giving the characteristic striated appearance. Z lines mark the point of distinction between two adjacent sarcomeres, where thin actin filaments extend at a right angle from the Z lines forming the I band. Tropomyosin is the molecular structure which runs in the groove of the actin helix, and every seventh actin molecule in the chain is attached to another molecule called troponin (Davidson, 2010). Thick myosin filaments run parallel and interdigitate with the actin filaments, the centre of the sarcomere is comprised of thick filament forming the A band. ATPase is contained in the cross-links between actin and

myosin, catalysing the hydrolysis of ATP to ADP providing the energy needed for contraction to occur (Davidson, 2010) .

Enveloping the cardiomyocyte is a phospholipid membrane called the sarcolemma with regular invaginations that penetrate deep into the myocyte along its longitudinal axis called transverse tubules, mostly referred to as t-tubules. Ion channels and pumps are expressed within these t-tubule membranes. In the rodent experimental model L-type calcium channels (or Cav1.2) are highly concentrated within t-tubules (Glukhov et al., 2015), their role is to facilitate synchronised contraction of the whole cell, through uniform, timely delivery, and sequestration of essential ions-most notably Ca^{2+}.

For contraction of cardiomyocytes to occur, Ca^{2+} ions enter through L-type calcium channels located within the t-tubules, triggering calcium-induced calcium-release of calcium ions from the sarco-endoplasmic reticulum (SR) store within each myocyte. Ca^{2+} binds to troponin triggering a conformational change in the troponin-actin complex to expose a binding site on the actin molecule and allow the ATPase on the myosin head to form a crossbridge with the actin filament. ATP is hydrolysed and the energy produced rachets the myosin head, exerting a direction force on the actin filament towards the centre of the sarcomere and shortens the sarcomere length (Davidson, 2010). Once contraction is complete, the majority of calcium returns to the SR store through an ATP reliant calcium pump known as sarco-endoplasmic reticulum calcium-ATPase or SERCA (Naish et al., 2009). As the calcium concentration drops, calcium ions unbind from the troponin complex, thus conformational change is reversed and the crossbridge is broken allowing for the actin to slide into its initial position and the sarcomere lengthens as the cardiomyocytes relax. This mechanism is illustrated in Figure 1.2.2.

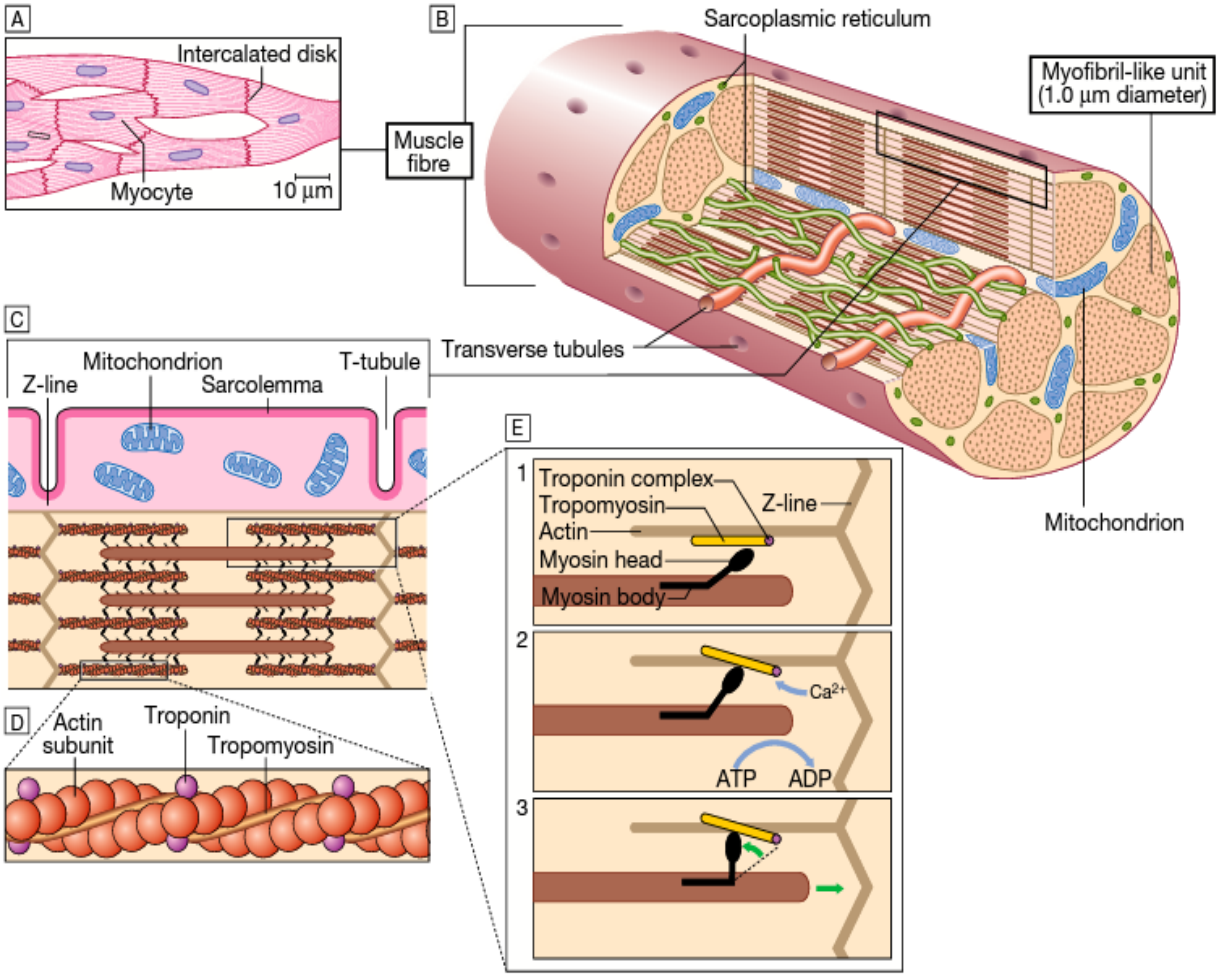

Figure 1.2.2 The cardiomyocyte & contraction

Panel A: illustration of how cardiomyocytes are conjoined through the intercalated disks. Panel B: Cross section of muscle fibre made up of myofibril units. Panel C: 2-dimentional diagram of an isolated section of a myofibril. Panel D: zoomed in illustration of the Actin/tropomyosin/troponin structure. Panel E: Diagram of the Actin-Myosin contraction mechanism. Adapted from (Davidson, 2010).

The force of contraction is heavily dependent on the concentration of calcium ions (Wannenburg et al., 2000) thus more actin-myosin cross-bridges form and greater shortening of the sarcomere will increase the force of contraction. Inotropic drugs such as Digoxin, and hormones such as adrenaline act on this system to maximise sarcomere shortening (Davidson, 2010).

1.2.3 Electrical activity of the heart

The synchronicity of the cardiac cycle, and hence the capability of the heart to function as a pump, rests on the strictly co-ordinated initiation, conduction, and resolution of the action potential (AP). An action potential describes the flow of charge in and out of the cell through various transmembrane ion channels and pumps. The key ions involved in this process are sodium (Na^+), potassium (K^+) and calcium (Ca^{2+}). The tight regulation of timing, amplitude, and distribution of these ions throughout the cellular myocardial structures is critical for proper cardiac function.

1.2.3.1 Ion distribution and membrane potentials

Differences in ionic concentrations, along with the selective permeability by the plasma membrane, creates a difference in charge which in a resting cell is termed *the resting membrane potential (V_r).* Table 1.2.1 shows the differing concentration of sodium, potassium, calcium, and chloride ions inside and outside human cells i.e. myocytes in a resting state.

Table 1.2.1 Differences in extracellular & intracellular ionic concentrations of sodium, potassium, and calcium

Adapted from (Naish et al., 2009)

Ion	Extracellular Concentration (mM)	Intracellular Concentration (mM)
Na^+	145	12
K^+	4	139
Ca^{2+}	1.8	<0.0002
Cl^-	116	4

Extracellular fluid is plentiful in Na^+ in the form of dilute sodium chloride and in Ca^{2+}, whereas the intracellular space has more concentrated K^+. Both Na^+ and Ca^{2+} have a natural affinity to move down their concentration gradients into the cell, known as depolarising currents. Whereas K^+ move down their concentration gradient out of the cell as a repolarising current. Within the cell, organic acids, phosphates and proteins act as anions (negatively charged bodies) which are impermeable to the phospholipid bilayer of the cell, balancing the positive charge of intracellular potassium. Ion transporters such as the Na^+/K^+ pump shift ions against their concentration gradients using energy through the hydrolysis of ATP and are essential for the maintenance of the resting membrane potential. The *equilibrium potential* describes a state where both the chemical force of the concentration gradient and the electrostatic force of the difference in charge are balanced, calculated for each ion using the Nerst Equation (Archer, 1989).

$$V_{\text{Eq.}} = \frac{RT}{zF} \ln\left(\frac{[X]_{\text{out}}}{[X]_{\text{in}}}\right)$$

Equation 1.1 The Nerst equation

V_{eq} = equilibrium potential, R= the universal gas constant, T=temperature in Kelvin, z= the valence of the ionic species (e.g z= +1 for Na^+ & K^+or +2 for Ca^{2+}or -1 for Cl^-), F= the Faraday constant, $[x]_{out}$= ion concentration outside the cell, $[x]_{in}$= ion concentration inside the cell.

$$V_{\text{m}} = \frac{RT}{F} \ln\left(\frac{p_{\text{K}}[\text{K}^+]_{\text{o}} + p_{\text{Na}}[\text{Na}^+]_{\text{o}} + p_{\text{Cl}}[\text{Cl}^-]_{\text{i}}}{p_{\text{K}}[\text{K}^+]_{\text{i}} + p_{\text{Na}}[\text{Na}^+]_{\text{i}} + p_{\text{Cl}}[\text{Cl}^-]_{\text{o}}}\right)$$

Equation 1.2 The Goldman-Hodgkin-Katz equation

V_m=membrane potential, P_k= permeability of potassium, P_{Na}=permeability of sodium, P_{cl}= permeability of chloride, $[x]_o$ = concentration of the given ion outside the cell, $[x]_I$ concentration of the given ion inside the cell.

Using data in Table 1.2.1 and the Nerst equation we can calculate the equilibrium potential of K^+ is -94.8mV, whereas the resting membrane potential of K^+ is -90mV (Enyedi & Czirják, 2010). Consequentially, this creates a slight outward electrostatic force which results in a leak of K^+ out of the cell during repolarisation. Whereas using the Nerst equation for sodium ions we can appreciate that V_{EqNa} = +66.6mV, a strong inward electrostatic force, which drives these ions into the cell when the channels are activated during depolarisation. To calculate the overall membrane potential, all of the ions which are permeable to the cell are taken into consideration within the Goldman-Hodgkin-Katz equation, which is an extension of the Nerst equation:

1.2.3.2 The action potential

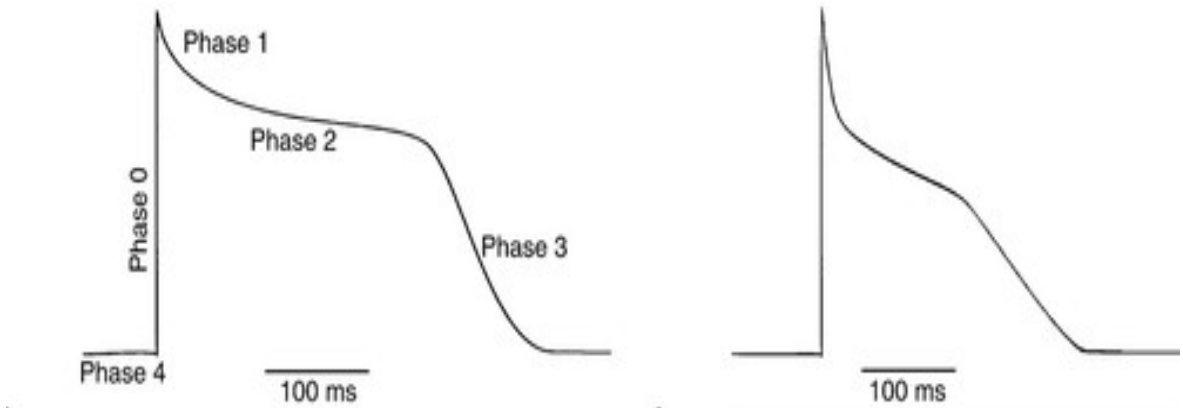

Figure 1.2.3 Comparison of ventricular (left) and atrial (right) action potential morphologies

Adapted from (Nerbonne & Kass, 2005)

The flow of charge by ions across the cell membrane creates currents, and in the case of muscular tissue such as the myocardium, electrical excitation fundamentally underpins the process of contraction which is termed excitation-contraction coupling. The cardiac action potential differs in morphology, speed, and velocity depending on the region of

the heart. The action potential profile of both atrial and ventricular myocytes have 5 distinct phases (phase 0 to phase 4); depolarisation (phase 0), early repolarisation (phase 1), plateau (phase 2), repolarisation (phase 3) and resting state (phase 4). Atrial action potentials have a shorter refractory period, forming a more triangular shape. This is illustrated in Figure 1.2.3.

The resting membrane potential is predominantly due to the sarcolemma's permeability to K^+-during this phase there is a steady efflux of K^+ ions. Depolarisation is initiated by positively charged Na^+ ions passing through gap junctions of an adjacently depolarised cell to elevate the membrane potential. At threshold of the voltage-sensor of voltage-gated sodium channels (VGSC) triggers a massive and rapid influx of Na^+ ions moving down a highly charged diffusion and electrostatic gradient. The AP upstroke causes a near immediate depolarisation of the cell to a positive membrane potential. The timing of activation and inactivation of VGSC during depolarisation is a key determining factor for the maximum upstroke velocity (V_{max}). When VGSC close, the cell enters the effective refractory period (ERP) spanning the entire plateau phase and the first part of phase 3, in which the cell cannot undergo another AP. Disturbance to the ERP by aberrant depolarising currents is a focal point of arrhythmogenesis.

The depolarisation of the cell during phase 0 further activates voltage-gated L-type calcium channels at around -45mV, allowing a slow and long influx of $Ca^{2+}$and triggers calcium-induced calcium-release from the SR via RyR2 receptors (Bers, 2002). Following the AP upstroke is the initial repolarisation (phase 1) which is more prominent in Purkinje myocytes, much less so in the atria whereas the SA and AV nodes do not have an initial repolarisation phase at all. Phase 1 is a transient opening of voltage-gated potassium channels known as $I_{TO,}$ an efflux of K^+ ions move out of the cell causing a slight

repolarisation of the membrane potential. Phase 2 is a consequence of the balance between depolarising and repolarising currents causing a plateau in the AP profile, due to open channels of L-type calcium along with the action of the sodium/calcium exchanger. The present consensus is that 1 Ca^{2+} ion is exported for 3 Na^{+} ions imported leading to an overall +1 charge in the intracellular space (Curran & Mohler, 2015).

These depolarising currents are counteracted by fast (I_{kr}) and slow (I_{ks}) rectifier potassium channels. During the main repolarisation phase (phase 3), L-type calcium channels close whilst voltage-gated potassium channels continue to open. The dominant current is therefore outward repolarisation, pulling the membrane potential back down towards the resting state at -80mV to -90mV (phase 4). During this phase ion pumps such as the NCX, Na^{+}/K^{+}ATPase and outward Ca^{2+} pumps continue working after voltage-gated channels close, restoring the cell back and maintaining the resting membrane potential until the next action potential is triggered, and the cycle repeats.

AP morphology differs greatly depending on the region of the heart observed (Nerbonne & Kass, 2005). There is a clear difference between the atrial and ventricular AP waveforms. The action potential in the atria is shorter overall, more triangular in shape with a less distinct plateau phase. This is partly due to a significantly reduced Ca^{2+} current. With Ca^{2+} being the principal ion in the binding of the troponin complex regulating the force of contraction of the sarcomere, along with a much thicker myocardium constituting the fundamental structure of the ventricles (as a greater force is required) it is therefore logical that ventricular cardiomyocytes have a much more enhanced Ca^{2+} current in comparison to their atrial counterparts. Atrial cardiomyocytes also possess a specific potassium current known as 'Ultra-rapid delayed rectifier current' (I_{Kur}) which is not found in ventricular cells (Eisner et al., 2017). This current further

shortens the plateau period by enhancing the outward repolarising potassium currents. The SA and AV nodes also have vastly different AP waveforms than anywhere else in the heart primarily due to the pacemaker function where is no resting state, rather a diastolic potential. Both exhibit a pacemaker potential in which slow spontaneous depolarisation occurs immediately after repolarisation, hence the SA and AV nodes are key regulators of the heart's conduction pathway.

1.2.4 Voltage-gated sodium channels

Table 1.2.2 Properties of VGSC isoforms

Adapted from (Catterall et al., 2005).

VGSC isoform	Tissue	Gene	Amino acid length	Activated	Inactivated	Associated β-subunits
$Na_v1.1$	Brain	SCN1A	2009aa (human and rat)	-33 mV	-72 mV	β_1, β_2, β_3, β_4,
$Na_v1.2$	Brain	SCN2A	2005aa (human), 2006aa (rat)	-24 mV	-53 mV	β_1, β_2, β_3, β_4,
$Na_v1.3$	Brain	SCN3A	1951aa (human and rat)	-23 to -26 mV	-65 to -69 mV	β_1 and β_3
$Na_v1.4$	Skeletal muscle	SCN4A	1836aa (human), 1840aa (rat)	-26 mV to -30 mV	-56 mV	β_1
$Na_v1.5$	Heart	SCN5A	2016aa (human), 1951aa (rat)	-47 mV	-84 mV	β_1, β_2, β_3, β_4,
$Na_v1.6$	Brain	SCN8A	1980aa (human), 1976aa (rat)	-37.7 mV	-98 mV	β_1 and β_2
$Na_v1.7$	PNS	SCN9A	1977aa (human), 1984aa (rat)	-31 mV	-61 mV to -78 mV	β_1 and β_2
$Na_v1.8$	PNS	SCN10A	1957aa (human)	-16 to -21 mV	-30 mV	Not established
$Na_v1.9$	PNS	SCN11A	1792aa (human), 1765aa (rat)	-47 to -54 mV	-44 to -54 mV	Not established

VGSCs are transmembrane protein complexes which produce the depolarising influx of sodium ions at the initiation and duration of the action potential (DeMarco & Clancy, 2016). There are nine subtypes of voltage gated sodium channels that are expressed within the mammalian class. Each isoform has specific features; activation/inactivation voltage threshold, amino acid sequence and gene. VGSCs are expressed proportionately differently depending on the bodily tissues. The standardised nomenclature for these channels was first proposed by Goldin et al in the year 2000 (Goldin et al., 2000). Na_v 1.1, 1.2, 1.3 and 1.6 are predominantly expressed in the central nervous system (Goldin). Na_v1.4 is dominant in skeletal muscle. Na_v 1.5 is the predominant cardiac isoform, making up nearly 90% of all sodium channel isoforms expressed in the heart; responsible for over two thirds of the total sodium current (Kaufmann et al., 2013). Finally, Na_v 1.7, 1.8 and 1.9 are abundantly expressed in the peripheral nervous system (PNS) (Catterall et al., 2005).

1.2.4.1 Fast & late sodium currents

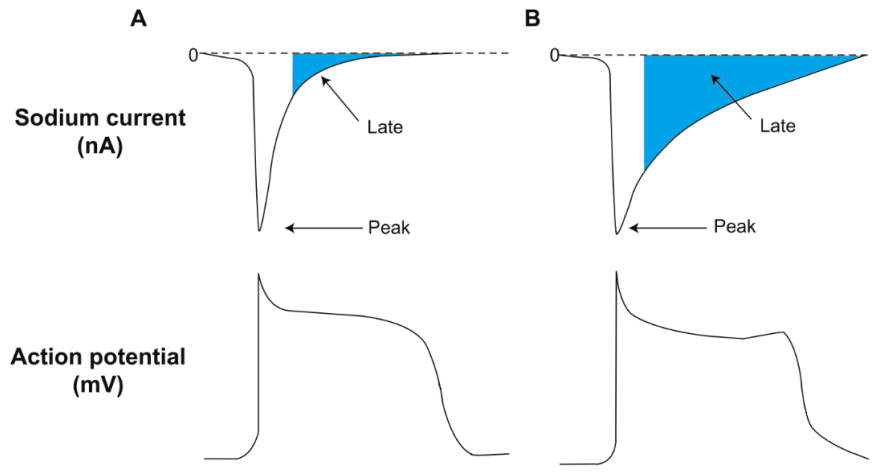

Figure 1.2.4 The effect of peak and late sodium currents on action potential morphology

Panel A shows the typical action potential of a ventricular myocyte, juxtaposed above it is the measurement of a typical sodium current; divided into peak (white) and late(blue). Panel B shows the effect of an enhanced sodium current on the action potential-elongated plateau phase with an afterdepolarisation. Adapted from (Vadnais & Wenger, 2010).

The sodium current (I_{Na}) can be appreciated as two phases; the peak (fast) sodium current and the late (slow) sodium current (I_{NaL}). The majority of the depolarising Na^+ current is generated by the fast I_{Na} of which $Na_v1.5$ the predominant channel responsible (Kaufmann et al., 2013). This produces the AP upstroke and 'maximum upstroke velocity' (V_{max}). The late sodium current is produced by a slow, steady influx of Na^+ which persists throughout the duration of the action potential. These two currents determine not only the peak of the action potential and velocity of depolarisation, but also in shaping action potential morphology through the length of the plateau phase, and therefore the refractory period. As illustrated in Figure 1.2.4 an enhanced I_{NaL} prolongs AP duration. This is directly linked to early afterdepolarisations. (Burashnikov & Antzelevitch, 2013; Horvath et al., 2013; Rivaud et al., 2018b). An unusually heightened late current slows repolarisation of the cell due to an uncharacteristically persistent influx of Na^+ ions maintaining a positive membrane potential. This prolonged plateau phase allows for L-type calcium currents (I_{CaL}) to recover from inactivation leading to a depolarising inward current of Ca^{2+} ions. Prolonged AP duration within the atria underpins the increased prevalence of AF in congenital long QT syndrome (Johnson et al., 2008). Na_v 1.8 specifically has been implicated in this process as blocking the channel has been shown to reduce the late sodium current, supressing the development of afterdepolarisations in the myocytes of mice and rabbits (Yang et al., 2012a). After depolarisations in regard to AF mechanics is discussed in further detail in section 1.4.3.

1.3 The human atria

1.3.1 Macroscopic architecture of the atria

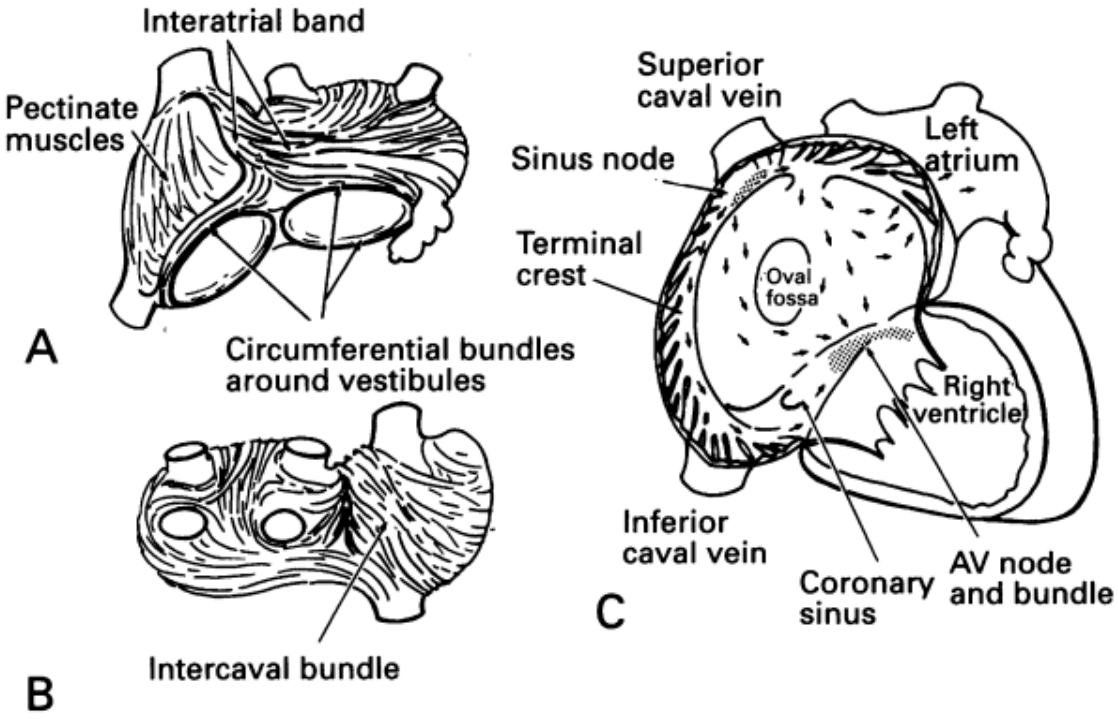

Figure 1.3.1 Diagrammatic representation of the muscular arrangement of the atria

A) Anterior view of the atria illustrating the longitudinal direction of the pectinate muscles and the circumferential arrangement of the interatrial band and bundles around the vestibules. B) Posterior view of the atria illustrating how the musculature wraps around the caval and pulmonary vessels. C) Internal perspective Illustrating of the direction of bundle flow through the right atrium, the pathway towards the left atrium as well as key anatomical landmarks of the oval fossa and coronary sinus. Key structures of the conduction system (SA node & AV node) juxtaposed. Adapted from Yang et al (1995).

The atria are complex structures forming the top two chambers of the heart. Each atrium is comprised of a venous component, an appendage, a vestibule of the atrioventricular valve and a septum which separates the two chambers. The right atrium receives blood from the superior and inferior vena cava, whereas the left atrium from the pulmonary veins. At the base of the right atria, there are circumferential bundles which encircle the vestibule attaching to the non-conductive fibrous tricuspid ring (Wang et al., 1995) Figure 1.3.2.

The internal architecture of the right atrium is much less uniform than the left; with the primary difference being the absence of the terminal crest & pectinate muscles in the left antrum Figure 1.3.2 A&B. As illustrated by Wang et al. 1995 the terminal crest is the largest muscular bundle in the right atrium, thought to provide structural reinforcement to the relatively thin chamber wall. It forms a longitudinal ridge which originates from the anterior septum, extending in front of the opening of the superior vena cava and continues inferiorly merging near the orifice of the coronary sinus. Along its course it branches into the pectinate muscles, of which the upper bundles extend at right angles into the right atrial appendage. Studies investigating the role the right atrial appendage in arrhythmia are scarce, though very recently Liu et al explored the mechanics and clinical outcomes of AF driven via this structure. Out of 20 patients in this study, AF cycle length in the right atrial appendage was the shortest compared to other atrial structures (134ms) with the fastest frequency potentials located here in 65% of patients. AF could be successfully terminated with ablation at the base of the right atrial appendage with excellent outcomes- only 2 patients presenting with recurrent arrhythmia in the form of atrial flutter (Liu et al., 2022).

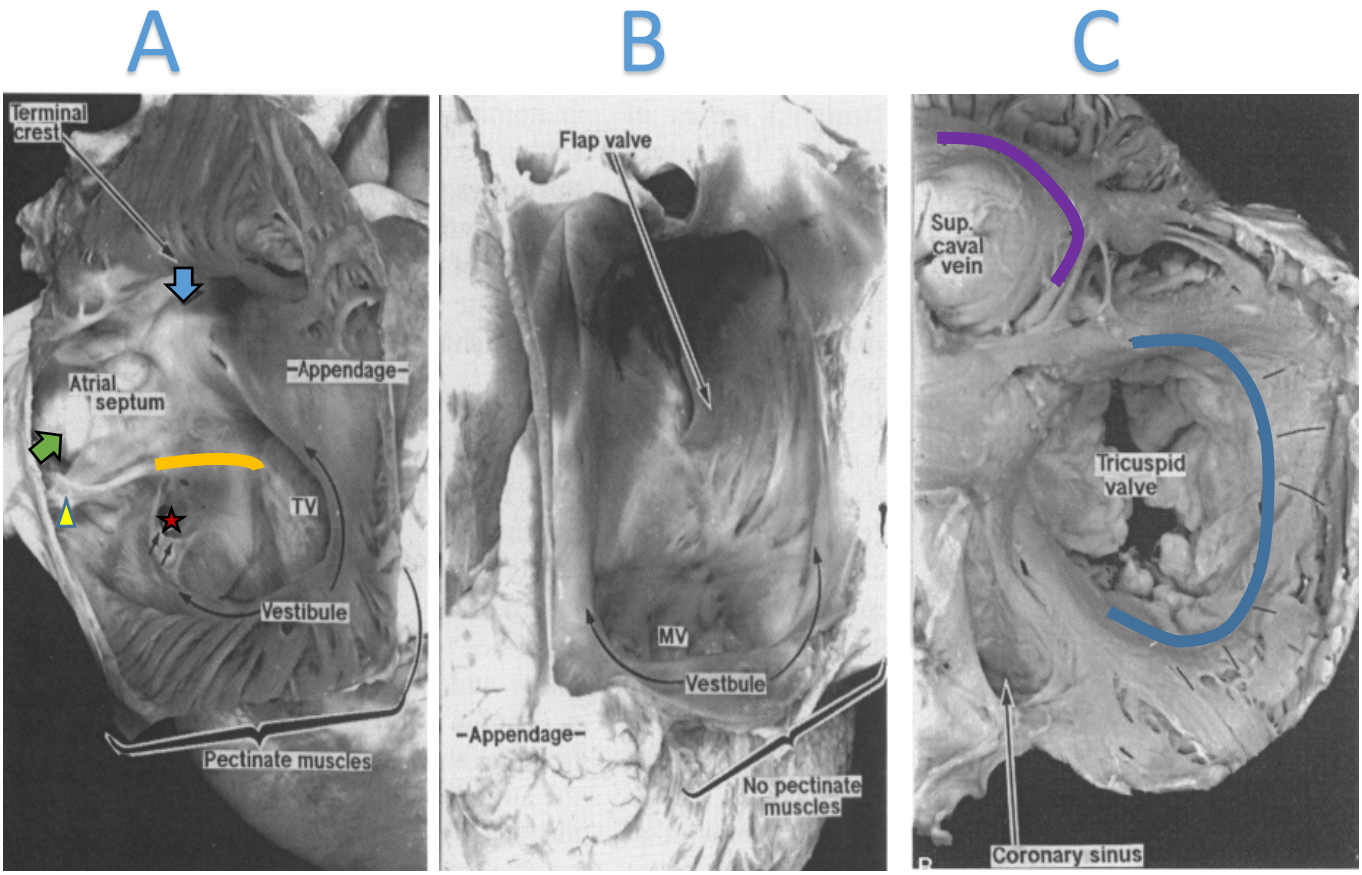

Figure 1.3.2 Anatomical dissection of the human atria

Panel A, Internal aspect of the right atrium displayed after dissection of the right atrial appendage. The incision cuts through the pectinate muscles displaying the complex internal arrangement of the atrial septum, terminal crest, opening of the superior vena cava (blue arrow) and inferior vena cava (green arrow). The coronary sinus is displayed an red star. The orange line highlights the tendon of Todaro. The Eustacian valve demarked by the single yellow arrowhead, the Thebesian valve by the small double arrows and the tricuspid valve labelled TV. Panel B, Internal view of the left atria. Notice the absence of pectinate muscles, creating a smooth uniform vestibule that leads to the mitral valve (MV). Panel C, Top view of the right atrium revealing the muscular orientation of the terminal crest encircling the superior vena cava (purple line) and circumferential bundles encircling the vestibule leading towards to the tricuspid valve (blue line). Adapted from (Wang et al., 1995).

The circumferential bands of the left atrium are thicker and stronger than those of the right (Wang et al., 1995). The Interatrial band (known as Bachmann's bundle) forms the principle circumferential bundle connecting the two atria Figure 1.3.3. This band of tissue was observed in the mammalian heart in 1916 by Jean George Bachmann who found that clamping this bundle of fibres in canines causes severe conduction delay (Bachmann, 1916).

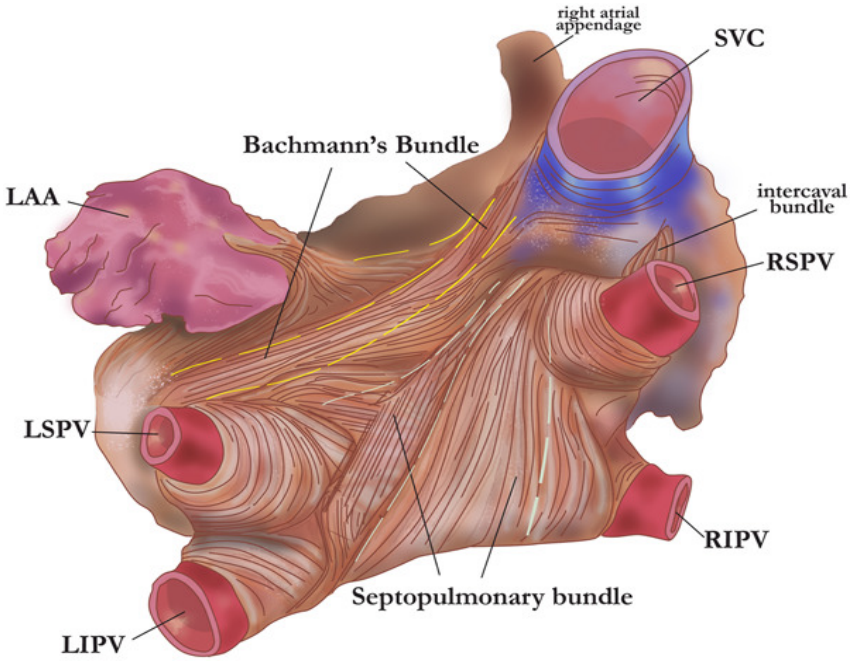

Figure 1.3.3 Posterior view of the left atria illustrating Bachmann's bundle, the septopulmonary bundle and insertion of the pulmonary veins.

adapted from (Clarke et al., 2021) .

It originates from the superior vena cava and extends along the anterior wall of the left atrium transversely approaching the left atrial appendage encircling the opening. The upper branch extends beyond the left atrial appendage towards to orifice of the left pulmonary vein, whereas the lower branch extends downwards towards the atrial base encircling the vestibule attaching to the mitral ring. The role of Bachmann's bundle in the initiation and maintenance of arrhythmia has become widely recognised as

illustrated by Ariyarajah et al. 2007 who studied the clinical significance of Bachmann's bundle in AF, and proposed that a conduction defect in this structure may be a substrate for the evolution of AF. The study showed that 29% of patients with inter-atrial block (n=44) had developed AF at their 12-month follow-up appointment, in contrast to patients without inter-atrial block their AF incidence was only 9%; and furthermore 75% of patients who had developed AF showed interatrial block on electrocardiography (Ariyarajah et al., 2007).

Beneath Bachmann's bundle forming the posterior wall of the left atrium are the septopulmonary bundles, which are fibres that fan out in front, between and around the insertion of the pulmonary veins. The sleeve of atrial musculature is conjoined with the vein, creating a smooth inlet into the chamber (Ho & Sánchez-Quintana, 2009). The presence of electrical activity in the pulmonary vessels has been recognised since the 1970s (Zipes & Knope, 1972). A couple of decades later it was observed that the region of the pulmonary veins could spontaneously initiate electrical activity (Haïssaguerre et al., 1998). The population of individual pulmonary vein cells from this region were shown to share electrical activity features with the sinoatrial node, and possess unique electrical features that predispose to the development of spontaneous activity which could lead to a AF susceptibility (Jones et al., 2008). Moving forward with advanced technologies clinicians have now been empowered to isolate specific regions of the posterior wall, and pulmonary veins, as targets for catheter ablation (Clarke et al., 2021).

1.3.2 The atrial cardiomyocyte

Histological examination of cardiac tissue reveals important differences in the dimension, structure, and organization of atrial and ventricular cells: Firstly, the atrial cardiomyocyte is shorter and more elliptical in shape, and Legato also commented that unlike their ventricular counterparts, most atrial cells appeared not to possess a t-tubular system (Legato, 1973).

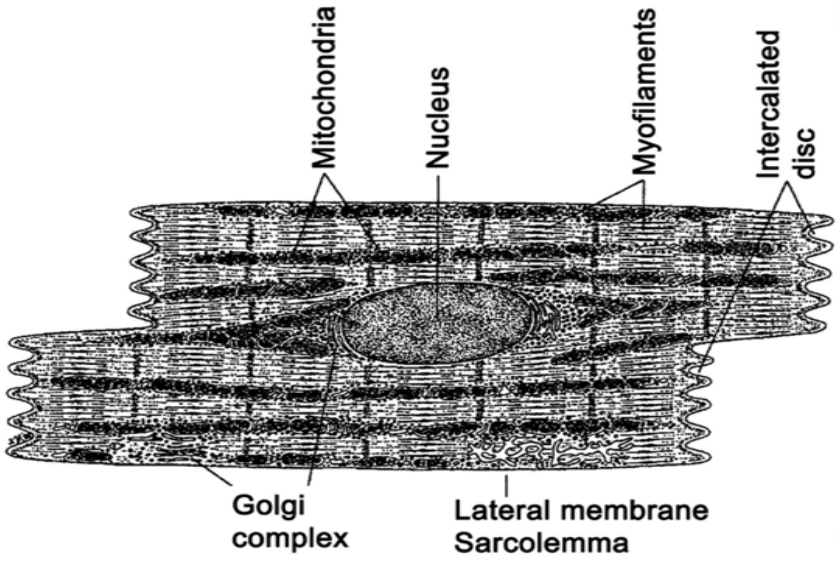

Figure 1.3.4 Illustration of an atrial cardiomyocyte

Adapted (Brandenburg et al., 2016).

Recent technological advances in confocal and epi-fluorescence microscopy have led to the dismissal of this observation from the 1970s. Richards et al. demonstrate that t-tubules are a common feature in the atrial cells of large mammals including humans; with 69% of human atrial cells demonstrating some form of t-tubular network (Richards et al., 2011), although due to the heterogenous nature of cells within the atrial myocardium he recognised that the number of cells with t-tubules and quantity of t-tubules in atrial cells are varied.

Atrial cardiomyocytes also have a unique arrangement in terms of their intercellular organisation. Atrial muscle tends to be constituted of bundles of cells which connect along their longitudinal boarder Figure 1.3.4. This is a distinct contrast to ventricular myocytes which are closely packed in a broad sheet like arrangement, conjoined more typically end-to-end through their interdigitating protrusions (Legato, 1973). The unique arrangement of atrial myocytes, connecting not only end-to-end but side-to-side, allows for impulse transmission along both axes. Therefore, there is more opportunity for disorganised patterns of impulse propagation.

In comparison to ventricular myocytes, atrial myocytes have a less negative resting potential, abbreviated phase 2 plateau phase and shorter action potential duration, creating the distinct short, triangular shaped action potential (Grandi et al., 2011) Figure 1.3.5. One of the most important distinctions of the atrial action potential is the presence of the ultra-rapid delayed rectifier current (I_{Kur}). As the name suggests, this is a rapid outward potassium current during phase 2 which is responsible for shortening the plateau phase and action potential duration. This is regulated predominantly by the Kv1.5 channel which is exclusively expressed in the atria (Wang et al., 1993).

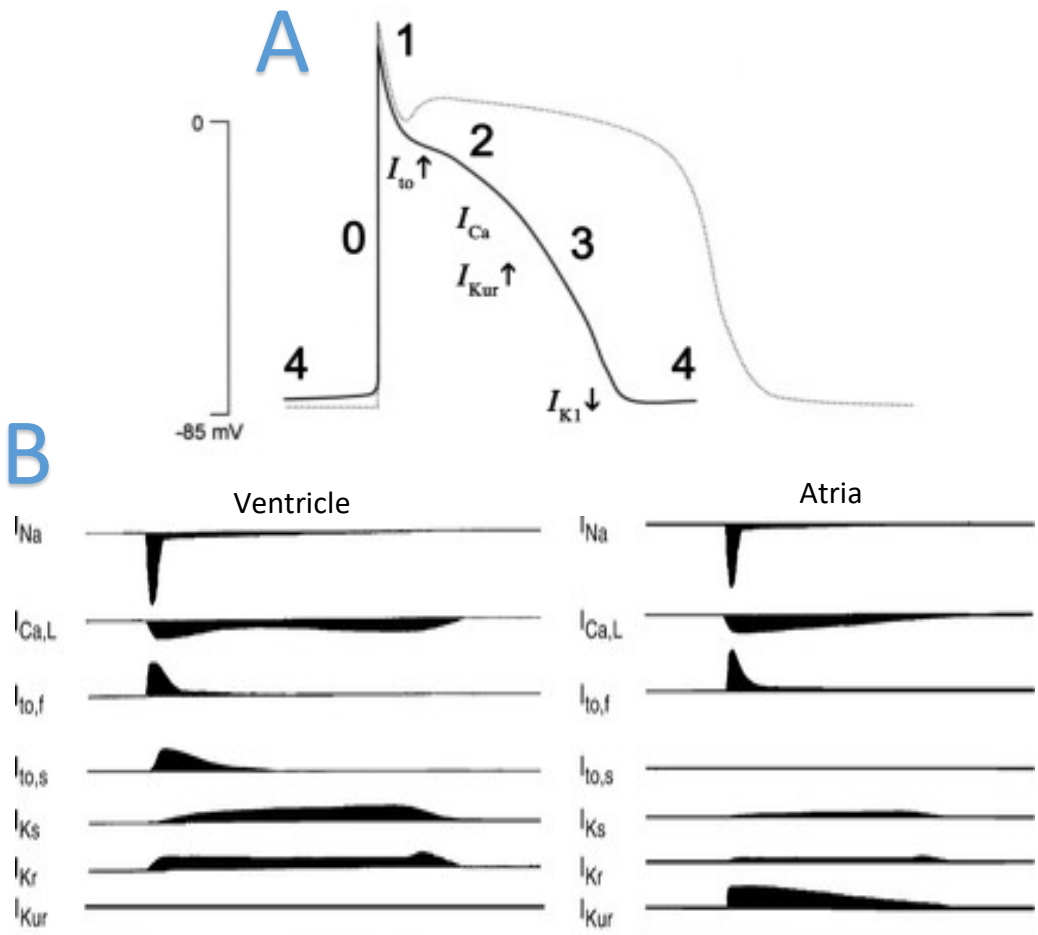

Figure 1.3.5 Juxtaposition of atrial vs ventricular action potentials

Panel A: The atrial action potential is illustrated by the bold black line, with the ventricular action potential juxtaposed with the dotted line. Numbers 0-4 highlight the phases of the action potential. The affecting currents on the atrial myocyte contributing to its shape during specific phases demonstrated under the atrial AP curve. Adapted from (Brandenburg et al., 2016).

Panel B: A side by side comparison of ion currents between the ventricles and the atria. Adapted from (Nerbonne & Kass, 2005)

1.4 Atrial fibrillation

1.4.1 General overview

Atrial fibrillation (AF) is a supraventricular tachyarrhythmia characterised by uncoordinated electrical activity in the atria, leading to a decline of mechanical function (Fuster et al., 2006). This erratic excitation throughout the atria creates irregular, chaotic and rapid contractions of the atrial myocardium with around 300 discharges per minute in comparison to 60-80 of a heart beating in sinus rhythm (Bootman et al., 2011). This disturbed electrical activity in the atria means there is a loss of normal pacemaker function. Clinically on the ECG a patient in AF will typically lose the 'P wave' (representing atrial depolarisation) which is replaced by an uneven, fibrillating isometric line Figure 1.4.1. The fine-tuned co-ordination between atrial and ventricular contraction is lost. Of the many discharges occurring in the atria, a sporadically timed impulse will propagate through the AV node leading to irregularly timed contraction of the ventricles. On the ECG this is demonstrated by unevenly spaced QRS complexes (representing ventricular depolarisation) (Fuster et al., 2006).

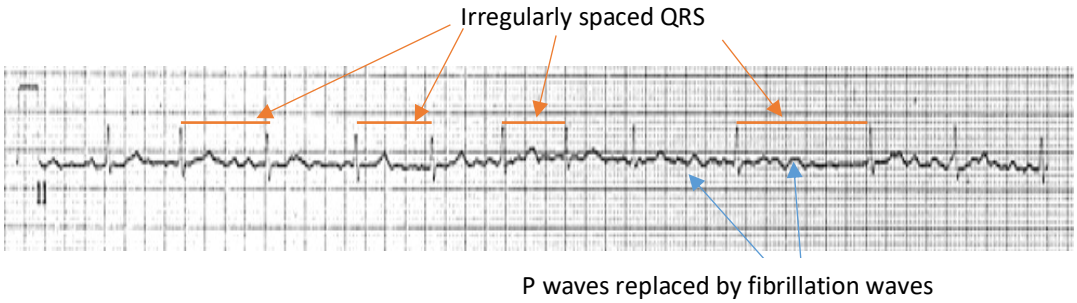

Figure 1.4.1 ECG of a patient in AF

Blue arrows highlighting the loss of P waves by a fibrillating isometric line. Orange lines illustrating the irregularly timed QRS complexes. Adapted from (Fuster et al., 2006)

Patients with AF will typically experience symptoms of breathlessness, palpations, dizziness, fatigue and syncope (Davidson, 2010). This is due to the uncoordinated contraction of the atria impairing blood flow through the hearts chambers, reducing output by 20-30% (Alpert et al., 1988). Due to poor emptying into the ventricles, static blood will pool in the atria and clot, consequently thromboembolic events are a principal concern in the AF population with the risk of stroke increased to between 300-500% (Benjamin et al., 1998).

1.4.2 Epidemiology and healthcare burden of AF

AF is the most common arrhythmia worldwide affecting an estimated 33.5 million people (Chugh et al., 2014). The prevalence of AF increases with age with 80.5% of cases seen in patients aged 65 and over (England., 2017). With age as the primary risk factor for the development of AF, inevitably an ageing population will result in an increased prevalence of the disease (Go et al., 2001; Weng et al., 2017) Figure 1.4.2. Within Europe

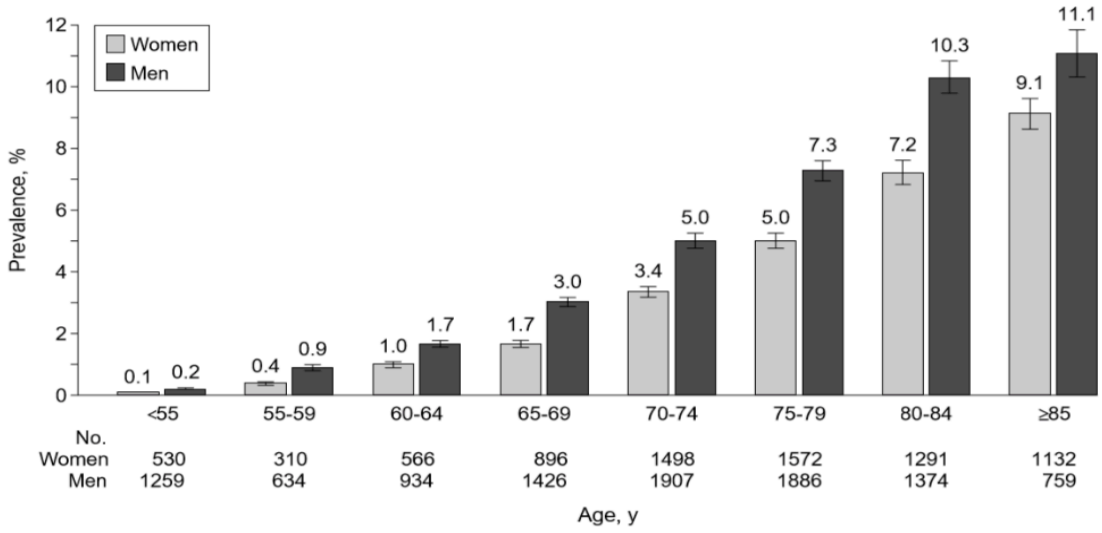

Figure 1.4.2 Prevalence of AF in relation to sex and age

adapted from (Go et al., 2001)

incidence of AF is expected to more than double in the over 55 population by 2060 (Krijthe et al., 2013). AF carries notable morbidity and mortality with patients at significantly higher risk of stroke (Wolf et al., 1991), heart failure (Ragbaoui et al., 2017), myocardial infarction (Ruddox et al., 2017) and death (Benjamin et al., 1998).

Healthcare resources continue to be strained as inpatient hospitalization specifically due to AF continues to rise by roughly 1% each year (Freeman et al., 2017). Within the UK alone, the direct cost of AF sharply rose from £244 million to £458 over a five-year period. When considering the long term cost of community care as a consequence of hospitalisation with AF an additional £111 million is tallied onto this in the year 2000-more than double that of 1995 (Stewart et al., 2007). Furthermore, management of AF-particularly anticoagulation-carries notable risk which also contributes to the economic impact. In Korea, the cost of AF related hospital admissions due to bleeding because of anticoagulation rose from €68.4 million to €388.4 million over a nine-year period.

1.4.3 Mechanics of AF

The pathophysiology of AF is a complex, multi-factorial process. Simply put, the evolution of AF can be appreciated as an interplay between trigger and substrate. The trigger is often the rapid firing of a local ectopic focus (Figure 1.4.3 A) and occurs in some atrial myocytes which exhibit enhanced automaticity. When the normally supressed pacemaker current (I_f) overwhelms the inward rectifier potassium current (I_{k1}) which maintains resting potential, an action potential is discharged Figure 1.4.4 A (Stillitano et al., 2008).

After depolarisations are another mechanism of spontaneous ectopic firing. Early after depolarisations (EADs) are dependent upon prolonged action potential duration which

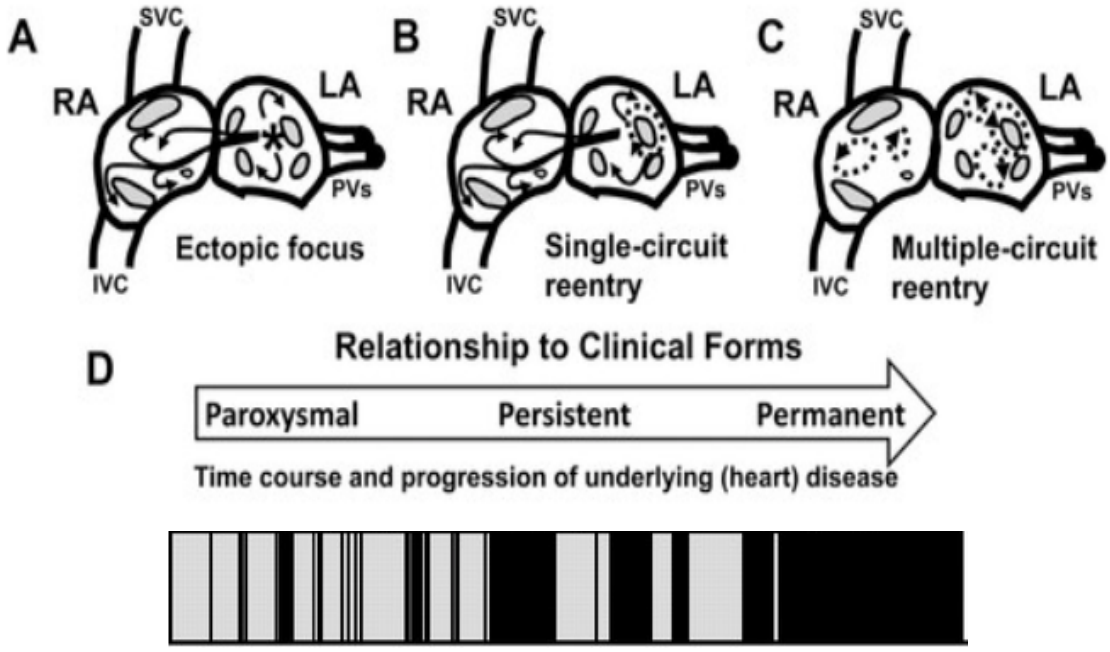

Figure 1.4.3 Progression of AF over time

Panel A) Illustration of an ectopic impulse origination from around the pulmonary veins and propagating through the atria. **Panel B)** Illustration of a single re-entry within the left atrium. **Panel C)** Illustration of multiple re-entry circuits throughout both atria. **Panel D)** Arrow demonstrating the progression of AF over time. Block illustration with grey space representing sinus rhythm, black space representing AF. As time progresses AF becomes more frequent, lasts for longer, and eventually becomes permanent.

Adapted from (Schotten et al., 2011) & (Iwasaki et al., 2011)

allow L-type calcium currents (I_{CaI}) to recover from inactivation Figure 1.4.4 B. Delayed afterdepolarisations (DADs) occur through the abnormal diastolic release of Ca^{2+} ions creating an overload of cytoplasmic Ca^{2+}. This triggers a calcium induced calcium release from via RyR2 receptors-a key process in excitation-contraction coupling. Overloaded cytosolic Ca^{2+} must be removed by the Ca2+/Na+ exchanger (Voigt et al.). Three Na+ ions move into the cell for one Ca^{2+} ion out leading to an overall positive charge and therefore a further depolarising current (Horvath et al., 2013) Figure 1.4.4 C.

The substrate is the structural and electrophysiological environment within the atria which promote the propagation and maintenance of the arrhythmia. Between 70-80% of patients with AF have some form pre-existing structural heart disease (Lévy, 1998). Furthermore, the time course for permanent AF to set in is much more rapid in those with structural heart disease than patients with AF alone (Kato et al., 2004; Kerr et al., 2005). There are important clinical conditions which promote the substrate for AF to occur. Hypertension is found between 60-80% of patients with AF (Nabauer et al., 2009).

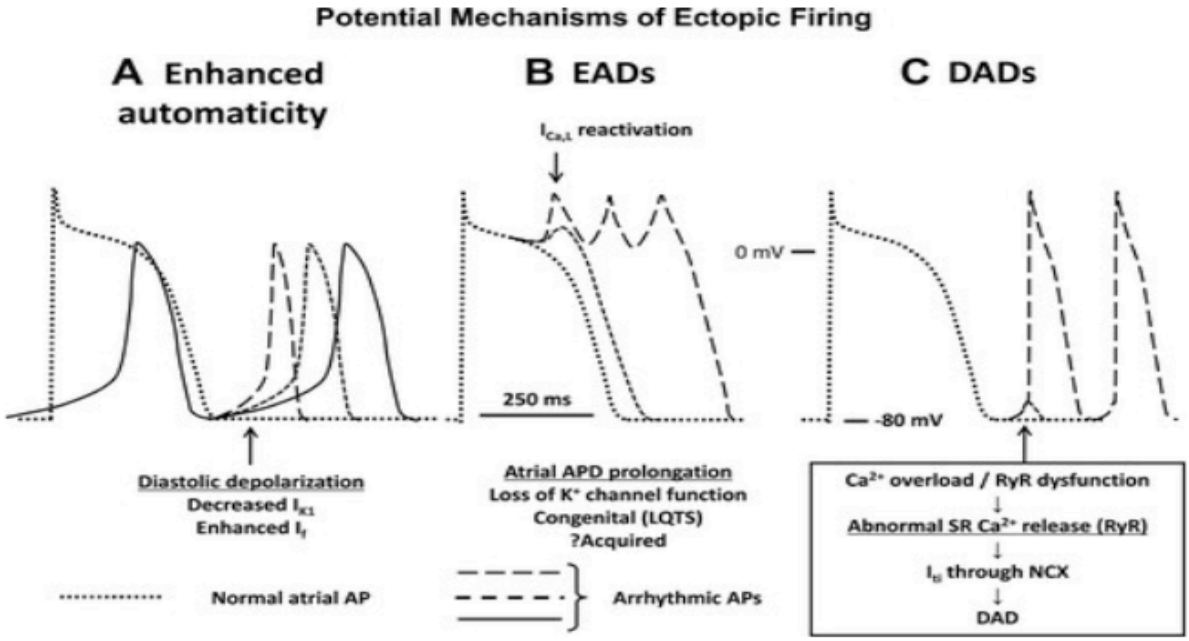

Figure 1.4.4 Mechanisms of ectopic firing in AF

Panel A) Enhanced automaticity, Panel B) EADs, Panel C) DADs

Adapted from (Iwasaki et al., 2011)

Vascular disease-in particular coronary artery disease-is present in roughly 30% of patients with AF (Nabauer et al., 2009) as is heart failure and diabetes (Nieuwlaat et al., 2005). Heart failure and AF tend to promote each other as AF compromises left ventricular function. This in turn causes pressure overload in the atria and atrial dilatation which is a prime condition for re-entry circuits to form Figure 1.4.5 C.

One of the main determinants of re-entry is the refractory period. A reduced effective refractory period in a region of myocytes results in less time for the cells to have recovered from depolarisation, and hence that tissue is susceptible to the conduction of an ectopic beat. Figure 1.4.5 illustrates the factors promoting re-entry and their mechanism. Initially episodes of AF tend to be asymptomatic, short, and self-terminating. Over time more frequent attacks occur with longer duration thus eliciting symptoms, and more sustained forms AF begin to take root (Israel et al., 2004) Figure 1.4.3 D. As AF progresses from paroxysmal to permanent, there is a shift from trigger to substrate driven pathology. Hence AF is a self-perpetuating and progressive disease ("AF-begets-AF"). As it becomes permanent, atrial remodelling cements and re-entrant circuits dominate the atria (Iwasaki et al., 2011). The diseased atrium in permanent AF therefore creates a substrate to which ablation has limited efficacy.

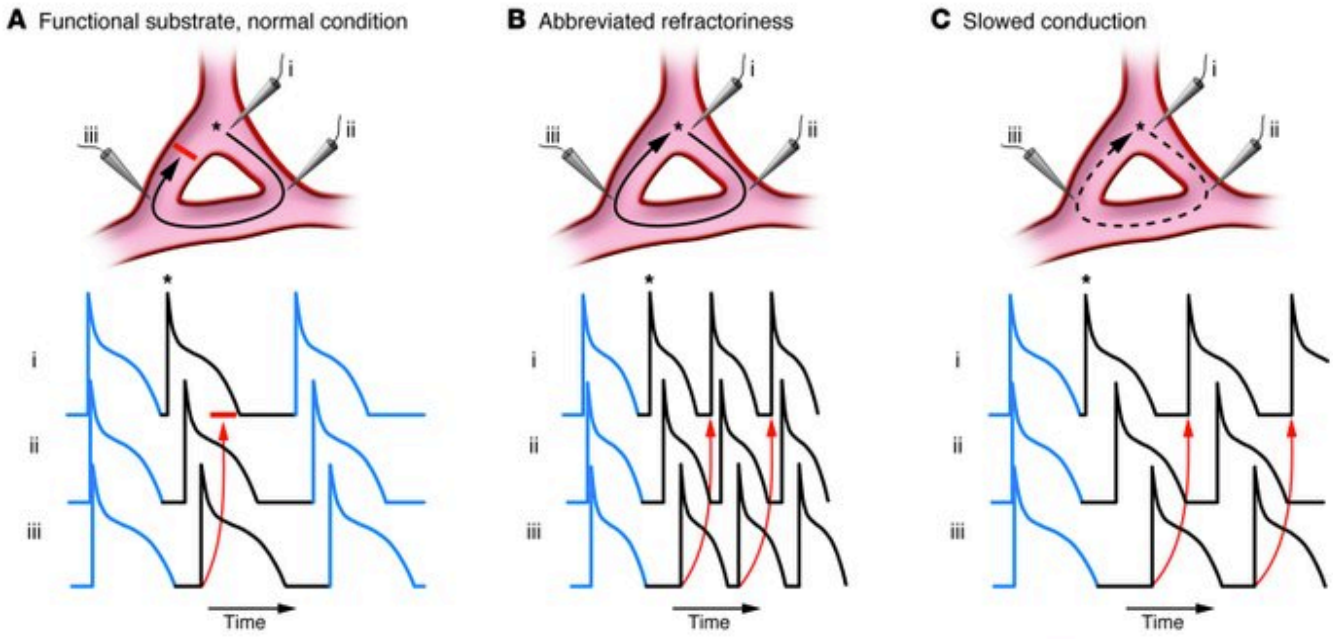

Figure 1.4.5 Factors promoting re-entry

These diagrams represent a hypothetical piece of cardiac tissue with 3 electrodes placed around a non-conductive substrate; i, ii, iii- which correlate to the action potential readings seen below each panel. The * represents an ectopic focus discharging an action potential. Blue action potentials represent normal functional electrical activity, black action potentials are ectopic.

Panel A) This represents cardiac tissue under normal electrophysiological conditions. As the ectopic is discharged, it circulates around the substrate, passing probes i, ii & iii. As it comes back to its starting point, the impulse in unable to re-excite the myocytes of where it originated as they're still in their refractory period and hence unable to depolarise again (illustrated by the red line). The potential re-entry arrhythmia is avoided, and the tissue continues to conduct action potentials as normal.

Panel B) This panel represents the effect of a reduced refractory period. An ectopic is fired just before probe i. Due to the shortened refractory period, myocytes within the starting region have recovered from the previous action potential and hence will conduct the ectopic impulse. Here, a re-entry circuit has formed and will continue to spiral.

Panel C) This panel represents the effect of slowed conduction around the substrate. By the time the impulse has propagated back to its starting point, due to the slowed conduction myocytes within the starting point have repolarised, recovered from the refractory period and hence susceptible for re-excitation. Slowed conduction may be a consequence of a multitude of factors e.g atrial stretch due to dilatation, fibrosis, ion channelopathy, ischaemia.

Adapted from (Wakili et al., 2011)

1.4.3.1 Atrial remodelling in AF

Atrial remodelling describes changes in structure and function which promote arrhythmia. AF and remodelling have a circular interdependent relationship; they give rise to each other, and one promotes the other though it's unclear precisely which comes first. It is however widely accepted that progressive atrial remodelling promoting re-entrant pathways are a hallmark feature of AF-with the severity of remodelling correlating with the disease duration (Manning et al., 1994; Yue et al., 1997). There are two main forms of remodelling to appreciate in AF; structural remodelling and electrical remodelling.

Structural remodelling

One of the earliest observations of a structural substrate for AF came from Frustaci et al. who sampled biopsies from the atrial septal wall and ventricles in patients with lone AF. These studies showed consistent findings of inflammation and tissue fibrosis confined to the atria, demonstrating histological evidence of fibrotic remodelling in AF (Frustaci et al., 1997). Fibroblasts play an integral part of the healthy myocardium by offering a cellular scaffolding to support the three-dimensional muscular network. This electrically insulative structure not only ensures uniform excitation and direction of propagation of electrical activity throughout the myocardium, but also slows down conduction in response to mechanical stretch (Kohl et al., 1994; Kamkin & Kiseleva, 1998). However, the upregulation of fibroblasts in AF leads to replacement fibrosis uncoupling myocytes, impairing cell to cell communication, hindering standard conduction pathways and priming the atria for re-entrant circuits to form (Yue et al., 2011). The over proliferation of fibroblasts as seen in AF creates a heterogenous,

unorganised, heavily disrupted muscular architecture. This further impedes co-ordinated electrical excitation, creating a pro-arrhythmogenic substrate (Begg et al., 2016) Figure 1.4.6. In a canine study, atrial pacing increased fibronectin production by 430% (Burstein et al., 2007).

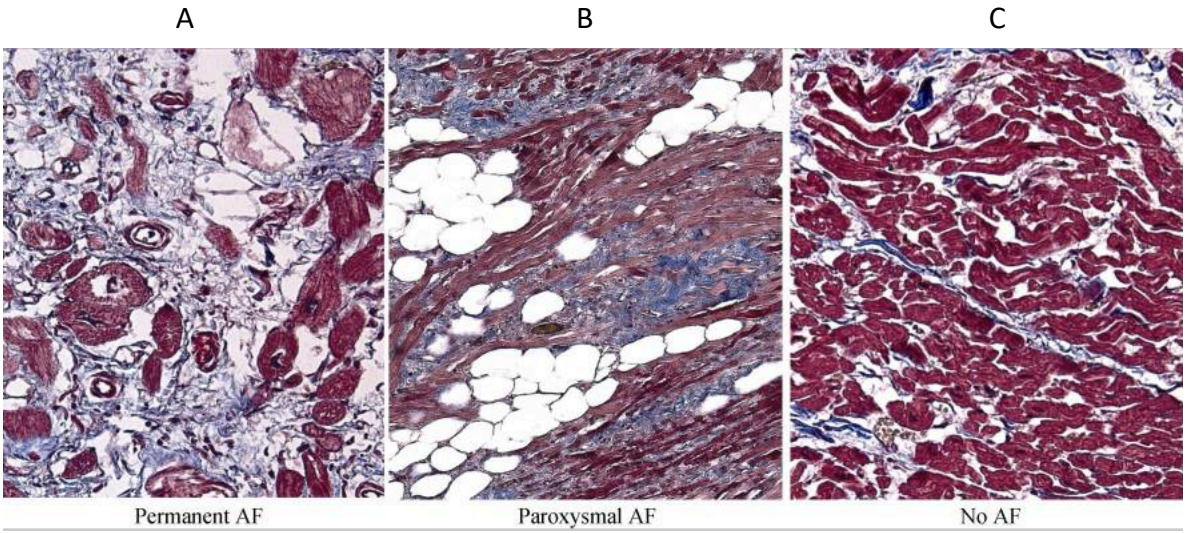

Figure 1.4.6 Light microscopy of myocardial samples demonstrating replacement fibrosis

Tissue collected at post-mortem from patients with permanent AF (panel A), Paroxysmal AF (panel B) and sinus rhythm (panel C). Adapted from (Platonov, 2017)

Electrical remodelling

Electrical remodelling involves alterations to the expression and function of ion channels which govern action potential mechanics and conduction through tissue. This creates multiple feedback loops which further promote arrhythmia Figure 1.4.7. During electrical remodelling, there are significant disruptions in calcium and potassium handling which increase the susceptibility for re-entrant arrhythmia (Grandi et al., 2011). Ca^{2+} enter the cell with each action potential-therefore rapid atrial rates increase Ca^{2+} loading. Compensatory homeostatic mechanisms become initiated to reduce Ca^{2+} entry; Ca^{2+} current inactivation through the direct downregulation of I_{CaL} and inward rectifier K^{+} enhancement which reduce Ca^{2+} loading through shortening the action potential

duration(Brundel et al., 2001; Grandi et al., 2011). However, by shortening action potential duration myocytes become susceptible to ectopic beats and hence these changes stabilize re-entry rotors increasing AF vulnerability(Pandit et al., 2005). Furthermore, disrupted calcium handling will promote diastolic calcium release and ectopic activity through DADs (Pandit et al., 2005).

With regards to the sodium current, AF has been associated with a diminished I_{Na} conduction velocity, shortening of the re-entry wavelength and disrupted electrical excitation (Pathak et al., 2013). Mutations in the SCN5a coding for the $Na_v1.5$ channel have been associated with the arrhythmia (Darbar et al., 2008), and the neuronal $Na_v1.8$ channel has been implicated frequently in the literature as a culprit for arrhythmogenic currents and even the target of therapeutic approaches (Yang et al., 2012b; Chen et al., 2016; Macri et al., 2018b). The specific role of sodium channels in AF will be discussed in detail in Chapter 4.

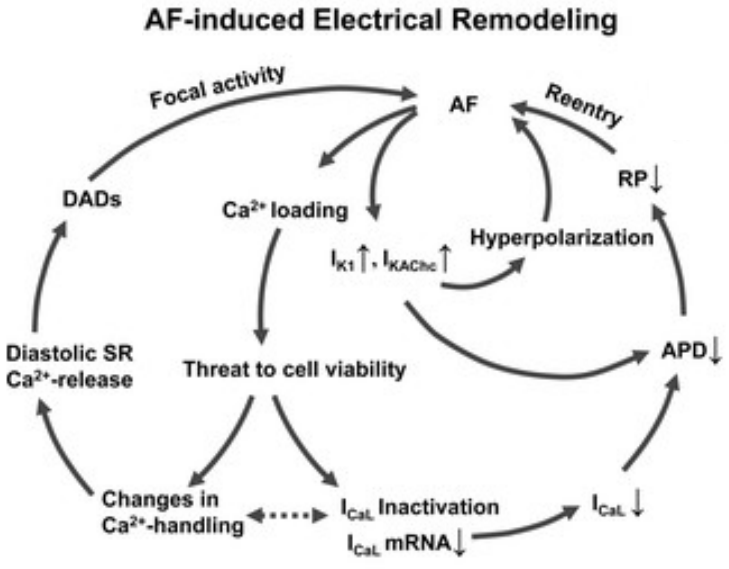

Figure 1.4.7 AF-induced electrical remodelling

Adapted from (Iwasaki et al., 2011)

1.5 Study hypothesis

1) This study aims to investigate the expression of voltage-gated sodium channels in the human right atria. We propose that with increasing age, there will be a reduction in the expression of the native cardiac isoform $Na_v1.5$, coupled with an increase of the neuronal isoform $Na_v1.8$.

   Null hypothesis: Elderly patients in sinus rhythm will exhibit no change in the expression of $Na_v1.5$ or $Na_v1.8$ in comparison to younger patients.

2) This study will compare the expression of $Na_v1.5$ and $Na_v1.8$ in the human right atria of patients with AF to those in sinus rhythm. We propose that there will be a significantly reduced expression of $Na_v1.5$ and increased expression of $Na_v1.8$ in patients diagnosed with AF in comparison to their sinus rhythm counterparts.

   Null hypothesis: Patients in AF will exhibit no significant difference in the expression of $Na_v1.5$ or $Na_v1.8$ in compassion to patients in sinus rhythm.

3) This study will aim to develop a protocol for pharmacological manipulation of $Na_v1.5$ and $Na_v1.8$ expression in the human right atria through the JNK pathway. This study will also investigate the relationship of p-JNK and total JNK expression with age. We propose that p-JNK and total JNK expression will be increased with age. We further hypothesise that with the activation of JNK with Anisomycin, $Na_v1.5$ expression will decrease whereas there will be a relative increase in the expression of $Na_v1.8$. Furthermore, with the inhibition of JNK through SP600125, $Na_v1.5$ will increase whereas expression of $Na_v1.8$ will go down.

   Null hypothesis: There will be no difference in P-JNK expression or total JNK expression with age. Manipulation of JNK expression will have no effect on the expression of $Na_v1.5$ or $Na_v1.8$.

Chapter 2

Materials and Methods

Chapter 2 Materials and methods

2.1 Consent and recruitment

This project utilises human tissue in the form right atrial appendage. Tissue was sampled from patients undergoing routine cardiac surgery of valve repair/replace or coronary artery bypass at Castle Hill Hospital. Suitable patients for tissue donation were identified using the University of Hull Teaching Hospitals IT systems; Lorenzo and ORMIS. Patients were initially contacted by phone to discuss the study, and on follow-up if they were interested a consent form and patient information leaflet was sent by first class post, usually at least one week prior to the date of surgery. This allowed time for the patients to read the study material carefully, discuss the study with relatives/friends and formulate any questions they would like to ask regarding the study: An email and phone number was enclosed to enable patients to ask any questions prior to admission.

On the day of admission, a formal consultation would take place on Ward 26. Each patient had the opportunity to ask any questions pertinent to the study and sign the consent form, which was witnessed by a member of staff. Whilst the original consent form was returned to the University of Hull study Director, a copy was given to the patient and another copy was placed in the patient's medical notes. At the same meeting, a patient history was taken for the study including their age, rhythm, operation, medication, general medical & surgical history, family history and smoking status.

2.2 Tissue acquisition

Once tissue was obtained from theatre it was placed in sterile, cold cardioplegic solution and transferred to the adjacent laboratory. Tissue was divided in to two halves to be used for the techniques of western blotting and immunocytochemistry. For western blotting, the tissue was finely sliced with a scalpel or scissors, placed in a cryogenic vial and flash frozen in liquid nitrogen: The vial was initially stored in a -80^{o}C freezer at Castle Hill Hospital.

For immunocytochemistry the tissue was cut into larger pieces and adhered to a cork disk using Tissue-Tek® O.C.T gel. The cork disk was submerged using large plastic forceps into a container of isopentane which had been pre-cooled by liquid nitrogen. The frozen tissue and cork bound samples were wrapped in tin foil and stored in a -80^{o}C freezer at Castle Hill Hospital. All samples were transported on dry ice to the University Hull, and again stored at -80^{o}C until experimentation took place.

Table 2.2.1 Components and concentrations of cardioplegic solution used for tissue acquisition

Cardioplegic Solution	
Component	**Concentration (mM)**
Glucose	277.5
KCL	30
$NaHCO_3$	20
Mannitol	34.3

2.3 Western blotting

2.3.1 Preparation of biological Samples

Tissue was ground using a pestle and mortar under liquid nitrogen to a pale pink powder and suspended in homogenisation buffer to protect the integrity of contained proteins in 1ml cryogenic vials. Suspended samples were flash frozen in liquid nitrogen and subjected to one freeze-thaw cycle on ice to ensure cell disruption. Once thawed, Eppendorfs were centrifuged (MicroCL 17R, Thermo Scientific UK) at 5000g for 5 minutes at 4^{o}C until a clear formation of a lysate and pellet. The pellet was discarded and the lysate supernatant containing proteins was pipetted off, collected and stored at -80^{o}C. Supernatant protein concentration was determined using the bicinchoninic acid (BCA) assay.

Table 2.3.1 Component and amounts of homogenisation buffer used for preparation of biological samples

Homogenisation Buffer	
Component	**Concentration(mM) & Amount**
Protease Inhibitors	1 tablet Pierce Protease Inhibitor Mini (Thermo Fisher UK)
EDTA	10mM (14.6mg)
Sucrose	300mM / <1% (500mg)
1% SDS	0.35mM (4.5ml)

2.3.2 Determining protein concentration using bicinchoninic acid (BCA) assay

A Pierce BCA Assay Reagent Kit was used for determining protein concentration.

Table 2.3.2 Contents of Pierce BCA protein assay kit

Pierce BCA Assay Reagent Kit	
Reagent A	BCA solution: 25mM BCA-Na_2, 160mM $NaCO_3.H_20$, 7.0mM Na_2tartrate, 0.1M NaOH and $NaHC0_3$; PH 11.25.
Reagent B	160mM $CuSO_4.5H_20$
Bovine Serum Albumin (BSA)	2mg/ml in 0.15< NaCl with 7.7mM NaN_3

BSA of 2mg/ml was diluted to a stock solution of 250 µg/ml. This was further diluted to form protein standards:

Table 2.3.3 Dilution of stock 2mg/ml of BSA to create protein standards

Protein concentration (µg/ml)	**0**	**25**	**50**	**100**	**150**	**200**	**250**
BSA (µl)	0	50	100	200	300	400	500
DH_20 (µl)	500	450	400	300	200	100	0

Reagent B and Reagent A were mixed in a ratio of 1:50 to create a fresh solution for immediate use (Reagent C). Samples for protein analysis were made using a 1:50 dilution of the original lysate in deionised water. In a 96-well plate, triplicate wells containing 20µl of standard or sample were mixed with 200µl of Reagent C. The plate was incubated

for half an hour at 37°C. Once the plate had cooled to room temperature, absorbance was measured at 562nm using a Tecan plate reader.

Average absorbance of each standard was plotted against protein concentration to create a standard curve:

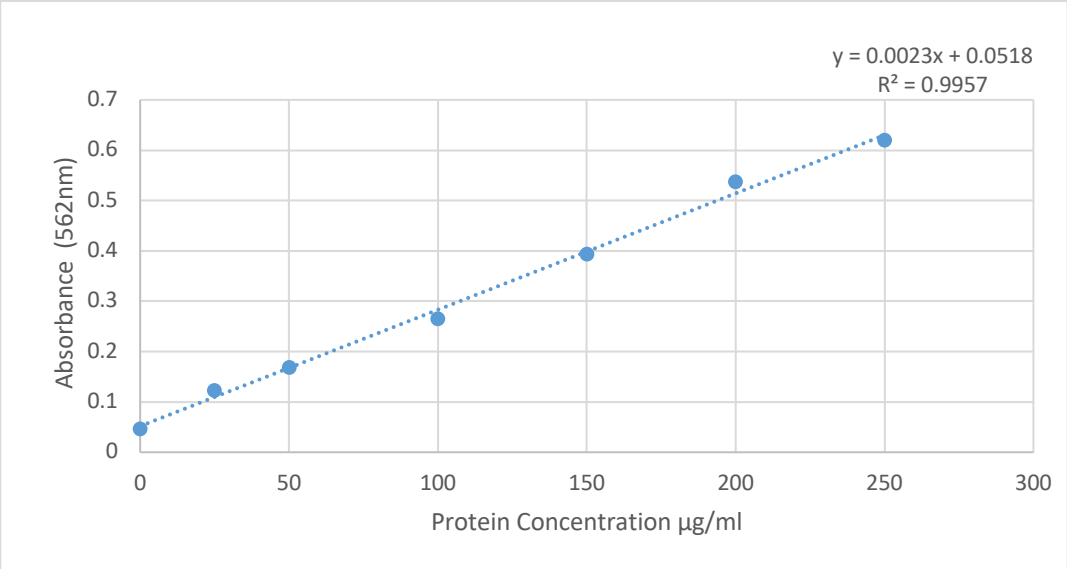

Figure 2.3.1 BCA standard curve

The linear relationship between absorbance and protein concentration of standards allows for determination of protein concentration in biological samples.

Average readings of triplicates for each patient sample were calculated and inputted into the equation to determine protein concentration. Example calculation:

y = 0.0023x + 0.0518

Average reading of Sample 1 = 0.4.

Therefore: *Y=0.4*

0.4=0.0023x +0.0518

X= (0.4- 0.0518)/0.0023

X= 151.39 µg/ml

Taking account of 1:50 dilution of original sample.

Therefore: *151.39 x 50*

Protein concentration of Sample 1 = 7569.6 µg/ml

100 µg of protein required to load into gel for electrophoresis.

Therefore: *7569.6 µg / 1000 µl* *(unit conversion)*

1 µg of protein = *1000 ÷ 7569.6*

= *0.132 µl*

100 µg of protein = *0.132 x 100*

13.2µl of Sample 1 to load into gel.

2.3.3 Polyacrylamide gels

Table 2.3.4 Reagents used to make polyacrylamide gels

Reagents	
Protogel	30% ($^{w}/_{v}$) acrylamide and 0.8% ($^{w}/_{v}$) bisacrylamide
Protogel Buffer	1.5M Tris-Hcl, 0.38% SDS. PH 8.8
Protogel Stacking Buffer	0.5M Tris-Hcl, 0.4% SDS, PH 6.8
Ammonium persulphate	0.44M in DH_20
TEMMED	6.7M in DH_20

Vertical slab gels of 10cm x 8cm x 1.5mm were formed using two short glass plates, two glass spacer plates and 10 well combs. Glassware was washed with deionised water and 4% ethanol and secured to the mounting apparatus.

A 10% running gel was favoured as the larger pores of the matrix allowed for clearer separation of middle to high molecular weight proteins through the polyacrylamide lattice. This consisted of 3.34ml of Protogel, 2.60ml of Protogel buffer and 3.96 ml of ultra-pure deionised water. To set the gel, 10µl of TEMED and 100µl of ammonium persulphate were thoroughly mixed into the solution and quickly poured in between two glass plates. A thin layer of butanol was poured on top of the mixture to prevent oxidation and remove any bubbles, providing a straight interface with the stacking gel.

Once the running gel had set, butanol was poured out and excess was absorbed using Whitman's paper. The 4% stacking gel was formed by 1.3ml of Protogel, 2.5ml of stacking buffer, 6.1ml of deionised water, 10 µl of TEMED and 50 µl of ammonium

persulphate and poured onto the set running gel. The comb was quickly placed on top of the poured solution ensuring no bubbles to form the wells. Once the stacking gel had set, the glass plates were removed from the mounting apparatus and placed in a Bio-Rad electrophoresis tank. The tank was filled with electrophoresis buffer and the combs were removed with the gels suspended in the buffer, ready for protein loading.

2.3.4 SDS-PAGE electrophoresis

Table 2.3.5 Reagents and equipment used for SDS-PAGE electrophoresis

Reagents & Equipment	
2x Laemmli SDS loading buffer ***National Diagnostics UK***	2% ($^{v}/_{v}$) 2-mercaptoethanol, 0.5M Tris-HCL (p.H 6.8), 4.4% ($^{w}/_{v}$) SDS, 20% glycerol, bromophenol blue
Electrophoresis buffer	0.25M Tris, 1.92M glycine and 1% SDS. (diluted from 10x stock)
Molecular Weight Markers: **(Amersham Life Sciences UK)**	Full Range Rainbow Markers (10-250kDa)
Bio-Rad MiniProtean Electrophoresis power pack and Tank.	

Patient samples were prepared for electrophoresis by mixing in equal amounts lysate and 2x Laemmli SDS loading buffer. The 2-mercaptoethanol contained within the Laemmli breaks the disulphide bonds and SDS acts as an ionic agent, wrapping around the protein creating negatively charged peptides. The mixture was vortex mixed and

reduced by heating for 5 minutes at 60^{o}C. Heating the mixture disrupts the 3D structure of the protein allowing for access to the epitope of which the antibody is derived.

Once the mixtures had cooled to room temperature, they were loaded to the wells of the polyacrylamide gel under electrophoresis buffer. One well of each gel contained 10 µl of molecular weight markers (10-250kDa). Electrophoresis was carried out using a Bio-Rad Cell Electrophoresis power pack and tank. 10mA was used to run the samples through the stacking gel. Once through, up to 40mA per gel was used to run through the running gel. The entire electrophoresis takes approximately 2 hours.

2.3.5 Electroimmunoblotting

Transfer of proteins from the gel to the nitrocellulose membrane was achieved through electroimmunoblotting. A sandwich stack was arranged between two electrode plates (Figure 2). Whitman filter paper was soaked in anode and cathode buffers to form the desired reservoirs. The gel was removed from between the glass plates and carefully placed onto the nitrocellulose membrane, ensuring no cracks or air bubbles. The gel was topped with the cathode reservoir, again ironing out any potential air bubbles. A constant current density of 0.8mA/cm2 (50mA per gel) was applied to the electrodes for two hours to ensure maximal transfer of proteins. Once the transfer was complete the membrane was placed in 10ml of blocking buffer and stored overnight at 4 ^{o}C.

Table 2.3.6 Reagents and equipment used for electroimmunoblotting

Reagents & Equipment	
Anode Buffer 1 (A1)	80% ($^{w}/_{v}$) 0.3M Tris (18.17g in 400ml of DH_20) 20% methanol pH 10.4
Anode Buffer 2 (A2)	80 % ($^{w}/_{v}$) 25 mM Tris (1.51g in 400ml DH_20) 20 % methanol pH 10.4
Cathode Buffer (C)	80 % ($^{w}/_{v}$) ε-amino-n-caproic acid (2.62g in 400ml DH_20). 20 % methanol pH 7.6
Nitrocellulose membrane	0.45µm pore size nitrocellulose membrane (Thermo Fisher Scientific UK)
Filter paper	Whitman 3MM chromatography paper (Thermo Fisher Scientific UK)
Equipment	TE 77 ECL™ Semi-dry blotter (Amersham Biosciences UK)
Blocking Buffer	5g of dried milk in 100ml of PBS (Pierce UK)

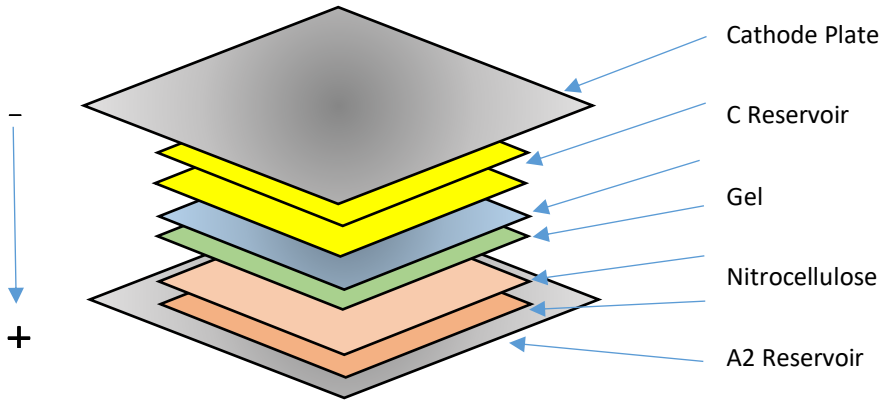

Figure 2.3.2 Components of semi-dry discontinuous blotting

Arrow on the left of the image represents the direction of current flow.

2.3.6 Probing the membrane

Table 2.3.7 Reagents used for probing the membrane

Reagents	
PBS	1 sachet in 1L of DH_20 (Premade from Pierce UK)
PBS-Tween	500µl of Tween20 in 1L of PBS
Blocking Buffer	5g of dried milk in 100ml of PBS
Secondary Antibody	25% ($^{v}/_{v}$) foetal calf serum (FCS) in PBS-Tween with Antibody.

Table 2.3.8 Primary antibodies used in western blot

Antigen	1° Antibody	Concentration	Dilution	Manufacturer	Host	Reactivity	Dilutant
$Na_v1.5$	Anti $Na_v1.5$	0.8mg/ml	1:500	Alomone, Israel	Rabbit	Human, rat and mouse	PBS-Tween
$Na_v1.8$	Anti $Na_v1.8$	0.8mg/ml	1:1000	Alomone, Israel	Rabbit	Human, rat and mouse	PBS-Tween
Desmin	Anti Desmin	0.03mg/ml	1:1000	Abcam UK	Rabbit	Human, rat, mouse and guinea pig	PBS-Tween

Table 2.3.9 Secondary antibody used for western blot

Immunogen	2° Antibody	Dilution	Manufacturer	Host	Reactivity	Dilutant
IgG (Rabbit)	Peroxidase-conjugated swine anti-rabbit	1:1000	Dako, Denmark	Swine	Rabbit	25% FCS in PBS-Tween

The nitrocellulose membrane was removed from the fridge, blocking buffer discarded and washed 3 times in PBS-Tween for 5 minutes to remove any trace of liquid milk whilst the milk proteins remain stuck on the membrane. Nitrocellulose was incubated in a 10ml solution containing the primary antibody in PBS-Tween and agitated for 1 hour at room temperature or left overnight in 4 ^{o}C fridge. Primary antibody was reclaimed and stored at 4 ^{o}C for future use. The membrane was washed again 3 times, each for 5-minute periods in PBS-Tween.

Nitrocellulose was incubated in a 10ml solution containing secondary antibody (FCS acting as non-specific blocking agent) and agitated for 1 hour at room temperature. Finally, the secondary antibody was reclaimed and stored at 4 ^{o}C, and the membrane washed for 3 periods of 5 minutes in PBS-Tween and a final wash for 15 minutes.

2.3.7 Developing the membrane

Table 2.3.10 Reagents & equipment used for developing the membrane

Reagents & Equipment	
ECL Kit (Pierce Scientific UK)	Reagent 1: Peroxidase solution Reagent 2: Luminol enhancer solution
Acetate	Photocopy machine acetate
Photographic Film	Amersham Hyperfilm (GE Healthcare UK)
Developer	Ilford multigrade diluted to 1:9 (Harman tech. Ltd UK)
Fixer	Ilford rapid fixer diluted to 1:5 (Harman tech. Ltd UK)
Equipment	Cassette Box

Equal volumes of reagent 1 and reagent 2 from the ECL kit were mixed and applied to membrane. The nitrocellulose membrane was sandwiched between two sheets of photocopy machine acetate and taken to a dark room. Under red light, the membrane was placed in a cassette box and exposed to photographic film for the detection of chemiluminescent signal. Typically, film was left exposed for 2 minutes, however the exposure time was altered accordingly with each nitrocellulose membrane development: the aim was to achieve clear, strong bands with limited background noise on the film.

Following exposure in the cassette box, the hyperfilm was placed in a tray of photographic developer and gently agitated until bands are seen. The film was removed immediately from the developer and dipped/rinsed in water to remove developer, then placed in a tray containing the fixer to prevent further band development. The film was gently agitated in the tray until clear. Once clear, the film was rinsed with tap water, it was hung by a clip on a line until completely dry.

2.3.8 Stripping the membrane

Table 2.3.11 Reagents for stripping the membrane

Reagents	
PBS-Tween	500µl of Tween20 in 1L of PBS
Stripping Buffer	Restore ™PLUS Western Blot Stripping Buffer (Thermo Scientific UK)
Secondary Antibody	25% (v/v) foetal calf serum (FCS) in PBS-Tween with Antibody.

To strip the nitrocellulose membrane for re-probing of a different protein of interest, the membrane was incubated in stripping buffer for 20 minutes and agitated at room

temperature. Stripping buffer was removed and membrane was washed 3 times for 5 minutes in PBS-Tween. Membrane was then re-incubated in a 10ml solution of secondary antibody and agitated for 1 hour. Secondary antibody is removed and membrane washed 3 times for 5 minutes and a final wash of 15 minutes. The membrane was developed to check for any remnant bands from previous probing. A clear film with no bands should appear, indicating that the previous primary antibody has been removed and the membrane is ready for re-probing. Typically, membranes were stripped and re-probed a maximum of two times.

2.3.9 Densitometric analysis.

A digital copy of the film was acquired by scanning the film. Alternatively, the film was placed on a lightbox in a dark room and a bird's eye digital photograph was taken using a Canon650D (18 megapixels), or a OnePlus6t (20 megapixels). Higher resolution images were obtained through digital photography rather than traditional scanners; hence this method was favoured. Images were analysed using Image J (Version 1.52p, NIH, USA).

Mean grey value was measured for each band of interest and the values were inverted (255-x). This was also done for the background and the two inverted values were deducted to give a net value. Net values for the band of interest were expressed as a ratio of Desmin which acts as a loading control, to give a final relative value. Hence:

$$\text{Final value} = \frac{(255 - \text{Protein X}) - (255 - \text{Background of Protein X})}{(255 - \text{Desmin}) - (255 - \text{Background of Desmin})}$$

For cleaved proteins of Nav1.8, each relevant band was analysed and the density per area was calculated. The net value was achieved by totally the density of all the bands and dividing them by the total area. Final values were achieved by normalising to desmin as above.

2.4 Method development

2.4.1 Optimisation of protein loading

To identify the ideal amount of protein to load to the wells which offer consistently desirable blots, three increasingly volumes of sample from the same patient, therefore three increasingly quantities of protein sample were loaded into adjacent wells and western blotted Figure 2.4.1. Other than increased volume=increasing protein quantity everything else remained the same: included using the same patient tissue for all 3 loaded samples, the membrane was equally submerged in antibody concentration of 1:500 and exposed to 10 minutes in the light box. The volume of 50µl produced extremely faint lines which would not have been reliable to analyse, however 100µl & 150µl both produced bands reliably. The lane with 150µl though produced the strongest bands required high volumes of sample which risked going through a patients sample quickly. Also, higher protein concentrations generally had a darker lane background, and this was considered may skew the analysis by blurring the boarders of the desired bands. As such, 100µl was selected as the optimum amount of volume to load as the heavy bands were clearly visible against the background, but with less background staining of the lane and less false bands appearing on the blot.

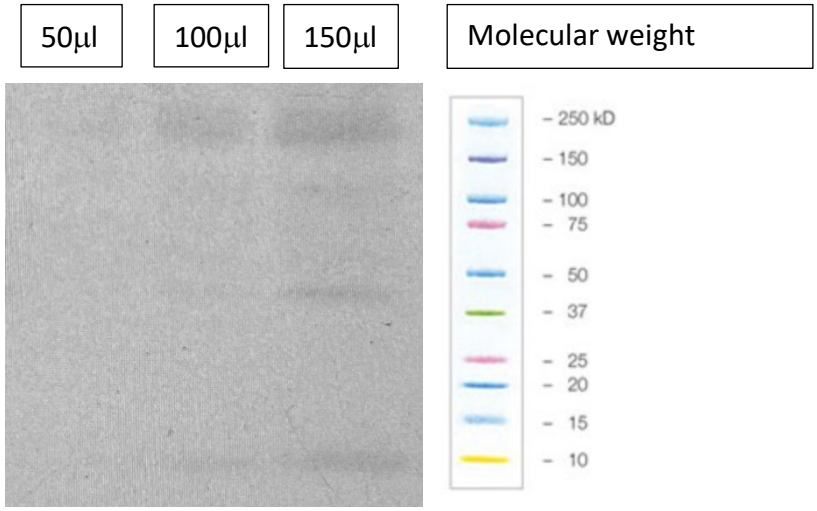

Figure 2.4.1 Optimisation of protein loading

Western blot of $Na_v1.5$ on human right atrial appendage from a single patient sample. Each lane was loaded with incrementally higher volumes, therefore incrementally higher quantities of protein; 50µl on the left, 100µl in the middle, 150µl on the right. The membrane was probed with a concentration of 1:500 of $Na_v1.5$ antibody. The film was exposed under the light box for 10 minutes.

2.4.2 Optimisation of antibody concentration

The next phase of optimisation experiments involved identifying which concentration of antibody to use for probing the membrane. To do this, a 100µl from a single patient (as determined in section Optimisation of Protein Loading) was loaded into pairs of wells as duplicate samples, three times as shown in Figure 2.4.2 and Figure 2.4.3 . Once protein transfer had taken place onto a membrane, the membrane was cut into 3 portions to create mini blots of duplicate sample. Each mini blot was probed using gradually decreasing concentration of antibody from 1:250, 1:500 and 1:750. Once the membranes were ready for development the mini blots were recombined to their original format and exposed under the light box for 10 minutes.

2.4.2.1 Na_v 1.5

The 1:250 ratio offered dense bands with a very murky, overexposed background hence this option was excluded. The 1:750 ratio produced bands however they were extremely faint and would be difficult to distinguish in a patient with low expression of the protein, this option was also excluded. The 1:500 ratio resulted in clear bands at the expected molecular weight without the murky background, and was the ratio used in in future work.

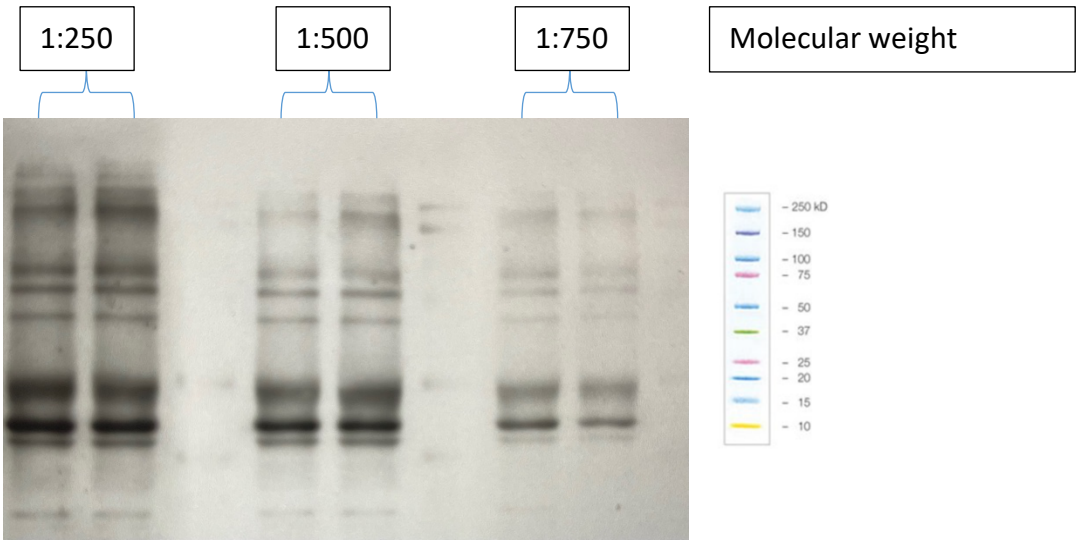

Figure 2.4.2 Optimisation of Na_v1.5 antibody concentration

Western blot of human right atrial appendage from a single patient. Each lane was loaded with 100μl of protein from the same sample. The membrane was divided into 3 sections containing 2 identical lanes in each section, creating mini blots. Each mini blot was probed with different concentration of Nav1.5 antibody; 1:250 on the left, 1:500 in the middle, 1:750 on the right. The developed film of membranes was re-joined and viewed.

2.4.2.2 Nav 1.8

In the optimisation blot for $Na_v1.8$, all 3 concentrations produced strong visible bands. The ratio 1:500 was selected as the optimum due to reduced visibly of secondary bands. Interestingly, the $Na_v1.8$ antibody took significantly less time in the light box to appear. The exposure time was gradually reduced until an optimum of 1 minute exposure produced the most consistent, cleanest bands.

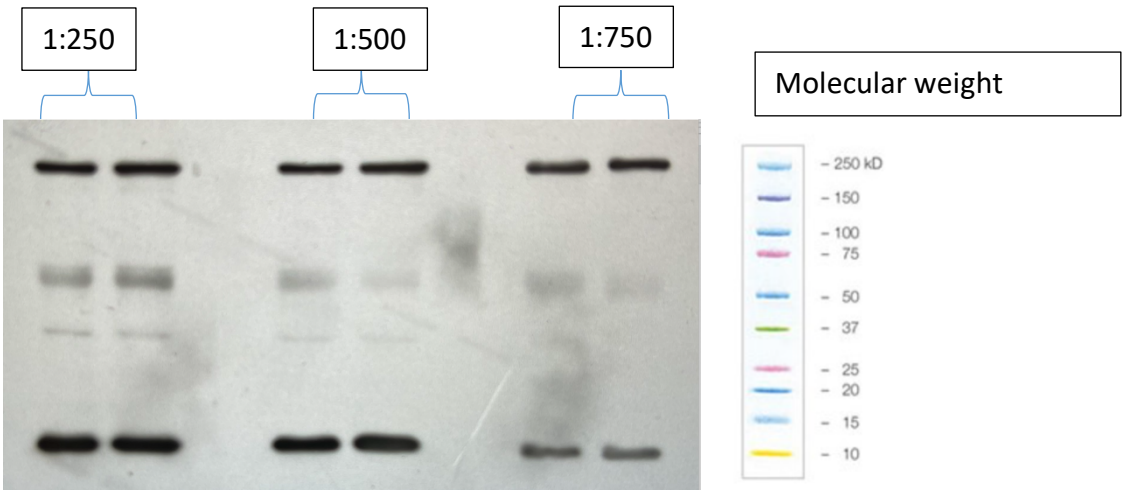

Figure 2.4.3 Optimisation of $Na_v1.8$ antibody concentration

Western blot of human right atrial appendage from a single patient. Each lane was loaded with 100µl of protein from the same sample. The membrane was divided into 3 sections containing 2 identical lanes in each section, creating mini blots. Each min blot was probed with different concentration of Nav1.8 antibody; 1:250 on the left, 1:500 in the middle, 1:750 on the right. The developed film of membranes was re-joined and viewed.

2.4.3 Identifying bands of interest & proof of antibody binding

Prior to analysis of bands to determine protein expression, the specific bands of interest. To do this, we used the manufacturers antigenic peptide for the specific primary antibody. The antigenic peptide acts as a competitive blocker of the primary antibody (1 ug peptide per 1 ug antibody for pre-adsorption for all Alomone antibodies), in this case

the sodium channel antibody, we expect protein-specific bands to disappear on a blot where the antigenic peptide was pre-incubated with the primary antibody, in comparison with a normal blot probed with same concentrations of primary and secondary antibody alone. Furthermore, we set out to prove the primary antibody would successfully bind with specific proteins on the membrane as well as the secondary antibody to emit the signal required to detect bands at the correct molecular weight.

Four lanes of an SDS-Page gel were loaded with 100μl of protein from a single patient. Following electrophoresis and protein transfer onto the nitrocellulose membrane, the membrane was cut into individual lanes and incubated in different solutions; (A) primary antibody only, (B) secondary antibody only, (C) primary antibody then conjugated to secondary antibody, and (D) primary antibody pre-incubated with antigenic peptide then conjugated secondary antibody. The developed film of membranes was re-joined and viewed.

2.4.3.1 $Na_v1.5$

Figure 2.4.4 illustrates the method development data with regards to the $Na_v1.5$ antibody. As expected, the lanes probes with only the primary, or only the secondary antibody, produced no visible bands (Figure 2.4.4 A & B). The primary antibody carries no fluorescent signal alone, so even though it will bind to the proteins on the membrane, those proteins are undetectable. Probing with the secondary antibody only also does not produce bands as it does not bind to the membrane due to the lack of primary antibody and it is simply get washed away. Figure 2.4.4C illustrates the correct methodology as when the membrane was probed with primary antibody which then conjugated to the secondary antibody bands appeared on the film at the correct

molecular weight as per manufacturer's datasheet. Figure 2.4.4D illustrates the outcome of exposure to the antigenic peptide as the specific bands are absent: there were 3 zones where we saw bands disappear completely 250kD, ~60kD and 25kD. Sodium channels are heavy proteins with a molecular weight of 260kD, hence the disappearing bands at the top of the lane are consistent with what we would expect in identifying these proteins, and these bands were selected for analysis. Those bands visible and faint in Figure 2.4.4 D are non-specific bands.

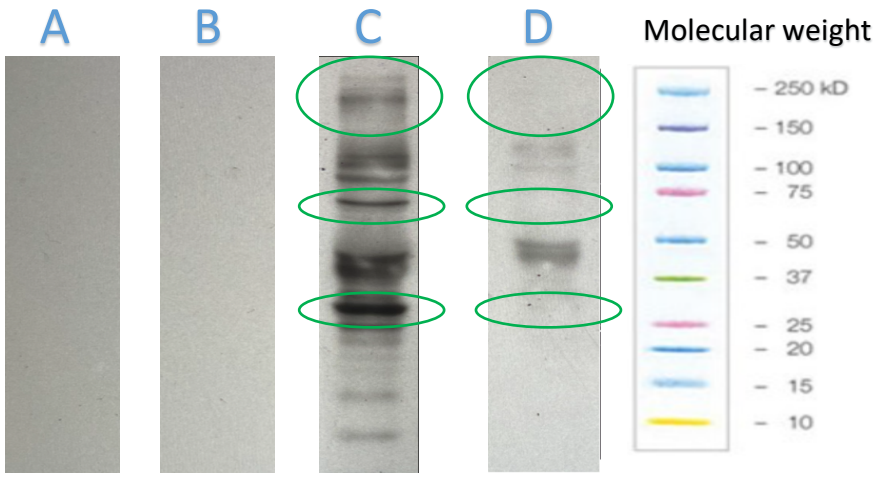

Figure 2.4.4 Antigenic peptide experiment for $Na_v1.5$

Panels A-D shows membranes with varies combinations of antibody. **A**, primary Nav1.5 antibody only. **B,** secondary antibody only. **C,** primary and secondary antibody. **D** competitive inhibition of primary antibody via antigenic peptide pre-adsorption. Green ovals highlight the region where specific protein bands usually appear (panel C) and disappeared using the antigenic peptide (panel D).

2.4.3.2 $Na_v1.8$

Figure 2.4.5 Illustrates the results of the antigenic peptide experiment for $Na_v1.8$ antibody. As expected, the lanes probes with only the primary, or only the secondary antibody, produced no visible bands (Figure 2.4.5 A & B). Figure 2.4.5 C illustrates the correct methodology as when the membrane was probed with primary antibody which

then conjugated to the secondary antibody bands appeared on the film at the correct molecular weight as per manufacturer's datasheet: We achieved two clear bands at 250kD and 10kD.

Figure 2.4.5 D illustrates the outcome of exposure to the antigenic peptide as the specific band was absent at 250kD consistent again with sodium channels with a molecular weight of 260kD. Hence the disappearing bands at the top of the lane was consistent with what we would expect in identifying these proteins and this band was selected for analysis. The lower 10kDa band was non-specific.

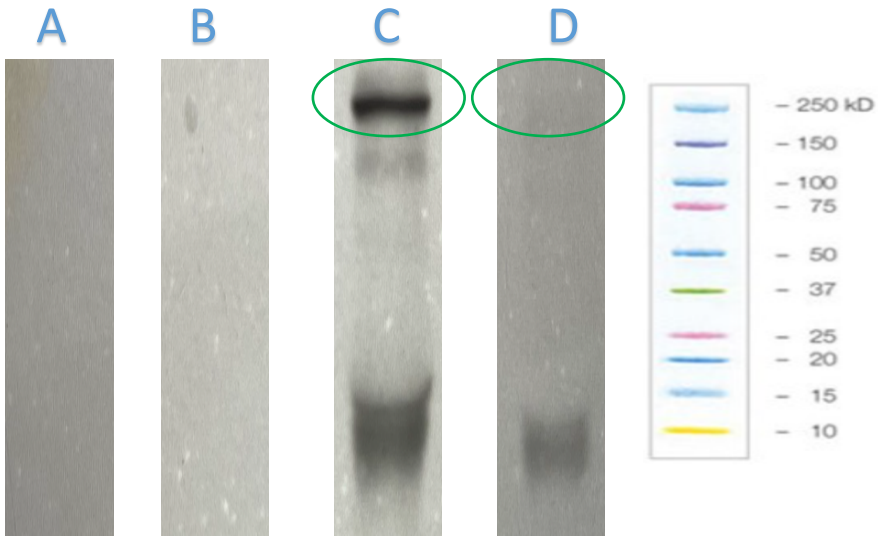

Figure 2.4.5 Antigenic peptide experiment for $Na_v1.8$

Panels A-D shows membranes with varies combinations of antibody.
A, primary Nav1.5 antibody only. **B,** secondary antibody only. **C,** primary and secondary antibody. **D** competitive inhibition of primary antibody via antigenic peptide pre-adsorption. Green ovals highlight the region where specific protein band usually appear (panel C) and disappeared using the antigenic peptide (panel D).

2.5 Immunocytochemistry

2.5.1 Cryosectioning

As described previously, tissue for sectioning was mounted onto a cork disk using Tissue-Tec OCT gel (ensuring complete coverage of the tissue) and frozen in cooled isopentane. A Microm HM505E cryostat (Microm, Germany) was used to achieve frozen sections. The cryostat was set to -20^{o}C and the tissue was sliced at 10µm thickness. Frozen tissue sections were collected from the cryostat with glass polysine slides. Glass slides containing tissue were stored at -80^{o}C.

2.5.2 Immunostaining

Table 2.5.1 Reagents & equipment used in immunostaining

Reagents & Equipment	
Wash	PBS (Pierce UK)
Fixative	4% ($^{v}/_{v}$) Paraformaldehyde (PFA) in PBS (Sigma-Aldrich, UK)
Detergent	0.05% ($^{v}/_{v}$) Triton X-100 in PBS (Sigma-Aldrich, UK)
Blocker	25% ($^{v}/_{v}$) Foetal calf serum (FCS) in PBS (Hyclone Perbio, USA)
Slides	Polysine glass slides (Thermo Scientific UK)
Resin Pen	ImmEdge Hydrophobic Pen (Vector Lab. UK)
Mounting medium	Vectashield (Vector Lab. UK)
Humidity box	Black humidity box with lid (Fisher Scientific UK)
Wheat Germ Agglutinin (WGA)	Rhodamine wheat germ agglutinin binds to membrane glycoproteins N-acetylglucosamine. Diluted to 1:1000 (Vector Lab. USA)

Table 2.5.2 Primary antibodies used in immunostaining

Antigen	1° Antibody	Concentration	Dilution	Manufacturer	Host	Reactivity	Dilutant
$Na_v1.5$	Anti $Na_v1.5$	0.8mg/ml	1:50	Alomone, Israel	Rabbit	Human, rat and mouse	25% ($^v/_v$) Foetal calf serum (FCS) in PBS
$Na_v1.8$	Anti $Na_v1.8$	0.8mg/ml	1:50	Alomone, Israel	Rabbit	Human, rat and mouse	25% ($^v/_v$) Foetal calf serum (FCS) in PBS

Table 2.5.3 Secondary antibodies used in immunostaining

2° Antibody	Immunogen	Dilution	Manufacturer	Host	Reactivity
Alexa Flour 488 F(ab') 2 Fragment of goat anti-rabbit IgG	IgG(Rabbit)	1:1000	Invitrogen by Thermo Scientific UK	Goat	Rabbit

Immunocytochemistry of patient tissue sections was used for determining relative protein quantity and to view subcellular spatial localisation. Slides were removed from -80^{o}C freezer and allowed to slightly warm for around one minute. Condensation was removed using blue laboratory tissue paper. Resin pen was used to draw a hydrophobic ring around each section. Tissue was fixed using the fixture solution for 20-40 minutes depending on the patient's age who donated the tissue and length of time stored in freezer. The PFA solution was removed, and slides washed 3 times for 10 minutes with PBS. Following this, sections for incubated in detergent solution for the same length of time as the fixative. The slides were washed again 3 times for 10 minutes with PBS. Tissue sections were incubated for a minimum of 40 minutes, up to 2 hours in the blocking solution to ensure non-specific binding sites were blocked with protein. Primary antibodies were diluted in blocking solution at a ratio 1:50. Slides were incubated in the primary antibody solution overnight in a humidity chamber at 4^{o}C.

Primary antibody solution was reclaimed and stored. Tissue sections were washed 3 times for 10 minutes in PBS. Slides were incubated for 1 hour in the dark with secondary antibody at a 1:1000 dilution in blocking solution and WGA. Secondary antibody was reclaimed, and slides were thoroughly washed 4 times for 15 minutes. Slides were mounted with vector shield and a glass cover slip was sealed in place with nail varnish.

It should be noted that the same primary antibodies are used for both protein analysis techniques, thus given confidence in the specificity of the antibody binding to the protein of interest. That is western blot bands are at the correct and expected molecular weight, and in immunocytochemistry the binds protein location is as expected with the protein of interest.

2.5.3 Confocal microscopy

Following the preparation biological samples, slides were taken for analysis under the confocal microscope. Fluorescence of VGSCs was observed under the 488 nm wavelengths, appearing in green, and rhodamine-labelled WGA was observed with the 561 nm wavelengths appearing in red. The two images were then superimposed to offer a view of the fibrous cell membranes along with the striated staining of VGSCs of interest.

Chapter 3

Age-associated remodelling of human cardiac sodium channels predispose the elderly heart to atrial fibrillation

Chapter 3 Age-associated remodelling of human cardiac sodium channels predispose the elderly heart to atrial fibrillation

3.1 Introduction

It is well understood that the prevalence of AF increases with age, with around 80% of cases identified in the over 65 population (England, 2017a). A comprehensive analysis over 50-year trends highlights ageing as the most prominent risk factor (Schnabel et al., 2015). These findings have been consistently supported over the last 15-years by epidemiological studies (Murphy et al., 2007; Rodriguez et al., 2015; Weng et al., 2017; Salih et al., 2021). Clearly, the effects of ageing on the heart predispose the elderly to arrhythmia. This is likely a consequence of age-associated remodelling; adaptions to structure and function of the heart due to the insults of disease, as well as the body's changing physiological demands as it grows older.

The heart is subject to four forms of remodelling; electrical, ionic, functional and structural (Pathak et al., 2013). Remodelling of the heart and AF are closely intertwined entities; the ageing heart promotes conditions for arrhythmia to occur, as well as the arrhythmic heart leading to further abnormalities within these four categories (Nattel et al., 2008). In this chapter we will explore the effects of ageing on the heart which promote AF, focusing more specifically on the ionic remodelling of voltage-gated sodium channels.

3.1.1 AF and the ageing heart

As we age, the heart is prone to structural remodelling in the form of fibrosis which creates myocardial stiffening (Tsuji et al., 1996). This in turn causes a functional deterioration in the heart's pump mechanics increasing the likelihood of failure. These fibrotic changes disrupt the normal continuity of bundle fibres, impairing cell-to-cell communication, hence compromising intercellular conduction (Kistler et al., 2004) (Burstein et al., 2009). This disturbance of the heart's standard electrophysiology is a primer for AF to occur as discussed in Chapter 1 section 1.4 & 1.5.

The ageing heart further undergoes electrophysiological remodelling which is at the core of the pathogenesis of AF. The elderly heart has been demonstrated to lose automaticity of the SAN due to poor excitability of SAN myocytes (Larson et al., 2013). The compromise of normal pacemaker function underpins part of the development of ectopic foci throughout the atrial myocardium, a pathognomonic feature of AF, at which point the electrical activity within the atria becomes dysregulated and chaotic.

3.1.2 Remodelling of voltage-gated sodium channels

Ionic remodelling describes changes in ion channel expression and thus their function. Pathological currents which are not observed during a normal action potential exert their effect on the cardiomyocyte creating electrical instability, altering the typical morphology of the action potential. $Na_v1.5$ is the predominant cardiac sodium channel isoform, responsible for the vast majority of sodium ion influx during the primary depolarisation phase of the action potential – the fast sodium current (Kaufmann et al., 2013). Downregulation with age (or faulty expression) of $Na_v1.5$ channel directly

contributes to arrhythmogenesis through shortening of the action potential upstroke and impairing the velocity of depolarisation (Figure 3.1.1) thus compromising the myocytes capacity for electrical conduction (Wu et al., 1997; Huang et al., 2015).

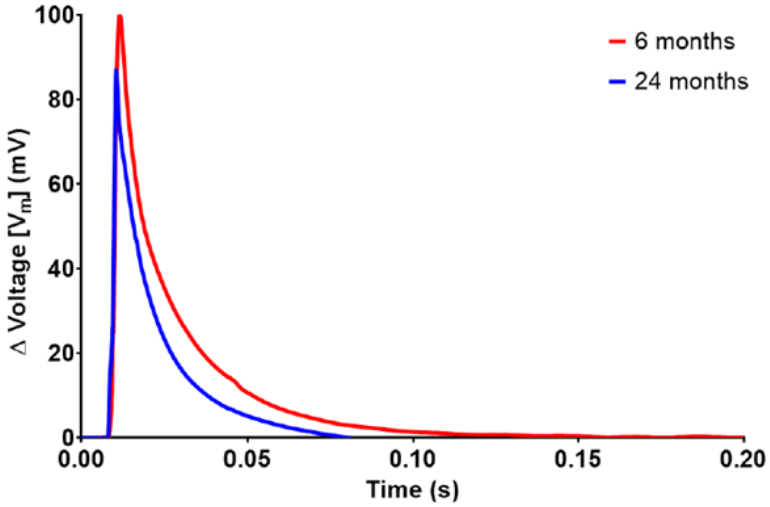

Figure 3.1.1 Action potential recordings from rat hearts

An illustrative example of recordings were taken from cells derived from rates aged 6-months (red) and 24-months (blue). Aged cells demonstrate a notably diminished AP velocity. *Data provided by SA Jones.*

This would align with studies which have identified reduced expression and faulty gating of the $Na_v1.5$ channel-due to loss-of-function mutations of the SCN5A gene- as being a principal genetic determinate for the development of AF (Dubois & Bergman, 1975; Zeng et al., 2013).

As well as being the responsible for phase 0 of the AP, VGSCs also contribute to the maintenance of electrical stability of the myocyte by regulation of the plateau phase and refractory period through the slow sodium current (Burashnikov & Antzelevitch, 2013; Horvath et al., 2013; Rivaud et al., 2018b). The sodium channel responsible for the slow sodium influx is $Na_v1.8$ (Macri et al., 2018a), and this isoform has been implicated in both animal and human models as the culprit of pathological late sodium currents and consequential arrhythmia (Yang et al., 2012a; Savio-Galimberti et al., 2014; Dybkova et

al., 2018; Rivaud et al., 2018b). This has drawn the attention of researchers in targeting the $Na_v1.8$ blockade as a potential therapy for AF (Chen et al., 2016). The literature has consistently alluded to a prolonged refractory period and AP duration-due to aberrant late sodium currents as being central to the pathogenesis of arrhythmia the elderly mammalian heart (Walker et al., 1993; Anyukhovsky et al., 2005; Huang et al., 2015).

3.2 Hypothesis

We hypothesize with increasing age of the patient that expression of the isoform $Na_v1.5$ will decline, conversely the isoform $Na_v1.8$ will increase expression within the right atrial appendage, which will lead to a predisposition of atrial fibrillation in the heart of the elderly patient.

3.3 Methods

In order to quantify protein expression of voltage-gated sodium channel isoforms, western blotting was utilised as described in Chapter 2. Specific bands for each isoform of interest were identified using the antigenic peptide experiments (discussed in the previous chapter) and analysed using Image J. Graphs were plotted using Microsoft excel with data arranged in order of individual chronological patient. Patients with AF were excluded from this analysis to focus specifically on the effects of aging on VGSC expression. Statistical analysis to determine significance was further performed using regression, ANOVA, Student's t-test and means ± SEM. Graph pad PRISM was used to calculate the P value of the graph and determine the significant of the slope from horizontal. Confocal microscopy was utilised, as described in Chapter 2, to observe altered location and expression of VGSC isoforms expression within atrial

cardiomyocytes. A total of 26 patients were recruited for this study aged 47-83 (mean age of 68).

3.4 Results

3.4.1 $Na_v1.5$ isoform expression in the heart tissue samples

Expression of the Nav1.5 was shown by use of an antigenic peptide to be a doublet of bands between 220-250kDa (Figure 3.4.1). Other bands not removed by competitive inhibition with the peptide were referred to as non-specific binding, thus not quantified in this study. Desmin expression was shown by one band at 52KDa – the loading control and therefore housekeeper to ensure no error due to inconsistent protein loading of the gel.

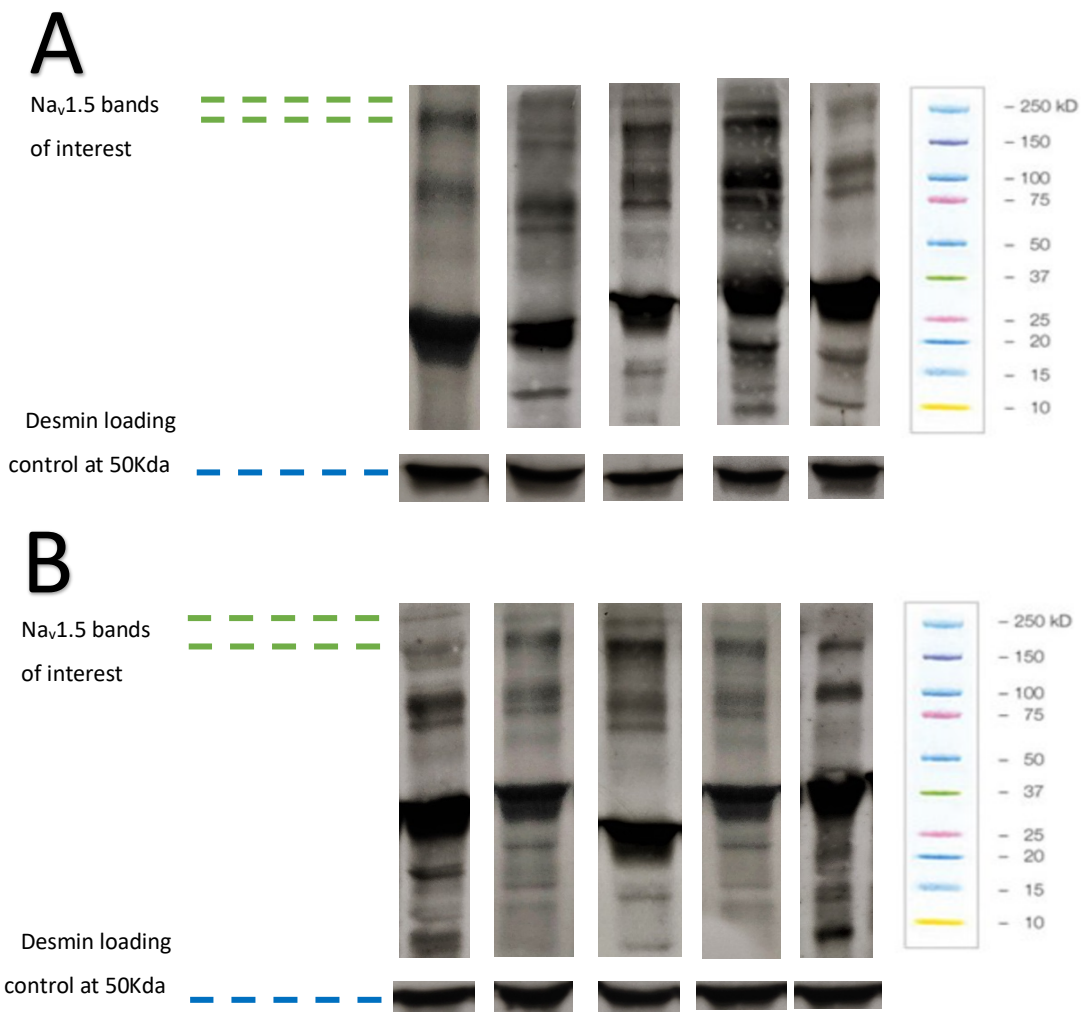

Figure 3.4.1 Western blots of Nav1.5 expression in hearts derived from younger patients (A) compared with older patients (B)

Green dashes represent bands of interest. Blue dashes highlight desmin loading controls Panel A, Ages from left to right: 47, 49. 51, 53, 57 years. Panel B. Ages from left to right: 76, 77, 79, 80, 83

3.4.2 $Na_v1.5$ isoform expression correlation with age

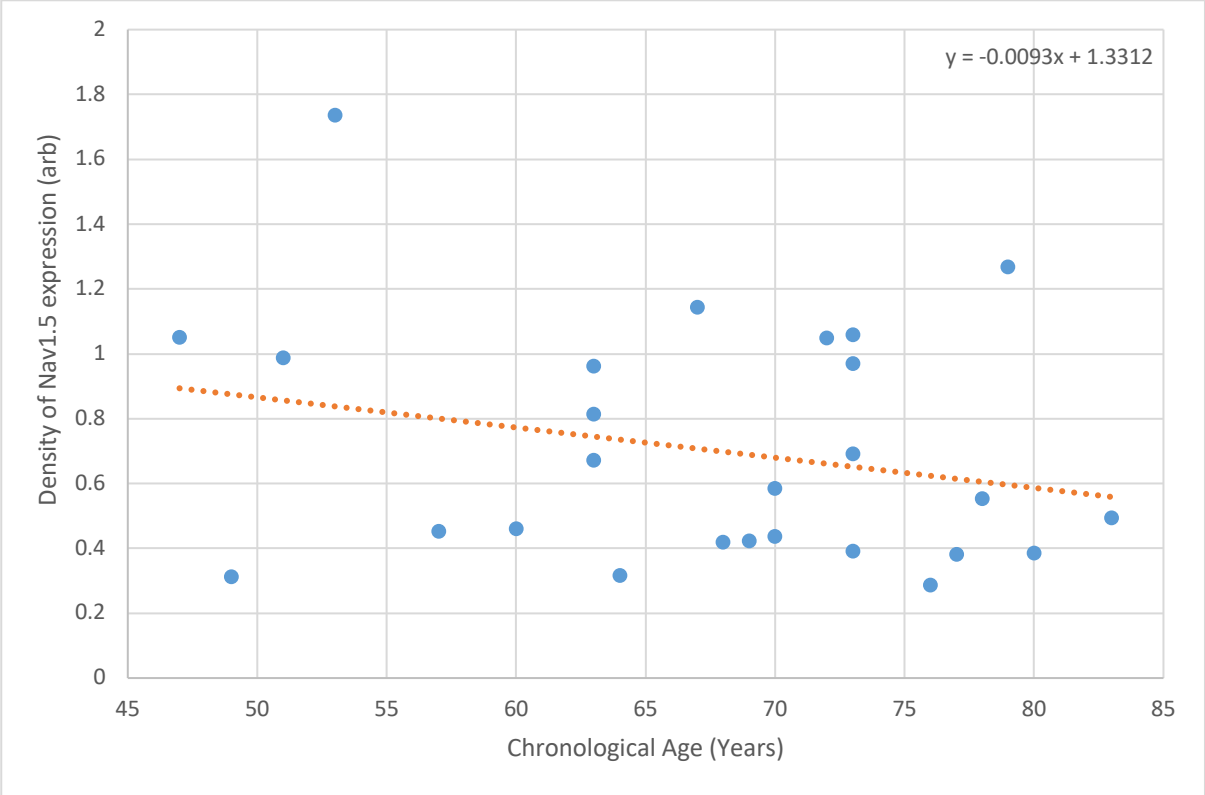

Figure 3.4.2 Negative correlation between increasing age and density of Nav1.5 expression

The band density of Nav1.5 protein expression were quantified and plotted against the patient's chronological age. This scatter gram presents a negative correlation between Nav1.5 expression and age (Pearson's correlation coefficient -0.25, n=26; R^2 = 0.0624, P= 0.2 with a slope deviation insignificant from 0).

Age-associated decline of $Na_v1.5$ in the human heart has been observed through the analysis of protein expression via western blot Figure 3.4.1. A downward trend in the expression of $Na_v1.5$ with age was observed in 26 patients between the ages of 47-83 with a Pearson's correlation coefficient of -0.25 Figure 3.4.2. Further study of this correlation was performed through regression analysis, and showed the gradient demonstrates a decline of 9% Nav1.5 protein per decade of ageing.

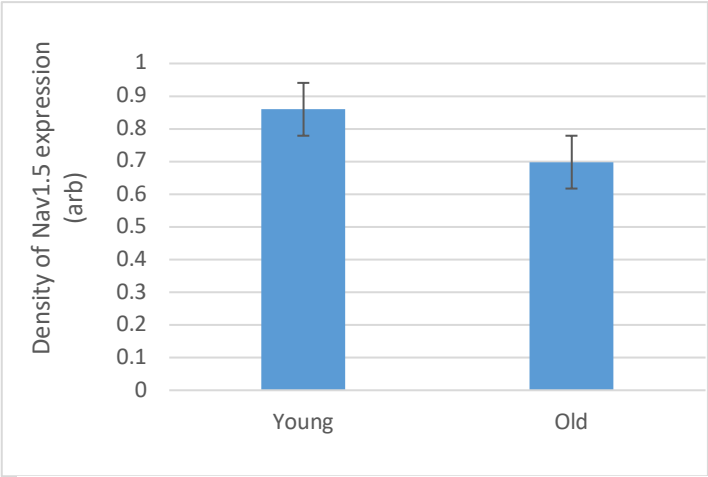

Figure 3.4.3 Average density of $Na_v1.5$ expression between young and old

Blots from the youngest 10 patients (ages 47-64) were averaged and compared with average of the Nav1.5 expression from the oldest 10 patients (ages 72-83). Student's T test, P=0.18.

When the difference in age was exaggerated by comparing the oldest 10 of the group with the youngest 10 of the group a 18.8% drop in the expression of $Na_v1.5$ was observed in the older group with P=0.18 Figure 3.4.3.

3.4.3 $Na_v1.5$ isoform expression located within the human atrial tissue

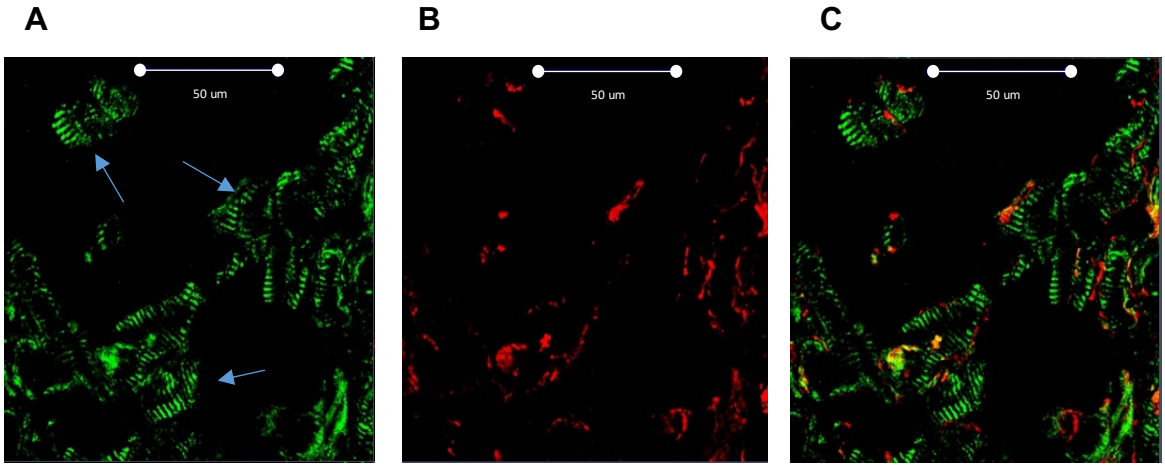

Figure 3.4.4 Confocal microscopy images of Nav1.5 in a patient aged 47

Panel **A,** Myocytes probed for Nav1.5 channels Alexa flour 488 showing high uptake at t-tubules in a striated pattern as pointed out by the arrows. Panel **B,** WGA staining demonstrating fluorescence of the cell walls. Panel **C,** Composite of the A+B images of WGA and Nav1.5. Scale bars at 50um.

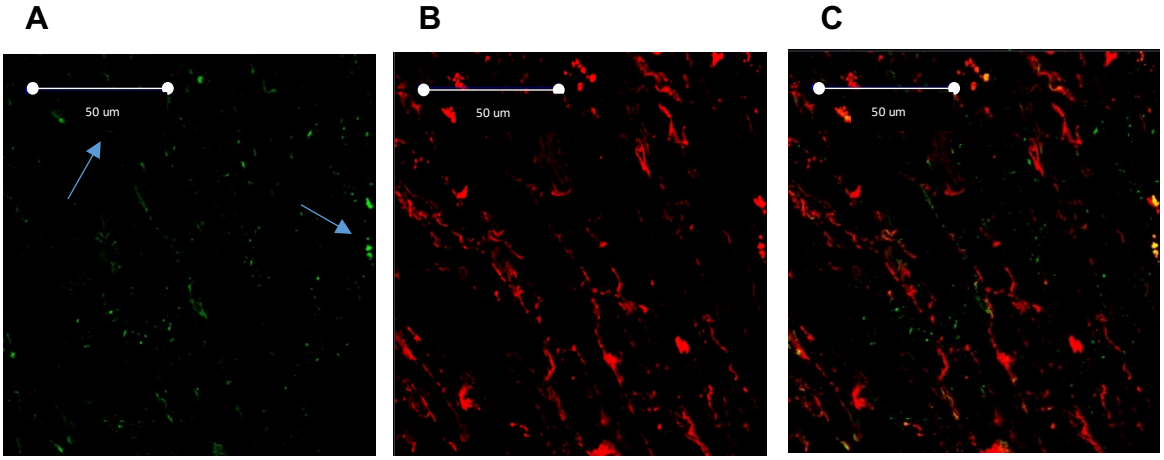

Figure 3.4.5 Confocal microscopy images of Nav1.5 in a patient aged 83

Panel A, Myocytes probed for Nav1.5 channels Alexa flour 488 showing poor uptake and weak due to reduced expression of protein. Panel B, WGA staining demonstrating fluorescence of the cell walls. Panel C, Composite of the A+B images of WGA and Nav1.5. Scale bars at 50um.

The loss of the predominant cardiac sodium isoform critically alters the cardiomyocytes capability for depolarisation during phase 0 of the action potential. Demonstrating this downregulation in older humans suggests that this ionic remodelling is at the very least influenced by the ageing process and may be a key step in the development of arrhythmia which we know is more prevalent in the older population. This downregulation has also been observed through confocal microscopy as illustrated in Figure 3.4.4 and Figure 3.4.5 through poor fluorescence of the $Na_v1.5$ probe in the older patient.

3.4.4 $Na_v1.8$ isoform expression in the heart tissue samples

Expression of the Nav1.8 was shown by use of an antigenic peptide to be a doublet of bands between 220-250kDa. Other bands not removed by competitive inhibition with the peptide were referred to as non-specific binding, thus not quantified in this study. Desmin expression was shown by one band at 52KDa – the loading control and therefore housekeeper to ensure no error due to inconsistent protein loading of the gel.

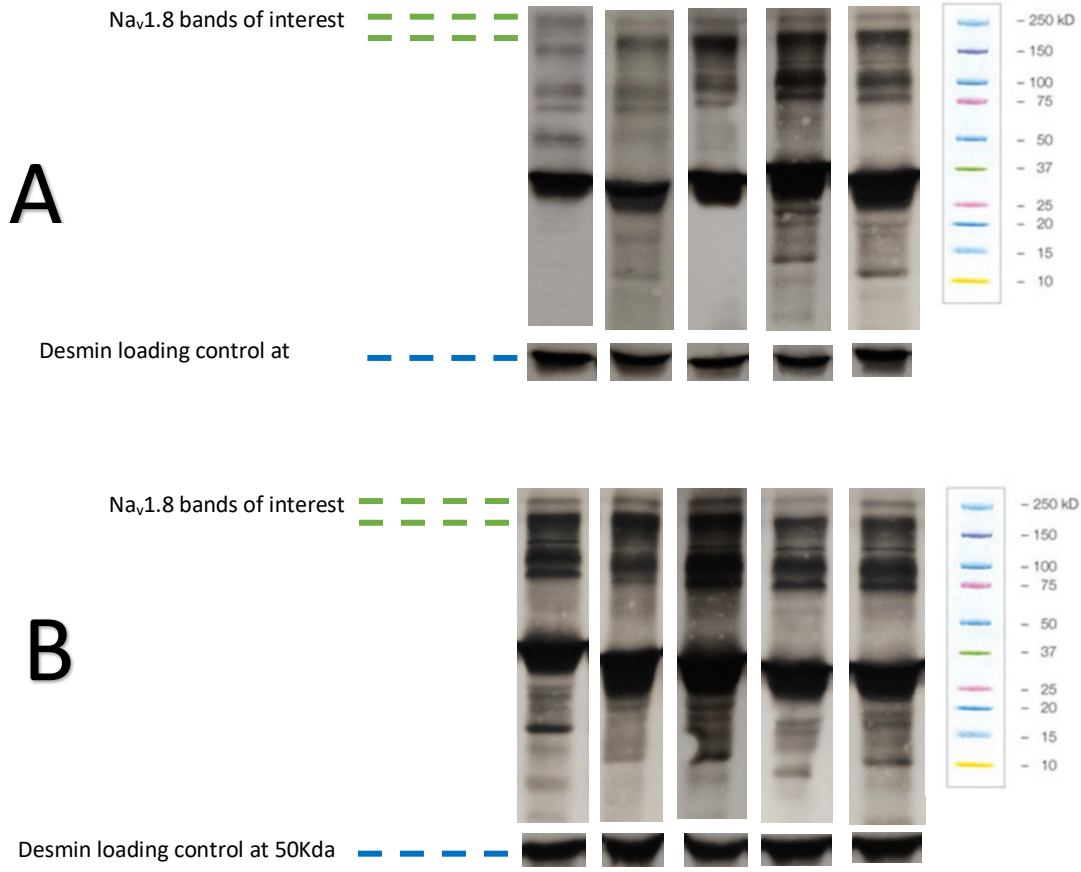

Figure 3.4.6 Western blots of Nav1.8 of younger patients (A) compared to the older patients (B)

Green dashes represent bands of interest. Blue dashes highlight desmin loading control. Panel A, Ages Top from left to right: 47, 49. 51, 63, 64 years. Panel B, Ages Bottom from left to right: 68, 69, 73, 77, 83 years.

3.4.5 $Na_v1.8$ isoform expression correlation with age

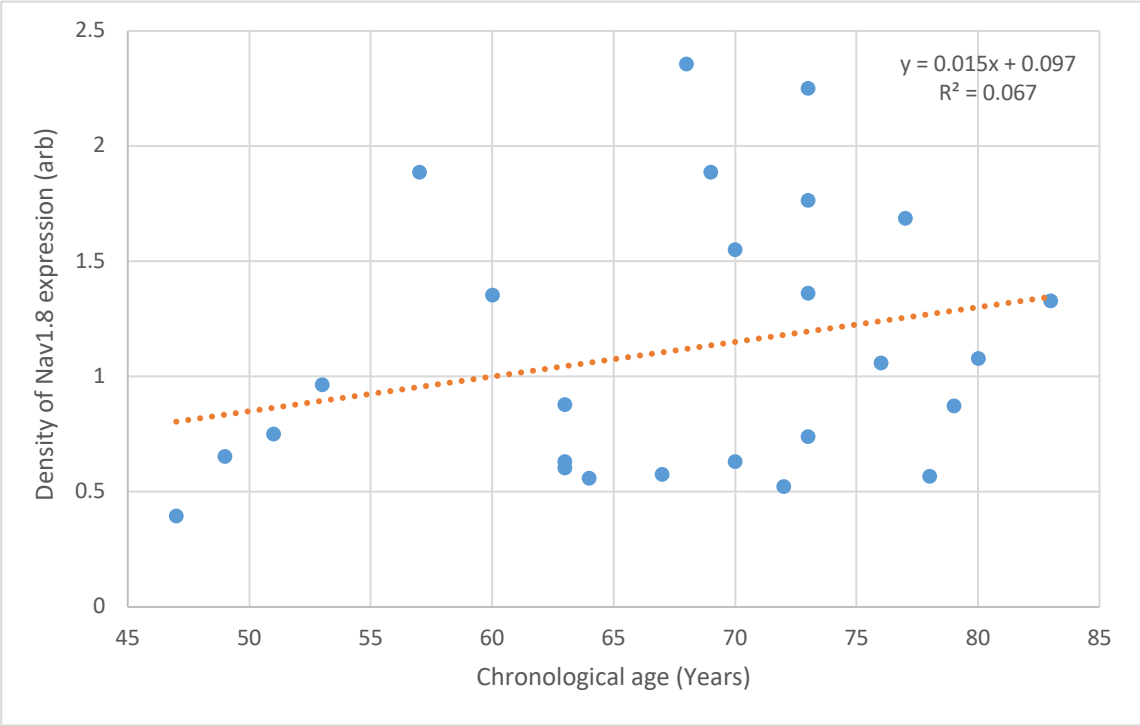

Figure 3.4.7 A positive correlation between increasing age and density of Nav1.8 expression

The band density of Nav1.8 protein expression were quantified and plotted against the patients age (n=26). This scatter gram presents a positive correlation between Nav1.8 expression and age (Pearson's correlation coefficient +0.26). With increasing age, expression of the Nav1.8 protein in the human right atrium is increased.

The line gradient demonstrates a rise of 16% $Na_v1.8$ protein per decade of ageing. With increasing age, expression of the Nav1.8 protein in the human right atrium is increased (n=26; R^2 = 0.067, P=0.21, deviation from 0 not significant).

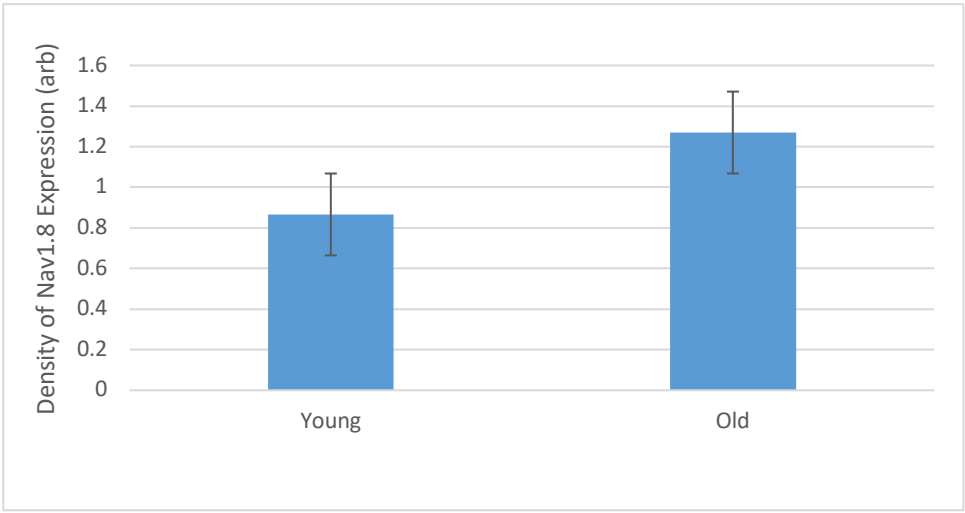

Figure 3.4.8 Average density of Nav1.8 expression of the youngest 10 pts vs the oldest 10 pts

Blots from the youngest 10 patients (ages 47-64) were averaged and compared with average of the blots from the oldest 10 patients (ages 72-83). Older group demonstrated a 32% increase in the density of Nav1.8 expression P= 0.039. Average age of the young group is 59.5, average age of the old group is 75.

Samples from the same patients demonstrated a positive correlation between the density of $Na_v1.8$ expression and age with a Pearson's correlation coefficient of +0.26 Figure 3.4.7. Regression analysis of this trend revealed a P=0.2. When the difference in age was exaggerated by comparing the average density of $Na_v1.8$ expression in the youngest 10 patients with the oldest 10 patients a 32% increase was observed in the older group with a P value of 0.039 Figure 3.4.8. This is statistically significant and hence we can reject the null hypothesis that ageing has no effect on the expression of $Na_v1.8$.

3.4.6 $Na_v1.8$ isoform expression located within the human atrial tissue

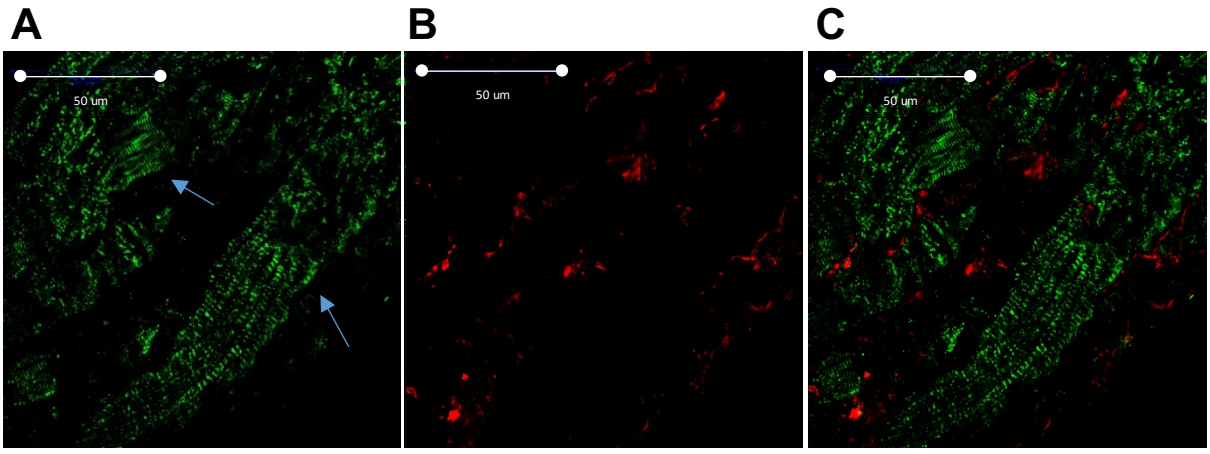

Figure 3.4.9 Confocal microscopy images of $Na_v1.8$ in a patient aged 83

Panel A, Myocytes probed for Nav1.8 channels Alexa flour 488 showing high uptake at t-tubles. Panel B. WGA staining demonstrating fluorescence of the cell walls. Panel C, Composite of A+B images of WGA and Nav1.8. Scale bars at 50um.

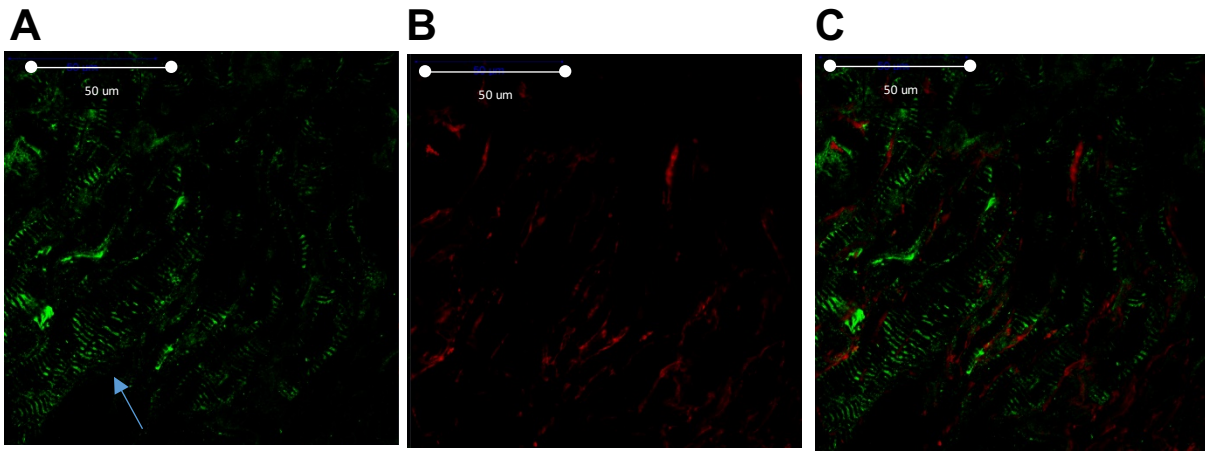

Figure 3.4.10 Confocal microscopy images of $Na_v1.8$ in a patient aged 47

Panel A, Myocytes probed for Nav1.8 channels Alexa flour 488 showing lesser fluorescence. Panel B, WGA staining demonstrating fluorescence of the cell walls. Panel C, Composite of images of WGA and Nav1.8. Scale bars at 50um.

We can appreciate this trend visually through the images of the confocal microscope in Figure 3.4.9 & Figure 3.4.10, with the higher uptake of $Na_v1.8$ in the older patient. This novel demonstration of the upregulation of $Na_v1.8$ in the older human population suggests that the effects of ageing on the human heart may prime it for an arrhythmia to occur, by enhancing the channel which is known to give rise to pathologically enhanced late sodium currents.

3.5 Discussion

3.5.1 General discussion

$Na_v1.5$ is the predominant cardiac isoform, generating the majority of the fast sodium current required for phase 0 depolarisation (Kaufmann et al., 2013). Velocity of depolarisation and action potential upstroke are therefore highly dependent on the abundance and functionality of this channel. Animal models have demonstrated that with increasing age the maximum upstroke velocity and action potential amplitude are diminished (Anyukhovsky et al., 2005; Ahmad et al., 2019c). In the SAN of aged mice, it has been observed that the expression and functionality of certain VGSCs is reduced- though within this study the expression of $Na_v1.5$ was not explored (Huang et al., 2015). From the existing literature, we could infer that one mechanism ageing may have on the impaired capacity of depolarisation in the mammalian heart is the downregulation of $Na_v1.5$. Indeed, Hao et al have suggested-though not directly observed- there may be a reduction of protein expression of $Na_v1.5$ in the hearts of older mammals due to the significant age-associated downregulation of SCN5a mRNA which codes for the protein (Hao et al., 2011). Furthermore, mutations in the SCN5a gene which impair protein

expression of $Na_v1.5$ have been strongly implicit with cardiac arrhythmias including AF (Darbar et al., 2008).

This study is the first to investigate the relationship of $Na_v1.5$ protein expression with age in human hearts. The negative correlation seen in Figure 3.4.2 would be in keeping with the existing literature. When comparing the average density of $Na_v1.5$ in the younger cohort (mean age of 59.5) with that of the older group (mean age of 75) an 18.8% drop in protein expression was observed Figure 3.4.3. Again, though not conclusive this data may imply a relationship between ageing and the direct expression of the cardiac isoform. A decline in protein expression would be consistent with observations that action potential upstroke and conduction velocity is diminished in the older mammalian heart and may be a key process in the evolution of arrhythmia. Reduced protein expression of $Na_v1.5$ has also been observed in human heart failure (Dybkova et al., 2018) and left ventricular hypertrophy (Ahmad et al., 2019b), conditions highly associated with AF as well as ageing..

$Na_v1.8$ is a sodium channel typically localised in the peripheral nervous system (Zimmer et al., 2014). This isoform has been the subject of close study in the context of arrhythmia, as it has consistently been implicated in enhancing the slow sodium current (Yang et al., 2012b; Savio-Galimberti et al., 2014; Macri et al., 2018a; Rivaud et al., 2018a). The slow sodium current regulates the effective refractory period and therefore action potential duration (Biet et al., 2012; Savio-Galimberti et al., 2014). We know that a prolonged action potential duration is an arrhythmogenic substrate, giving rise to afterdepolarisations on a cellular level, and therefore spontaneous ectopic firing on the macroscopic level (Savio-Galimberti et al., 2014; Rivaud et al., 2018a). Targeting the $Na_v1.8$ channel specifically has been shown to terminate the slow sodium current and shown to have profound antiarrhythmic effects. (Yang et al., 2012b). As such, many novel therapeutic approaches have evolved to induce a pharmacological blockade of this channel to terminate arrhythmia including AF (Burashnikov & Antzelevitch, 2013; Burashnikov et al., 2014; Caves et al., 2017; Ellermann et al., 2018; Carstensen et al., 2019). This will be discussed in detail in Chapter 4. At the time of this study and to the best current knowledge, there has been no efforts to investigate the relationship of age and $Na_v1.8$ protein expression in the mammalian heart.

This study has observed a positive correlation with the expression of $Na_v1.8$ protein in the human right atrium with age Figure 3.4.7. When comparing average density of protein between the youngest 10 patients (mean age 59.5) with the oldest 10 patients (mean age 75) a 33% increase of $Na_v1.8$ expression was observed with a P value <0.05. This is a statistically significant result allowing the dismissal of the null hypothesis. This finding consistent with the literature, filling in an important gap of knowledge. We know that ageing increases the likelihood of AF. We also know that the late sodium current

has been implicit in the arrhythmogenic process and increasingly becoming the target of pharmacological intervention to terminate arrhythmia. It would make sense that with increasing age, the expression of this isoform would also increase, enhancing the late sodium current and destabilising the electrical activity of cardiomyocytes through afterdepolarisations. Why ageing would lead to the increasing density of $Na_v1.8$ is not clear and may be the subject of further study. It's possible that this may be a compensatory mechanism for the loss of functional $Na_v1.5$protein in the ageing heart- though this is purely speculative.

3.5.2 Limitations

Firstly, the major limitation of extrapolating these results to the general population is that by the nature of sampling tissue from patients who undergo cardiac surgery, the patients studied have suffered severe insults of cardiac disease which have required a major operation to amend. The disease processes will likely have played a role in shaping the structure and function of these hearts which could skew the data. Furthermore, we do not know what effect the insults of surgery itself may have had acutely to the cellular physiological processes of the heart and how this may affect VGSC expression. Within this experiment ageing alone was considered as the determinant for altered VGSC expression. Other modifiable and non-modifiable factors such as sex, underlying cardiac disease, family history, co-morbidities, medication, and lifestyle may also have a role to play in this process. Unlike animal models, confounding factors are far more difficult to exclude in humans. Therefore, the isolated variable under study here is likely not to be the only influence on protein expression. Furthermore, this study only investigated the relative abundance of protein expression not functionality of protein, channel gating or

the currents they produce. Any inference of the potential arrhythmogenic effect has been drawn based on existing literature which have studied the functional electrophysiology. Finally, this study contains a relatively small sample size of a specific set of patients. For more conclusive results, a larger cohort of patients would be recommended.

Chapter 4

Voltage-gated sodium channel isoforms Nav1.5 and Nav1.8 protein expression in right atrial tissue from patients diagnosed with atrial fibrillation

Chapter 4 Voltage-gated sodium channel isoforms $Na_v1.5$ and $Na_v1.8$ protein expression in right atrial tissue from patients diagnosed with atrial fibrillation

4.1 Introduction

The role of sodium ion channelopathies in the development of arrhythmia is a rapidly evolving field of study. Faulty or altered expression of the cardiac isoform Nav1.5 has an established association with a spectrum of arrhythmias including Long QT syndrome, Bragada's syndrome and atrial fibrillation (Splawski et al., 2002; McNair et al., 2004; Darbar et al., 2008; Bezzina et al., 2013) . Mutations in the SCN5a gene encoding for Nav1.5 exhibit as either gain-of-function or loss-of-function of the channel (Wilde & Amin, 2018). Mutated expressions of Nav1.5, the critical player in depolarisation predispose the cardiomyocyte to electrical instability through pathological gating mechanisms, atypical sodium currents and distinctly abnormal action potential morphology (Darbar et al., 2008). Impaired function of the $Na_v1.5$ channel leads to fewer availability of Na^+ shortening the action potential upstroke impairing the cells capacity for conduction (Ellinor et al., 2008). Gain-of-function mutations on the other hand leads to a prolonged action potential duration which predisposes the cardiomyocyte to EADs & DADs. Both mutations have been observed to manifest in hereditary forms of AF in humans (Darbar et al., 2008; Ellinor et al., 2008; Makiyama et al., 2008).

In this chapter we will explore the relevance of mutated Nav1.5 channels to aid our understanding of sodium currents which may underpin the arrhythmogenic process, and we will discuss how the non-cardiac sodium channel $Na_v1.8$ contributes to these pathological currents increasing the likelihood for arrhythmia to occur. Additionally, we

will compare and contrast the expression of cardiac $Na_v1.5$ and the non-cardiac $Na_v1.8$ sodium channel isoform in the right atrium appendage from patients diagnosed with AF and those in sinus rhythm, whilst discussing clinical relevance of these mechanisms in evolving therapeutic approaches for treating and preventing atrial fibrillation.

4.1.1 Mutations of SCN5a in AF

Gain-of-function mutations in $Na_v1.5$ describe an alteration in the channel's gating mechanism where the sodium current influx is enhanced (Li et al., 2009). This is due to incomplete inactivation or late inactivation of the channel at more depolarized potentials (Li et al., 2009). Failure to completely terminate the current in a timely manner enhances the late sodium current, therefore prolongs the AP duration and sets the cardiomyocyte for afterdepolarisation (Rivaud et al., 2018a; Wilde & Amin, 2018). Furthermore, incomplete inactivation enhances the window current where channels may be reactivated. This presents an avenue for ectopic action potentials to evolve as there is a disruption in the regulation of Na^+ depolarisation. These mechanisms are illustrated & described in Figure 4.1.1.

Loss-of-function mutations describe the reduced expression of *functional* $Na_v1.5$ channels (Guzadhur et al., 2010; Zeng et al., 2013). Mutated channels exhibit a poorly operational voltage sensor domain which take a higher membrane potential to trigger channel activation. Delayed channel activation means fewer Na^+ ions are available at the crucial phase 0 of the action potential (Zeng et al., 2013). This culminates in a diminished AP upstroke and a slower depolarisation of the cell (Zeng et al., 2013; Wilde & Amin, 2018). The slow activation and quick inactivation means that the APD is shortened and

the cell is susceptible to re-excitation predisposing the cardiomyocyte for re-entry wavelets. This process is illustrated by Figure 4.1.2.

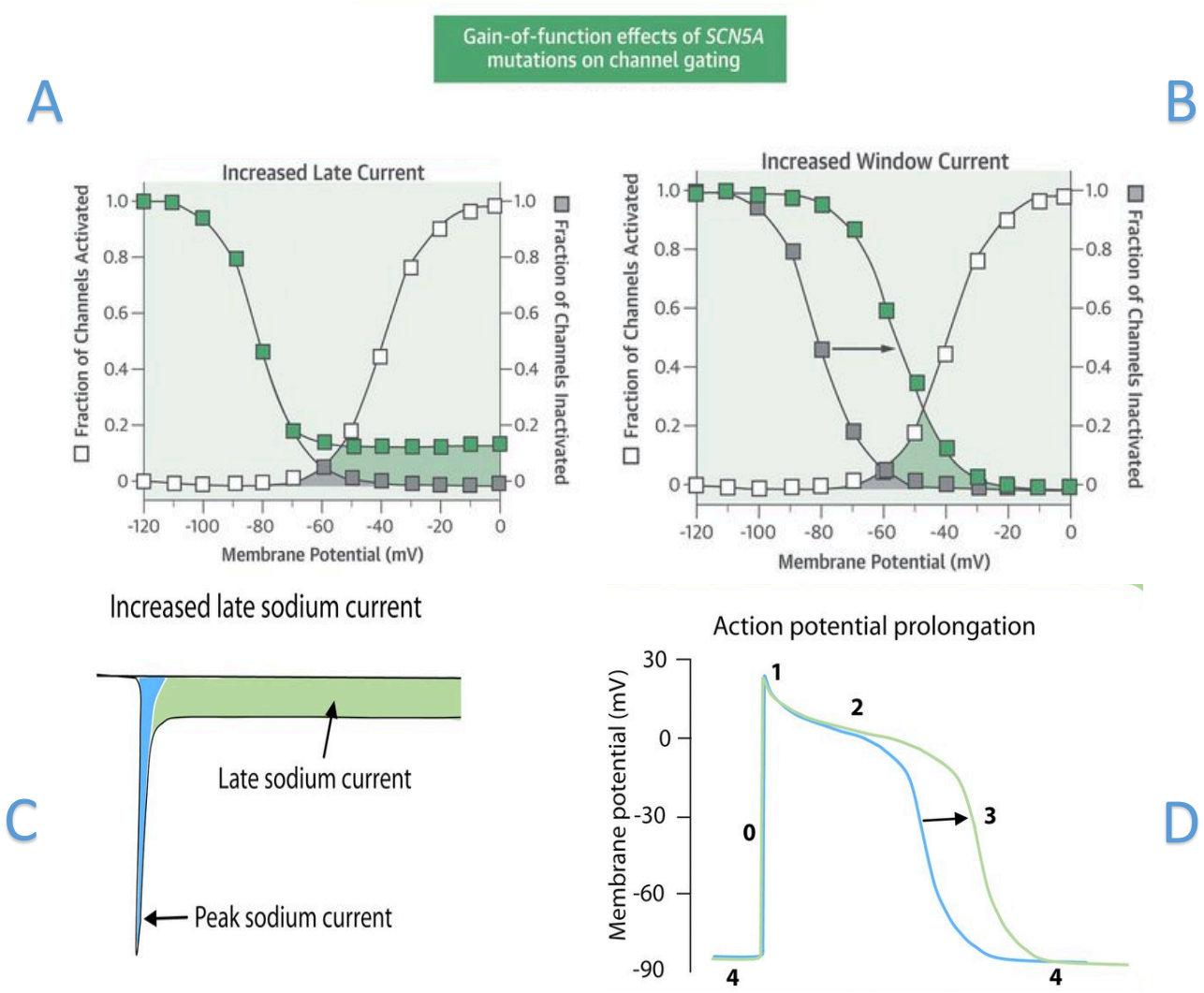

Figure 4.1.1 Gain-of-function effects of SCN5a mutations on channel gating

Panel A and C. Two curves overlapping illustrates the fraction of channels activated (white squares) vs the fraction of channels inactivated (grey squares) across the range of membrane potential in panel A. Green squares represent the channels where gain-of-function mutation as penetrated resulting in incomplete inactivation of sodium channels at a higher membrane potentials. The result is a higher fraction of channels inappropriately activated for a longer period of time, thus creates an enhanced late sodium current as shown by **panel C.**

Panel B. Two curves overlap illustrating the fraction of channels activated (white squares) vs the fraction of channels inactivated (grey squares) across the range of membrane potential. Green squares here demonstrate channels with gain-of-function mutation, where the whole curve has shifted to the right: therefore, a proportion of channels have a delayed inactivation. This increases the window current where channels may reactivate as shown by the dark green shading under where both curves overlap.

Panel D. Normal action potential illustrated in blue. Green curve demonstrates the prolonged plateau and repolarisation phases which come because of late inactivation and enhanced late sodium currents. During this prolonged phase 2 & 3, afterdepolarisations may occur disrupting the cells electrical stability.

Adapted from (Wilde & Amin, 2018)

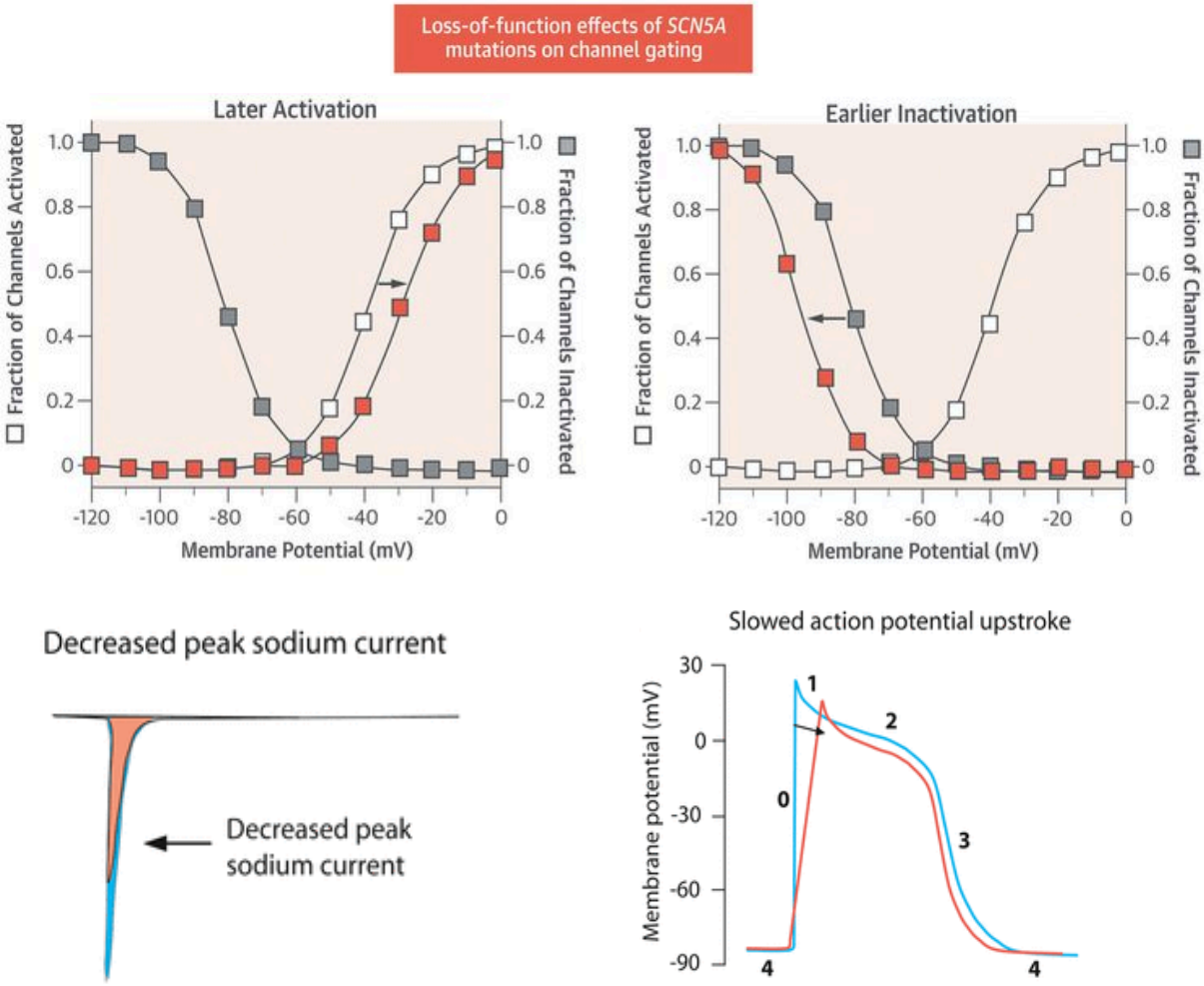

Figure 4.1.2 Loss-of-function effects of SCN5a mutations on channel gating

Panel A. Fractions of channels activated represented by the curve with the white squares and fraction of channels inactivated represented by the curve with the grey squares. The orange squares represent channels in which the loss-of-function mutation has penetrated. The white curve has shifted to the right, demonstrating an overall delay in channel activation, requiring much a higher membrane potential for channels to initiate their opening to allow the influx of Na^+.

Panel B. The grey squares representing channel inactivation has shifted to the left. This demonstrates an earlier inactivation of the sodium channel, again limiting the amount of Na^+ available for depolarisation.

Panel C. This is a culminative effect previously shown in panels **A** & **B,** exhibiting a diminished peak sodium current as illustrated here; normal current in blue, loss-of-function current in orange.

Panel D. Two action potentials juxtaposed; normal in blue and pathological in orange. The overall effect on a cellular electrophysiology is a delayed AP upstroke and an early repolarisation phase. Therefore, cells exhibiting Nav1.5 channels with a loss-of-function mutation will have a compromised capacity for electrical conduction, poor timing of said conduction and therefore likely exhibit irregular contractility.

Adapted from (Wilde & Amin, 2018)

4.1.2 The role of SCN10a in AF

$Na_v1.8$ isoform is coded by the SCN10a gene, and has been identified as responsible for the late sodium current as well as increasing susceptibility to arrhythmia in both mice and humans (Yang et al., 2012b; Savio-Galimberti et al., 2014; Dybkova et al., 2018; Rivaud et al., 2018a). Unlike other neuronal sodium channels, Nav1.8 is resistant to the neurotoxin TTX and has a functionally similarity to its Nav1.5 counterpart. In humans, the Na1.8 isoform encoding SCN10a gene is located adjacent to Nav1.5 isoform encoding SCN5a gene, and they interestingly share 65% of their amino acid sequence (Akopian et al., 1996). Their comparative similar genetic and functional properties, paired with an ever-growing association in their possible contributions to the arrhythmic process has made $Na_v1.8$ a target of close research in recent years (Macri et al., 2018b).

Clinically, we appreciate that patients with cardiac risk factors and co-morbidities are more likely to develop cardiac pathologies, including arrhythmias (Grubb et al., 2019). Dybkova et al demonstrated in human left ventricular myocytes, a significant increase in the expression of $Na_v1.8$ coupled with a significant downregulation of $Na_v1.5$ in patients with heart failure (Dybkova et al., 2018). They went on to illustrate the direct contribution of $Na_v1.8$ to AP duration through an enhanced late sodium current, and that inhibition of $Na_v1.8$ channel decreased the late current, therefore supressing arrhythmogenic triggers.

This finding is significant in both clinical and basic science domains. This supports the consensus in the literature implicating the Nav1.8 channel to an enhanced late current, it is demonstrated in human subjects in a manner which sheds new light on the susceptibility of the diseased heart to arrhythmia. The same research group later

published similar results regarding the inverse expression of these two isoforms in patients with left ventricular hypertrophy (Ahmad et al., 2019b). The same observation in two closely linked cardiac pathologies which often give rise to the other, offers a fresh and deeper perspective on the multifactorial problem of patients suffering with cardiac disease becoming prone to developing arrhythmia. As of yet, there are no studies comparing the expression of $Na_v1.5$ and $Na_v1.8$ in human subjects in sinus rhythm compared with those diagnosed with AF.

4.2 Hypothesis

We hypothesise that the right atrial appendage of patients diagnosed with permanent AF will exhibit an increased expression of $Na_v1.8$ coupled with a reduced expression of $Na_v1.5$ compared to patients in sinus rhythm.

4.3 Methods

Right atrial appendage from patients undergoing routine cardiac surgery in Castle Hill Hospital. Western blotting was performed (as discussed in Chapter 2) to determine the density of Nav1.5 and Nav1.8 protein expression observed between 225-200 kDa. Image J was used for densiometric analysis, and bands were normalised to Desmin (a band seen at 52kDa.) to determine equal protein loading. Prior to surgery patients were diagnosed as in sinus Rhythm, or post evaluation of ECGs during their routine clinic appointments diagnosed with AF and confirmed AF at the time of surgery. These two rhythm groups were best matched on age, operation type and co-morbidities to exclude as many confounding variables as possible. Student's T test was used to test for

statistical significance, and a P value less than 0.05 was considered significant. N= determines the number of patients within each group.

4.4 Results

Table 4.4.1 Table of patient groups

Best matched on age and comorbidities, when comparing sinus rhythm (S) in blue with atrial fibrillation (AF) in green.

Sinus Rhythm	Atrial Fibrillation
Age	Age
63	64
63	66
67	69
72	73
73	74
79	78
80	79

We demonstrated a correlation between VGSC expression and increasing chronological age in the previous chapter. It is important to minimise age as the primary confounding variable as much as possible when investigating AF (Table 4.4.1 illustrates the pairing of patient groups). In the total cohort of patient tissue we obtained, seven patient donors had clinically diagnosed permanent AF: This meant the vast majority of tissue studied was donated from patients who were in sinus rhythm, thus the best seven patients were selected to match the AF group in terms of their age at the time of operation, operation type and co-morbidities.

Expression of the protein isoforms Nav1.5 and Nav1.8 in tissue from patients with different rhythm status is shown in Figure 4.4.1. Bands between 250KDa. and 150KDa., indicated with a green dash and previously determined as specific to the protein of interest were analysed. Upon initial observation of Figure 4.4.1 Panel A it's clear that overall, the specific Nav1.5 sodium protein bands in the AF group appear much weaker than their sinus counterparts. The sinus group, clear doublet banding at the highest molecular weights as expected, observed as a thinner top band followed by a thicker and denser bottom band. However, in the AF group the banding is far less clear. Across multiple samples there appears to be a splitting of the heavy bands. To compensate for this, the pixel density within the area of each band was calculated individually and added to make a total, to eliminate the lighter background between bands which may falsely skew the analysis suggesting a weaker expression.

Observations of Figure 4.5.1 B blots of Nav1.8 in the sinus group appear to be extremely dense, often overlapping vertically, whereas the AF group appear to be quite varied in the expression with a clearer banding pattern. The sinus group were noted as overexposed as the background shade of the lanes also appears significantly darker than

their AF pairs. Furthermore, the images were compressed for the purpose of this publication which adds to the appearance of overexposed dense bands. Background changes were accounted for during analysis; firstly, the standardised control method of measuring the background pixilation of the lane in comparison to the bands of interest, and secondly by expanding the images during analysis to clearly identify the borders of the bands.

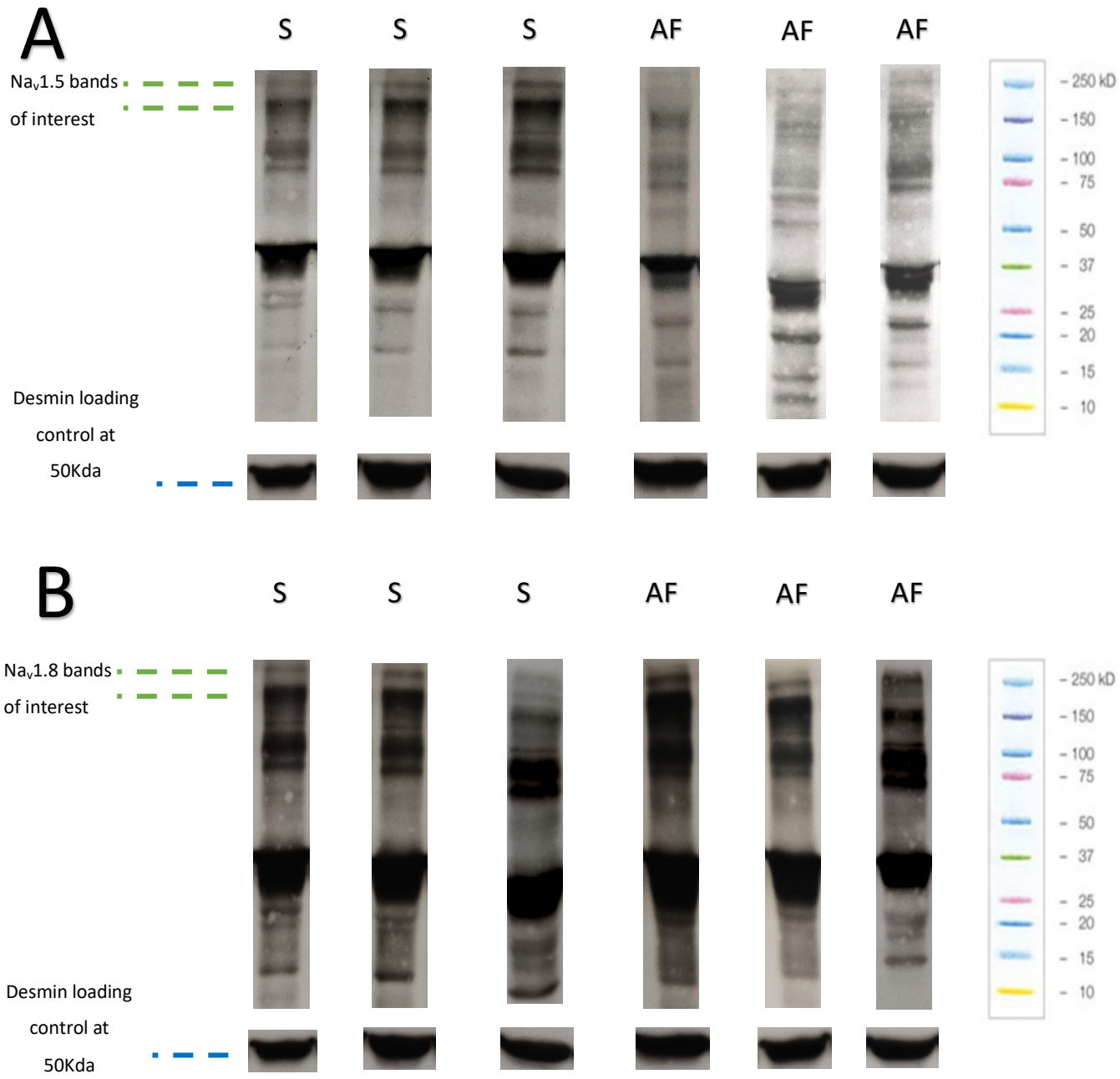

Figure 4.4.1 Expression of the protein isoforms Nav1.5 and Nav1.8 in tissue from patients with different rhythm status

Illustrative western blots show the protein expression of Nav1.5 (panel A) and Nav1.8 (Panel B) in tissue donated from patients in sinus rhythm (S) and those with diagnosed AF.

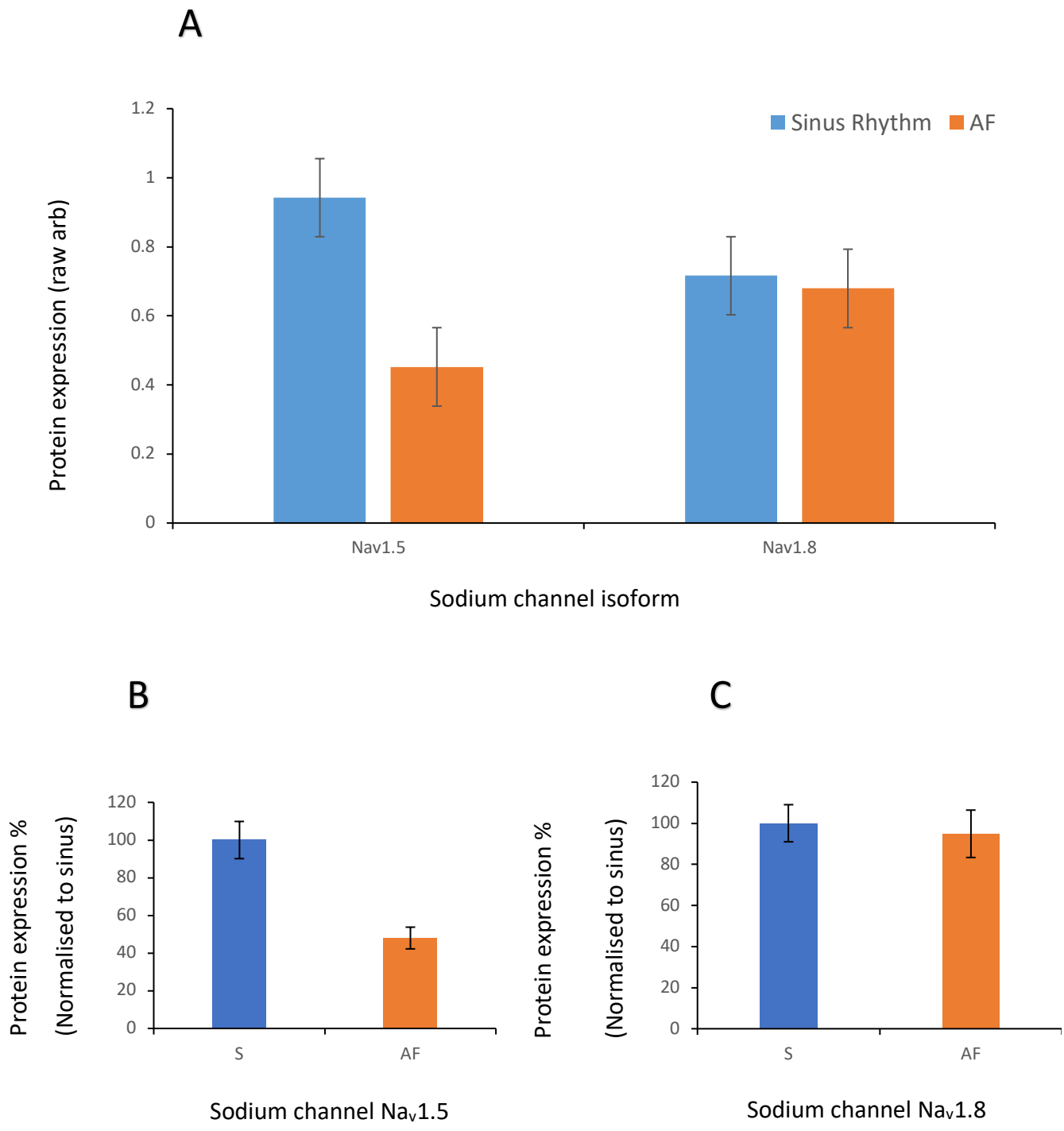

Figure 4.4.2 Nav1.5 and Nav1.8 protein expression in tissue from patients in permanent AF compared with sinus rhythm

A) the normalised to desmin per patient raw mean data plotted for both Nav1.5 and Nav1.8 protein expression to compare the effect of AF. B) the protein expression of Nav1.5 normalised to the sinus patient mean to compare AF. C) the protein expression of Nav1.8 normalised to the sinus patient mean to compare AF. n= 7, t-test p= 0.00046

Figure 4.4.2 A for each patient the raw density of bands of protein expression for Nav1.5 and Nav1.8 was normalised to their desmin content as housekeeping/even protein loading. For Figure 4.4.2 B&C, the mean density of protein expression of $Na_v1.5$ and $Na_v1.8$ in both groups the mean values for each isoform were expressed as a % of the sinus rhythm group (S) and a Student's t-tests to calculate P values to ascertain statistical significance. Figure 4.4.2 B for $Na_v1.5$ shows there was a significant decrease of protein expression by 52% in the AF patients compared with the sinus rhythm patients (n= 7, t-test * p= 0.00046). In contrast, the expression of $Na_v1.8$ protein showed no significant difference between the sinus and AF groups (P= 0.731).

4.5 Discussion

4.5.1 General discussion of results

Data in this chapter partially supports the original hypothesis with patients in AF exhibiting a marked reduction of $Na_v1.5$, of 52%. The physiological and clinical implication of these results as demonstrated in human tissue is significant as a reduction in $Na_v1.5$ in patients in AF means fewer availability of sodium ions, therefore a diminished peak of the fast sodium current and therefore phase 0 of the AP. The loss of $Na_v1.5$ protein in our AF cohort would be consistent with conclusions within the existing literature highlighting the susceptibility of AF due to coding variants of its SCN5a gene (Splawski et al., 2002; Darbar et al., 2008). To the best current knowledge, this is the first study to demonstrate that humans with AF have a significantly reduced expression of $Na_v1.5$ protein in the right atrium when compared to their counterparts in sinus rhythm.

Upregulation of $Na_v1.8$ was not observed as predicted by our hypothesis as there was no significant different between the AF and sinus groups of patients in Nav1.8 protein expression. This is unexpected as AF has been strongly associated with enhanced late sodium currents as regulated by the $Na_v1.8$ isoform (Savio-Galimberti et al., 2014; Macri et al., 2018b)-hence we would expect patients in AF to exhibit higher quantities of this protein, enhancing the pathological current. However, the blots were particularly dark in background with heavy close bands, and this may have hampered the analysis undertaken. The limits of this study were the low number of AF patient examined and no further data to examine function or gating mechanics. It is quite possible that the enhanced late sodium current associated with AF may not be solely due to the number of $Na_v1.8$ channels available, but more so depend on the activation and inactivation times of the channel. Patients with AF could exhibit pathological ion gating enhancing the late sodium current (Bezzina et al., 2013; Savio-Galimberti et al., 2014; Fang et al., 2016; Macri et al., 2018b).

An important limitation of this study which will influence the data is that the length of time the patient was living with AF was not considered. As previously discussed, AF is a self-perpetuating disease and remodelling is a hallmark feature of the condition; the longer a heart remains in AF the more extensive the remodelling (Manning et al., 1994; Yue et al., 1997). We do not know in this study whether the patients have been in permanent AF only recently, or if they've lived with the disease for many years. The length of AF duration will undoubtedly play a key role in ionic remodelling. Furthermore, the sample size within this study is extremely limited. For a more decisive conclusion as to the relationship of $Na_v1.8$ expression and AF, a larger cohort is required. Finally, it is worth appreciating in this case that although the confounding variable of age was

accounted for, there are undoubtedly a number of variables which are difficult to minimise in this study when sampling human tissue from diseased hearts.

4.5.2 Clinical approaches targeting VGSCs to treat and prevent AF

Sodium channel blockade is an exciting, evolving modality for the management of AF. Within the context of emerging laboratory research, specific blockade of the $Na_v1.8$ channel through an agent named A-803467 has been demonstrated in multiple studies in not only diminishing the I_{NaL} restoring physiologically normal AP morphology, but also in preventing electrical remodelling reducing the incidence and duration of paroxysmal AF in canines (Chen et al., 2016). Furthermore, it has been observed that this specific sodium channel blocker supresses ventricular arrhythmia induced via acute ischaemia (Yu et al., 2017). However this is only observed with this agent in experimental laboratory data.

Of the class I anti-arrhythmic drugs available for clinical use, Ranolazine is of particular interest. It is currently within the NICE guidelines for the management of stable angina (NICE, 2016). Unlike its counterparts, it is a potent and specific blocker of $I_{NaL,}$ as well as having a mild inhibitory effect on I_{Kr} and I_{ca}. (Belardinelli et al., 2006). Furthermore, it has a greater specificity over targeting atrial myocytes compared to ventricular myocytes (Burashnikov et al., 2007), and its capacity to target these cells has been demonstrated to be as potent in vivo as it is in experimental laboratory conditions (Antzelevitch et al., 2004; Song et al., 2004). Ranolazine has produced impressive results in terminating acutely induced AF in horses through pharmacological cardioversion (Carstensen et al., 2019), demonstrated to be protective against AF in chronic ischaemic

heart disease(Herruzo-Rojas et al., 2019), as well as effective in the reversing of post-operative AF following cardiac surgery (Simopoulos et al., 2018).

The efficacy of Ranolazine in terminating and preventing atrial tachyarrhythmia is most notable in clinical trials: The MERLIN-TIMI 36 study included 6560 patients who were admitted to hospital with non-ST elevation myocardial infarction. Patients were randomised to receive either Ranolazine or a placebo. With continuous ECG monitoring, the intervention group had a significantly reduced incidence of both ventricular tachycardia as well as new-onset AF (Morrow et al., 2007). The RAFAELLO study investigated the role of Ranolazine in preventing recurrence of AF following electrical cardioversion. 241 Patients received: 350mg, 500mg, 750mg of oral Ranolazine twice daily vs a placebo. The drug was tolerated well even at higher doses, with the top dose intervention group demonstrating a significant reduction in AF recurrence (De Ferrari et al., 2015). The HARMONY trial investigated the efficacy of Ranolazine in reducing AF burden in patients with paroxysmal AF and those with implanted pacemakers over 12 weeks. ECGs and symptoms diaries were reviewed at regular intervals. On its on Ranolazine had no notable effect. However, when paired with a moderate dose of dronedarone had a 59% reduction in AF burden, reduced outbreaks of AF, and qualitatively improved patients' symptoms than placebo or dronedarone alone (Reiffel et al., 2015).

Though the evidence for consideration of Ranolazine into more mainstream clinical practice continues to accumulate, there are important questions yet to be addressed. Long-term effects of the drug are yet to be understood due to its relative novelty compared with traditional agents. Whether Ranolazine can be used as a stand-alone agent is questionable as the most pronounced anti-arrhythmic effect has often been

observed when it was paired with procedural or other pharmacological strategies. Also to consider it that its safety in the elderly population and multi-morbid patients is yet to be fully studied. This is a particular point of contention as the appreciation of AF as a disease entity of the elderly is an established phenomenon. None-the-less, Ranolazine has expanded the toolbelt of anti-arrhythmic drugs for AF and catapulted sodium channel blockade forward as a viable therapeutic approach for acute atrial tachyarrhythmia.

The strategy of inhibiting aberrant sodium currents is limited in that by this point, remodelling of sodium channels has already occurred; the heart is already in arrhythmia or primed for it to occur. A more forward-thinking approach would be to attempt to prevent ionic remodelling in the first place. In canine models, Irbesartan has been demonstrated to prevent sodium channel remodelling, improving intra-atrial conduction, as well minimising the progression of atrial fibrosis (Kataoka et al., 2016; Wang & Li, 2018). Irbesartan is a commonly prescribed angiotensin receptor blocker utilised in the management of hypertension. Its renal safety profile is excellent, allowing use in patients undergoing haemodialysis under NICE guidelines. As the elderly population commonly have impaired renal function, either due to age, pathology or polypharmacy, Irbesartan may be an ideal and currently under-utilised agent. A meta-analysis of randomised control trials totalling 13,184 patients found that angiotensin-converting-enzyme inhibitors and angiotensin receptor blockers significantly reduced the recurrence of AF, with Irbesartan to be particularly effective(Han et al., 2013). Evidence across laboratory and clinical domains strongly suggests that this drug warrants careful consideration as a preventative strategy for AF-particularly in the elderly who are most at risk for developing the condition, likely to have element of

compromised renal function, as well to be taking antihypertensives anyway as part of their package of medical management.

4.5.3 Limitations

The biggest and most obvious limitation of this study is that it only contains 7 patients within each group. Clearly, this is not a broad enough sample size to be completely applicable to the general population. To have been able to contrast and compare these tissues non-the-less is of tremendous value. Furthermore, this study only compared protein expression and not channel function, hence there is a missing element to fully demonstrating the proposed hypothesis that AP peak will be reduced, and late current will be enhanced. The hypothesis was not supported in its entirety as there was not the spike in Nav1.8 expression as predicted which is a further weakness of this study.

Chapter 5

Drug Manipulation of voltage-gated sodium channels through the JNK pathway

Chapter 5 Drug Manipulation of voltage-gated sodium channels through the JNK pathway

5.1 Background

The c-Jun N-terminal kinase (JNK) is part of a family of mitogen activated kinases involved in the stress signalling pathway. It can be induced by inflammatory cytokines, bacterial endotoxins, osmotic shock, UV radiation and hypoxia (Bennett et al., 2001). An inverse relationship of activated JNK and connexin 43 (Cx43) has been previously observed in the elderly mammalian heart as with increasing chronological age, phosphorylated JNK was observed to increase whilst Cx43 decreased (Yan et al., 2018). This builds on evidence which has suggested that JNK has a central role in the regulation of Cx43 and is involved in altering the hearts capability for intercellular conduction, predisposing older hearts to a susceptibility to arrhythmia (Petrich et al., 2002). Total JNK has been identified as a biomarker for chronic cardiac stress, whereas phosphorylated JNK as a marker for acute cardiac stress (Chambers & LoGrasso, 2011; Yan et al., 2018). Recent studies have demonstrated that total JNK is elevated in patients with hypertension and hypercholesterolaemia, two major cardiac risk factors (Jones et al., 2018).

JNK has been the target of clinical trials over the last 20 years, and many variants employed for a variety of disease as possible attenuators. For example, Alzheimer's disease shows increased phosphorylation of JNK within brain samples of patients (Colombo et al., 2009), and is pursued as a new tool of attenuation. Whereas Koch et al., 2015 informed us that JNK derived compounds under clinical scrutiny: D-JNKi1 to treat stroke, bentamapimod for inflammatory endometriosis, tanzisertib to treat idiopathic pulmonary fibrosis and also to treat the chronic skin condition of discoid lupus erythematous.

We know from in vivo studies JNK can be pharmacologically manipulated to reduce or enhance its expression (Bennett et al., 2001). Anisomycin, also known as flagecidin, is classed as a protein synthesis inhibitor that specially binds to the JNK binding domain, activating JNK (Bogoyevitch et al., 2010). It has also been observed that anisomycin at an effective dose (10ug/ml in rat hearts (Ogawa et al., 2004) also reduces reactive oxygen species generation occurs (Chambers & LoGrasso, 2011). Comparatively, anthra[1,9-cd]pyrazol-6-(2H)-one, commonly referred to as SP600125, is a reversable ATP competitive inhibitor of JNK (Bogoyevitch et al., 2010) used in research studies to elucidate the role of JNK, particularly upregulation of P-JNK *in vivo* and *in vitro* studies.

The link between JNK and sodium channels is yet to be identified within the literature. Turnover of VGSC was first identified in Schwann cells of rabbits in 1988 to be around 3 days (Ritchie, 1988). More recently the functional half-life of VGSCs have been showed to be around 35 hours in the left ventricular myocytes of dogs (Maltsev et al., 2008). If JNK has been implicated as being a regulator of Cx43 expression, as well as observed to be elevated in patients with cardiac risk factors, as a biomarker of cardiac stress, it could be that JNK plays a key role in VGSC remodelling which we have observed with age and AF.

5.2 Hypothesis and objectives

Our hypothesis was that the expression of total JNK and phosphorylated JNK will be significantly greater in the human right atrial appendage with increased chronological age. Furthermore, pharmacological intervention *in vitro* will activate JNK (anisomycin) leading to a decrease in $Na_v1.5$ protein expression and increase in $Na_v1.8$ protein expression, which in contrast will be reversed by inhibition of JNK (SP600125).

This hypothesis will be answered through the following objectives.

- Determine whether there is a significant difference in the protein expression of phosphorylated JNK and total JNK between the extremes of age in our patient cohort.
- Develop a functional protocol for cardiac slicing of human right atrial appendage, and use these slice for *in vitro* pharmacological manipulation of the JNK pathway.
- Determine the effect of anisomycin, and SP600125, on JNK protein expression in the human right atrial appendage.
- Determine if pharmacological manipulation of JNK will change the protein expression of the voltage gated sodium channels isoforms $Na_v1.5$ and $Na_v1.8$.

5.3 Methods

Right atrial appendage was sampled from patients undergoing elective cardiac surgery at Castle Hill Hospital. In theatres, the tissue was placed in 50ml cardioplegia held at 4^{o}C: The components of the cardioplegic solution is outlined in table 5.1. The patient tissue sample was then transported to the University of Hull campus and the experiment set-up is illustrated in Figure 5.3.1.

Table 5.3.1 Constitution of cardioplegia

Cardioplegic Solution	
Component	**Concentration (mM)**
Glucose	277.5
KCL	30
$NaHCO_3$	20
Mannitol	34.3

5.3.1 Cardiac slicing

Slicing was performed using a Leica Vibratome (VT1200, Lecia Germany). This equipment was prepared with ice in the external chamber and cardioplegia in the slicing chamber to maintain a cold environment for the tissue to be submerged. We used gas of 5% CO_2 and 95% O_2 with a tube submerged into the slicing chamber to keep the tissue perfused with oxygen and maintain the correct pH while slicing. The tissue was glued onto the cutting place and submerged in the slicing chamber; a fresh blade was applied to the blade mount and aligned within the edge of the tissue. The tissue was cut at 0.03 mm/s with a step size beginning at 300 µm up to 600 µm, and I used 500 µm as this provided the most consistent slice reproduced from the same piece of patient tissue to gain multiple identical tissue samples.

5.3.2 Pharmacological manipulation

5.3.2.1 Pharmacological solutions

Anisomycin purchased from Alomone labs™ (lot#: A520AM02100 from Israel) had a molecular weight of 265.31, therefore a 500 mM concentration of stock solution required 0.133g of Anisomycin in 1ml of DMSO, which was aliquoted into 50µl lots and frozen to store at -20^{o}C. When required, one vial of 50µl 500mM stock Anisomycin solution, was added to 5 ml of Tyrode solution which would fill 1 well holding one piece of sliced cardiac tissue with around 2ml left over to top up the well if dried out. A control solution with 50µl DMSO was added to 5 ml of Tyrode solution for the zero drug well.

SP600125 was purchased from Abcam (lot#: APN17084 from Cambridge) had a molecular weight of 220.23, therefore a 500 mM concentration of stock solution required 0.110g of SP600125 in 1ml of DMSO which was aliquoted into 50µl lots and frozen to store at -20^{o}C. When required, one vial of 50µl 500mM stock SP600125 solution, was added to 5 ml of Tyrode solution. The constitution of Tryodes solution is outlined in table 5.2.

5.3.2.2 Experimental set-up

The slices of cardiac tissue were placed into wells of 6 well plates. These plates were adapted with acrylic backs, an inlet and outlet to allow temperature-controlled water to pass through, warming the plates contents to body temperature at 37 ^{o}C. A water bath generator was utilised to circulate water through the plates at 37 ^{o}C. One plate was dedicated to each drug of choice: the JNK activation via the use of anisomycin plate 1,

and plate 2 dedicated to JNK inhibition via SP600125. Each plate had 2 wells used as control, no drug in the Tyrode solution, the remaining wells had various drug of choice doses.

Table 5.3.2 Composition of Tyrode's solution

Tyrode's Solution	
Component	**Concentration (mM)**
NaCl	93
$NaHCO_3$	20
Na_2HPO_4	1
$MgSO_47H_20$	1
KCL	5
Glucose	10
Sodium acetate	20
Insulin	5 (U/L)
$CaCl_2$	1

Each well had a small tube from a manifold to allow maintain tissue perfusion with gas of 5 % CO_2 and 95 % O_2. As the experiment duration was 6 hours to allow as much time as possible for VGSC turnover, each hour the wells were checked to make sure the fluids

had not evaporated. If it was observed solution levels per well had dropped, they were topped up with appropriate solution for that well. After 6 hours all tissues were removed and frozen in individual Eppendorf's under liquid nitrogen and frozen at -80 ^{o}C. An illustration of the experiment set up is shown in Figure 5.3.1. The process of protein quantification by western blot was performed as highlighted in previous chapters.

5.3.3 Western blot

For probing JNK protein expression, polyclonal antibodies were purchased from Thermo Fisher Scientific (cat no: PA5-99529 for total JNK 1 & 2; 44-682G for Phospho-JNK 1 & 2). These antibodies were diluted to a concentration of 1:500, and employed as per the standard method. We compared JNK and P-JNK expression in 18 tissue samples, looking at the extremes by comparing the oldest 9 patients (mean age 76) and the youngest 9 patients (mean age 53) of our total patient cohort studied in Chapter 3. All patients were in sinus rhythm. Data was from the band densities was analysed using image J and Microsoft Excel.

Tissue samples which underwent drug manipulation with their control samples were probed for protein expression of total JNK, P-JNK (to assess the efficacy of the drug manipulation process) along with $Na_v1.5$ and $Na_v1.8$ protein expression to investigate if the drug manipulation process through the JNK pathway influenced the turnover of VGSCs.

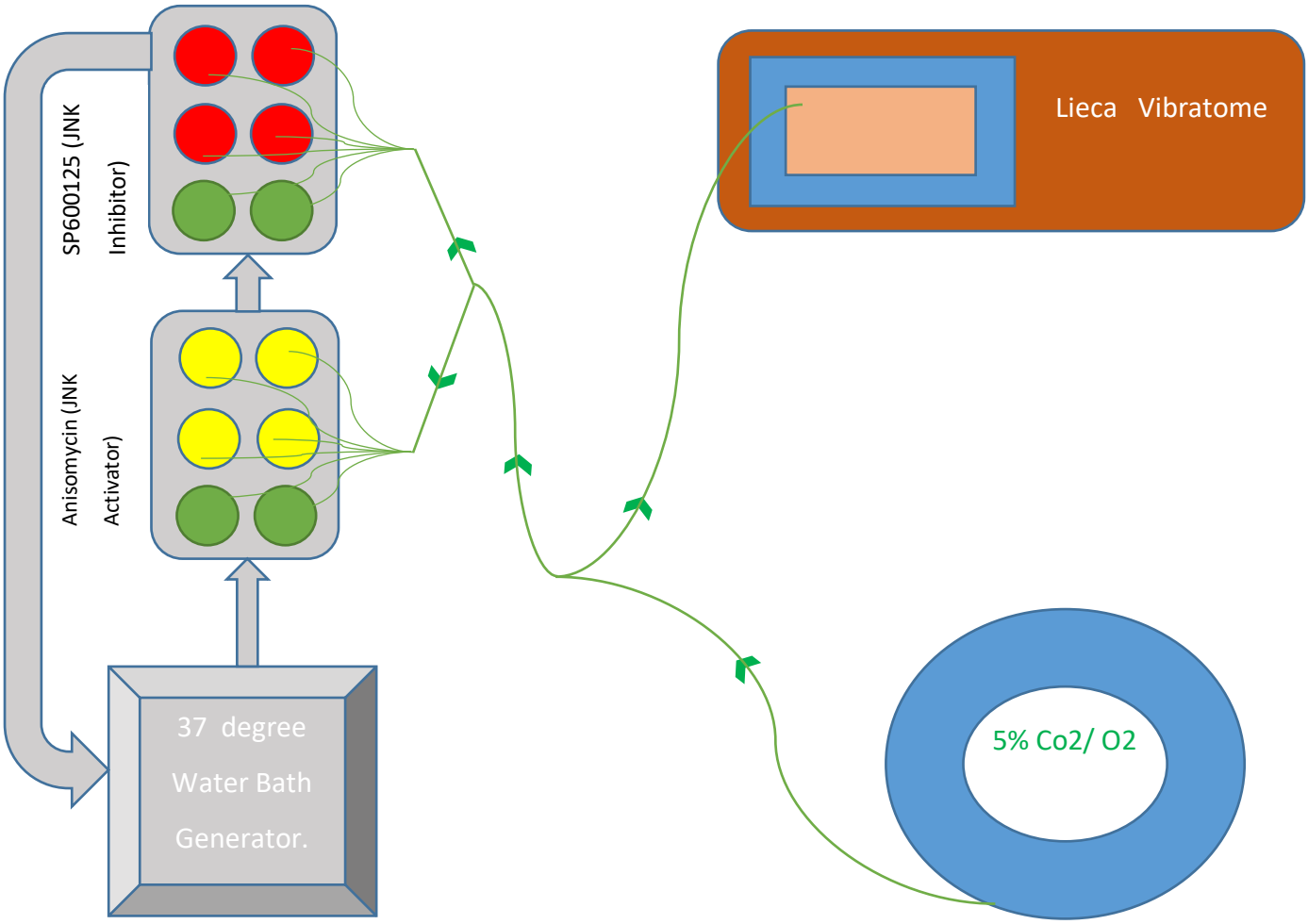

Ice well

Slicing chamber filled with Ice cold cardioplegia

Control well: Tyrode solution, no drug

JNK activator Anisomycin in Tyrode solution

JNK inhibitor SP600125Tyrode solution

Plastic connecting tubing

Direction of airflow

Figure 5.3.1 Drug manipulation experiment laboratory set up

5.4 Results

5.4.1 P-JNK and total JNK protein expression in relation to chronological age

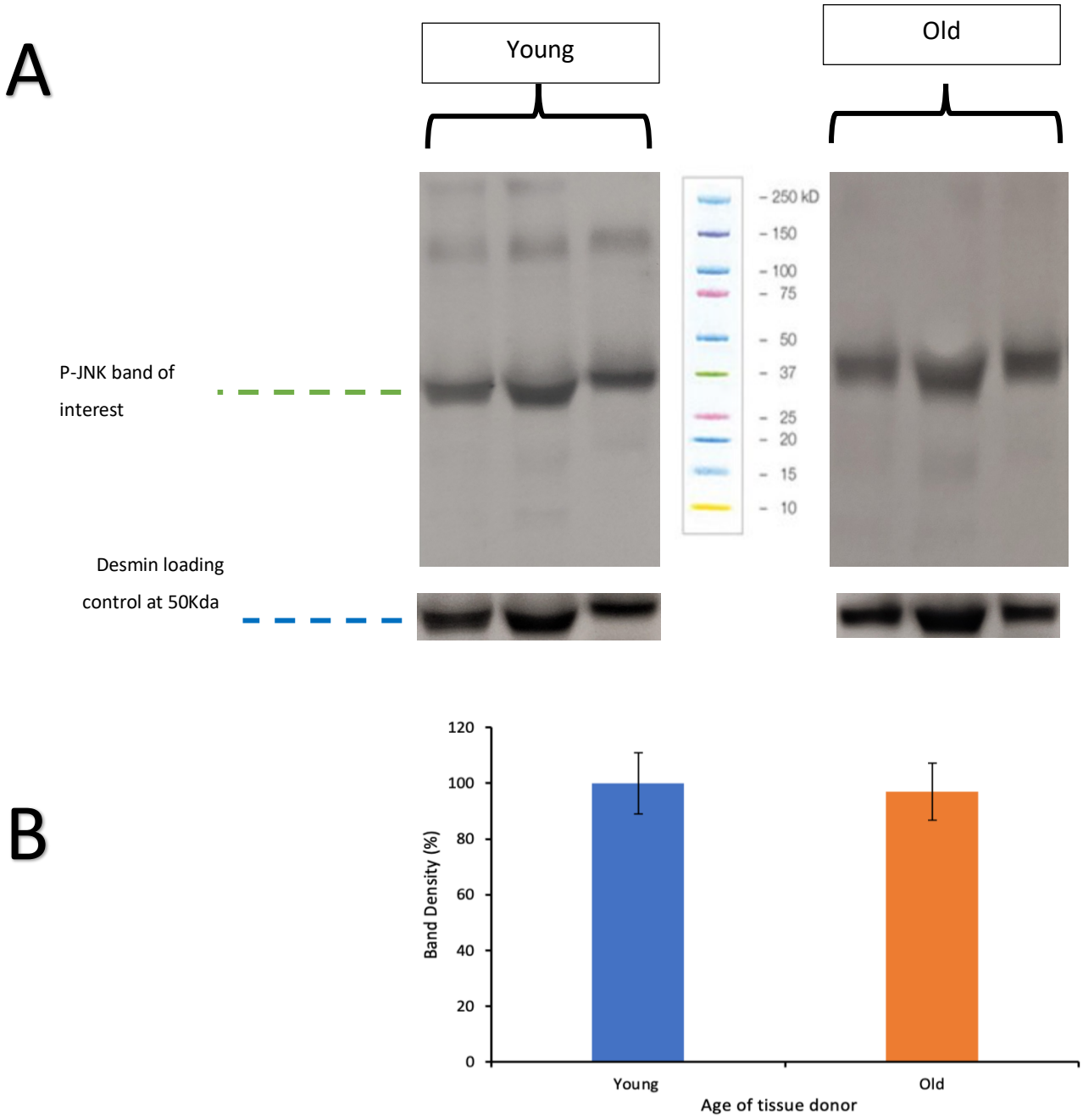

Figure 5.4.1 P-JNK protein expression

Panel A, illustrative western blot of bands specific to P-JNK protein expression, from tissue samples derived from the 9 youngest (mean age 56) and 9 oldest patients (mean age 76). **Panel B**, mean density normalised to the young patient mean value ± SEM, P-JNK protein expression per age group (n=9 young; n=9 old, t-test p=0.834).

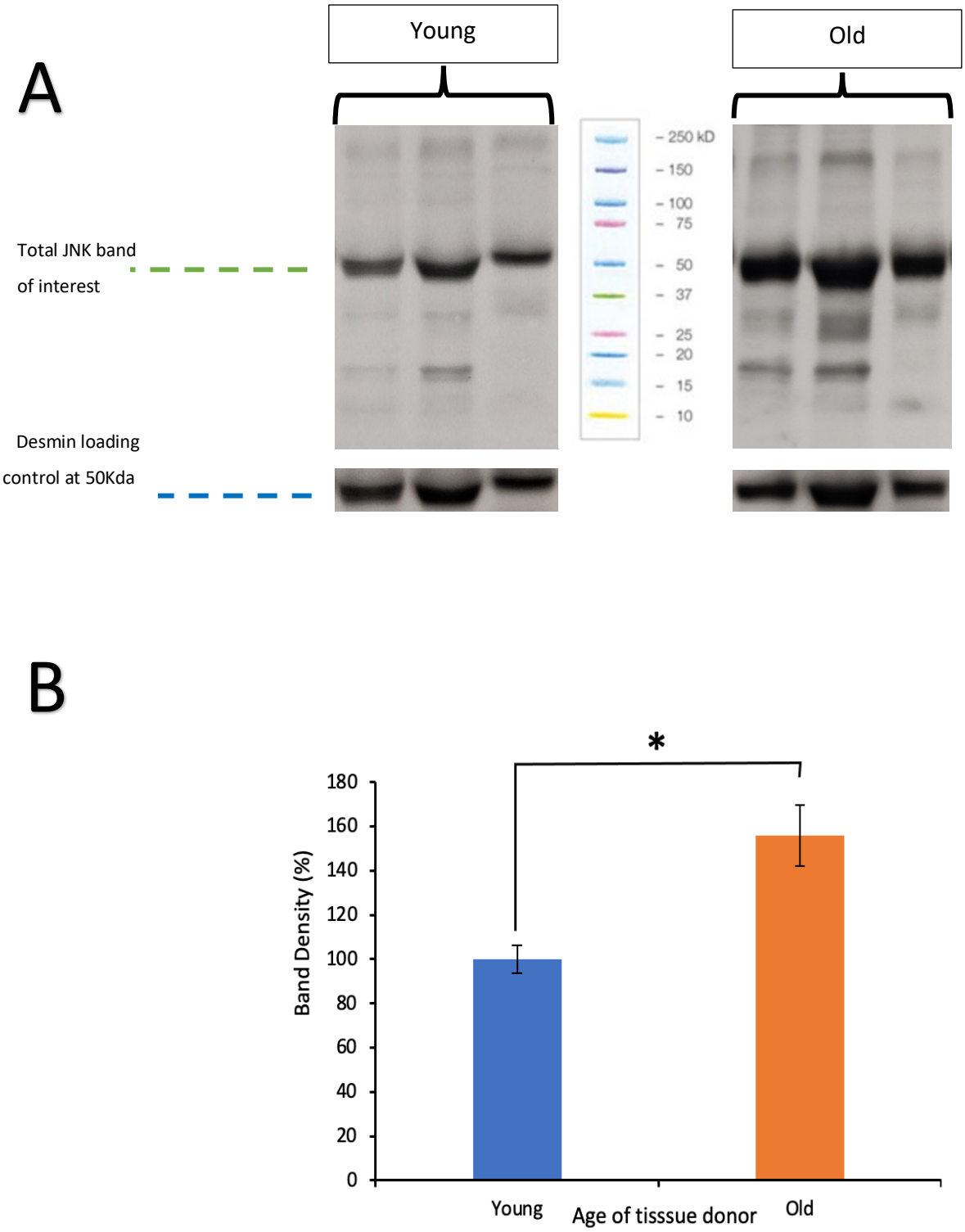

Figure 5.4.2 Total -JNK protein expression

Panel A, illustrative western blot of bands specific to total-JNK protein expression, from tissue samples derived from patients classed as young (mean age 53) and old (mean age 76). **Panel B**, mean density normalised to the young patient mean value ± SEM, total JNK protein expression per age group (n=9 young; n=9 old, *t-test p=0.0045).

Comparison of P-JNK and total JNK protein expression was examined between tissue samples donated from young and old patients as shown in Figure 5.4.1 & Figure 5.4.2. We can observe with a t-test that there is no significant difference between the young and old groups in P-JNK expression. The difference between these two group for total JNK can be observed by the blots alone Figure 5.4.2B. Data of total-JNK shows a significant increase of 56% band density in the older group when compared with the young group; with a Student's t-test there was a significant difference of p=0.0045 between the young and old groups for total JNK protein expression.

5.4.2 JNK pharmacological manipulation alters VGSC $Na_v1.8$ protein expression

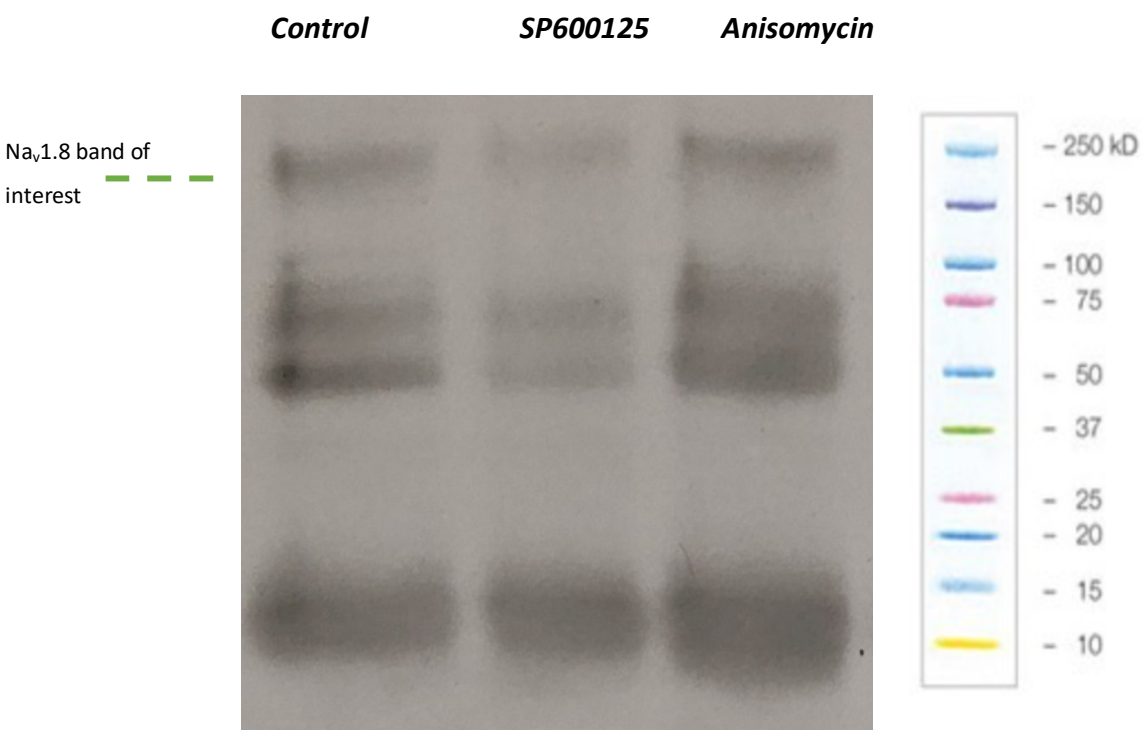

Figure 5.4.3 Nav1.8 protein expression of 1 patient sample following drug manipulation experiment

Left lane is the control without any exposure to a drug. The middle lane tissue was exposed to the JNK inhibitor SP600125, and the right-hand lane was exposed to the JNK activator Anisomycin.

Figure 5.4.3 shows a blot of $Na_v1.8$ protein expression of 1 patient sample sliced and used in pharmacological manipulation experiment as shown in Figure 5.4.1. Due to n=1 this is illustrative data; observed tissue exposure to the JNK inhibitor SP600125 had a much weaker banding density compared to the control, whereas in contrast the JNK activator Anisomycin exhibited stronger bands of $Na_v1.8$ protein expression.

5.5 Discussion

It should be noted that the experiments in this Chapter were severely disrupted, and abruptly terminated by the Covid-19 pandemic. Firstly, the western blot technique was used to compare JNK protein expression in the oldest and youngest groups, most notably demonstrated a significant increase of over 50% in the total JNK expression older aged group. This was expected and is consistent with the literature as with increasing patient age, the heart is vulnerable to the stressors of disease and physiological dysfunction (Anyukhovsky et al., 2005; Dun & Boyden, 2009; Biernacka & Frangogiannis, 2011; Ahmad et al., 2019c; Grubb et al., 2019). It was observed that P-JNK had a higher average protein expression in the older group compared with the young, this was a trend increase and not statistically significant: We needed to achieve a great number of patient sampling to determine if this was a true result, which was prevented due to the pandemic.

The drug manipulation technique illustrated by Figure 5.4.3 provided a striking result, although clearly an N value of 1 is not a cohort representative. The JNK inhibitor SP600125 decreased (observed on the blot as significantly) the expression of $Na_v1.8$, whereas the JNK activator observed to slightly increase the density of expression of the neuronal channel, when compared with the control (no treatment sample). This single

result suggests, though clearly not conclusively, that JNK activity could be linked with the expression of VGSCs. If JNK is a regulator of $Na_v1.8$ this provides novel and significant insight into the remodelling of cardiac sodium channels, deepening the understanding of the pathophysiological process behind the development of cardiac arrhythmia which $Na_v1.8$ has been almost unanimously implicated.

Identifying JNK as a critical player in this process, coupled with its potentially regulatory role in the expression VGSCs, could illuminate novel approaches in targeting this remodelling process. The proposed pathway for the evolution of arrhythmia could be that as JNK increases with age to upregulate $Na_v1.8$ protein expression, thus increasing the number of channels present. This in turn would enhance the late sodium current, causing a lengthening the action potential duration, then increase calcium loading and resultant DADs. This mechanism is illustrated in Figure 5.5.1. The influence of JNK on the expression of $Na_v1.5$ are currently unknown.

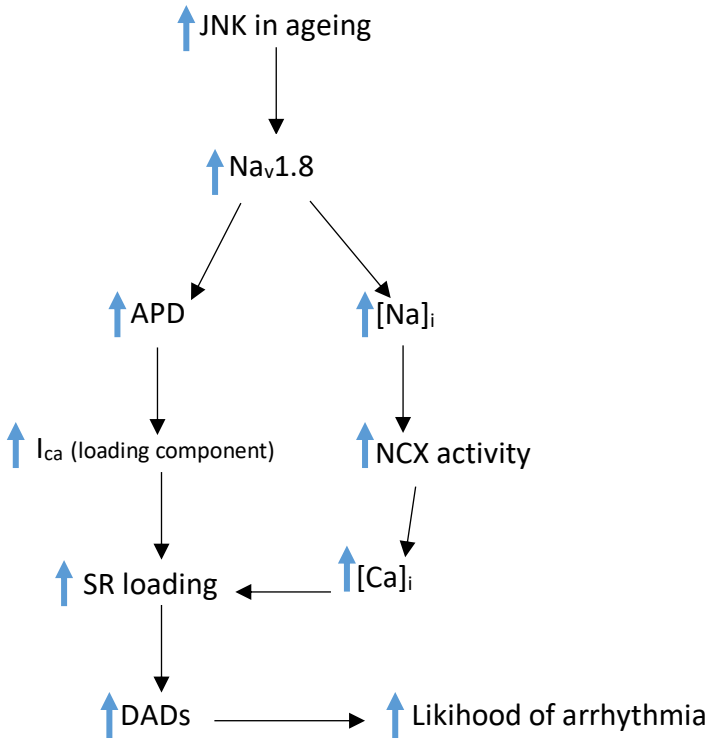

Figure 5.5.1 Influence of JNK on the evolution of arrhythmia

5.6 Limitations

The limitations to this study are substantial and many. Most obviously, an N number of one for the drug manipulation is clearly not significant or representative. Furthermore, the desmin has not been blotted for this sample and hence a major control variable of protein loading is lacking. $Na_v1.5$ data is completely absent and hence we have no insight into the effect of manipulating the JNK pathway has on the expression of this channel. The blots of total JNK and P-JNK following exposure of drug manipulation to confirm the pharmacological activity is also missing. Therefore, we cannot conclude that the results above are due to increased or decreased presence of JNK. Unfortunately, the impact of the Covid-19 pandemic has meant that access to our laboratory was prohibited and has resulted in a significant proportion of this study to be incomplete.

5.7 New results

Since the write up of this original study, new data has emerged from the SAJ laboratory. Right atrial appendage tissue from 5 patients had undergone the processes cardiac slicing followed by JNK manipulation and was stored in a -80^{o}C as work ceased by E Isaac due to the pandemic. Now resumed by Nneka Otti, a clear demonstration of the effects of anisomycin and SP600125 has been exhibited on the protein expression of total JNK in Figure 5.7.1. Leading to the study to reveal the effect of JNK activation and JNK inhibition on $Na_v1.5$ and $Na_v1.8$ protein expression in Figure 5.7.2.

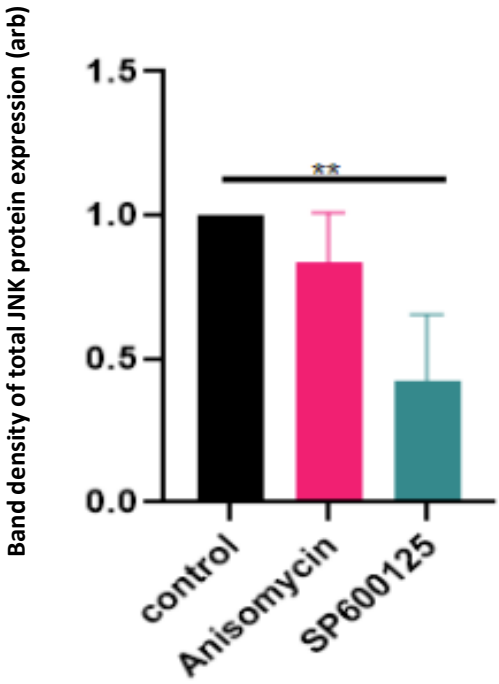

Figure 5.7.1 Effect of Anisomycin and SP600125 on total JNK expression in the human right atria

Bar chart analysis of the density of total JNK expression under three conditions; control (no drug), Anisomycin (JNK activator) and SP600125 (JNK inhibitor). Most notably there was a ~50% reduction in the expression of total JNK when tissue was exposed to SP600125, highlighting the potency of this agent in JNK inhibition.

(n=3; one-way ANOVA test and Tukey's multiple comparison tests p=0.014.)

(Acknowledgements; patient recruitment, cardiac slicing, drug manipulation E. Isaac; Western blotting and data analysis N. Otti).

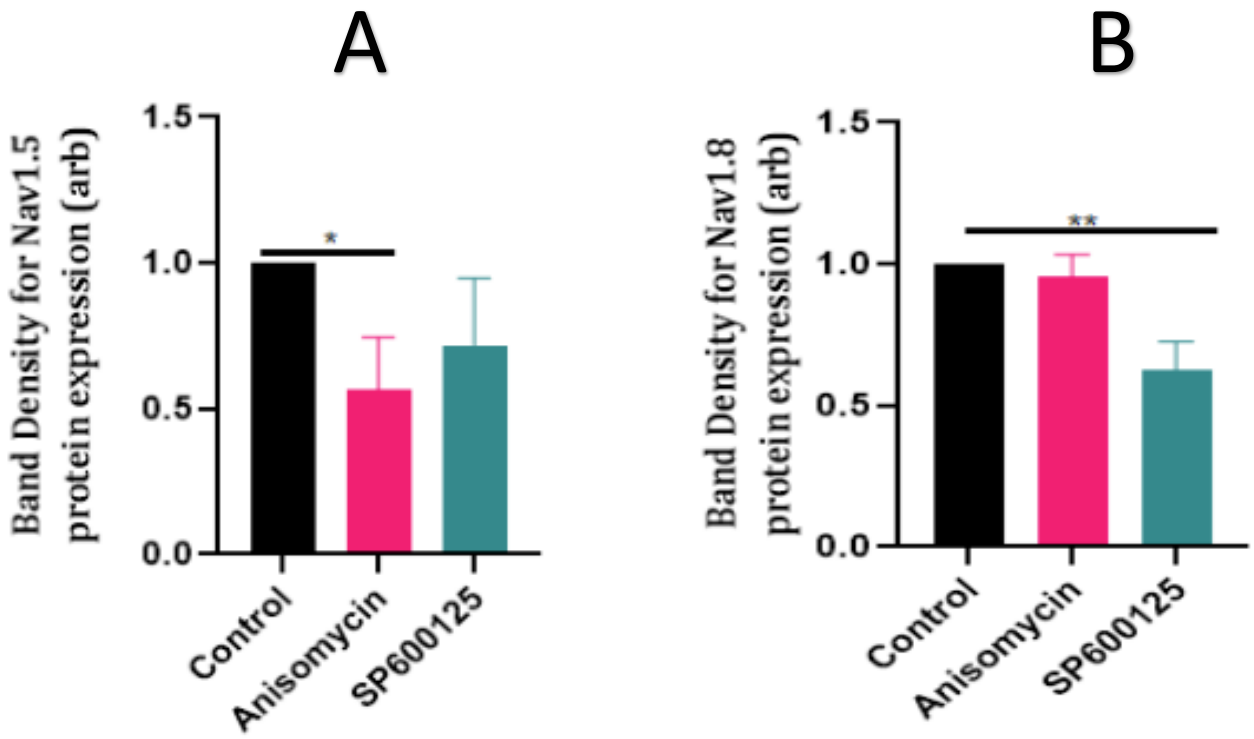

Figure 5.7.2 Effect of JNK activation and inhibition on Nav1.5 (A) & Nav1.8 (B)

Panel A, Compared to the control, there was a 46% reduction in the expression of $Na_v1.5$ protein when JNK was activated using Anisomycin. However, SP600125 produced a slightly upregulated expression of $Na_v1.5$ protein when compared to the JNK activator, with a 28% reduction in comparison to the control lane. (n=3; one-way ANOVA test and Tukey's multiple comparison test P=0.04).

Panel B, In comparison to the control SP600125 produced a significant 40% decline in the protein expression of $Na_v1.8$, whereas anisomycin showed no change in $Na_v1.8$ express when compared to the control lane. (n=3; one-way ANOVA test and Tukey's multiple comparison test p=0.048).

It should be noted that this result is consistent with the pilot data illustrated in Figure 5.4.2.

(Acknowledgements; patient recruitment, cardiac slicing, drug manipulation E. Isaac; Western blotting and data analysis N. Otti).

5.7.1 Discussion of new results

These new results bring to light novel insight that JNK expression seems to significantly influence the modulation of $Na_v1.5$ and $Na_v1.8$ in the human heart. When JNK is inhibited with SP600125 we see a 40% reduction in $Na_v1.8$ in comparison to control (P=0.048) supporting our original observation. Activating JNK with Anisomycin produced a significantly higher expression of $Na_v1.8$ in comparison to the inhibition lane. Coupling this with data in Figure 5.4.1, where we observed a significant increase in the expression of total JNK in older patients, and Figures 3.4.7 and Figure 3.4.8 where we observed increased $Na_v1.8$ expression in older age, we may elude that a higher JNK expression with age may be a determinant step in the remodelling of cardiac $Na_v1.8$ predisposing the elderly heart to pathological late currents through the upregulation of this channel.

With regards to $Na_v1.5$, JNK activation with Anisomycin seems to significantly reduce the expression of this channel by 46% in comparison to control P=0.04. This is consistent with the ageing data which has demonstrated a reduction in $Na_v1.5$ with age, and an increase of total JNK with age thus again eluding to JNK as potentially being a key player underlying the electrophysiological remodelling predisposing the heart to arrhythmia through the loss of its native sodium channel isoform critical for depolarisation to occur.

Though this data is novel and has demonstrated fascinating results as to the underlying biomechanics of VGSC remodelling in the human heart, this is still extremely preliminary as a N number of 3 is far from representative. This does however demonstrate the efficacy of the experimental method detailed in this chapter, that pharmacological manipulation of JNK can have a significant impact on the expression of VGSC.

Chapter 6

General discussion

Chapter 6 General discussion

6.1 Synopsis of study

This primary objective of this study was to investigate the relationship between ageing and VGSC expression of two specific isoforms, $Na_v1.5$ and $Na_v1.8$, within the right atrium of the human heart. The age-associated ionic remodelling process has been illustrated in the literature in animal studies, however not previously demonstrated in human tissue. Exploring this relationship offers a deeper, pathophysiological insight into the phenomenon of AF prevalent in the elderly population. The study was primarily to compare the expression of these two VGSC isoforms in humans with permanent AF and those in sinus rhythm, excluding as age as a factor by using age-matched samples. Secondly, by the employment of drug manipulation we explored the possibility of modulating VGSC expression through the JNK pathway.

6.1.1 Summary of findings

i. **Negative correlation between increasing age and expression of $Na_v1.5$.**

   Organised in chronological age order (n= 26 patients), we demonstrated $Na_v1.5$ expression of declined with a Pearson's correlation co-efficient of -0.25 (R^2=0.0624): The line gradient demonstrates a decline of 9% Nav1.5 protein per decade of ageing. When organised into groups of oldest and youngest patients in our cohort, the $Na_v1.5$ protein expression exhibited a 18.8% decrease in the older group (n=10; t-test, P=0.18).

ii. **Positive correlation between increasing age and expression of $Na_v1.8$.** In the same patients organised in chronological age order (n= 26 patients), we demonstrated $Na_v1.8$ expression rose with a Pearson's correlation co-efficient of +0.259 (R^2 = 0.067): The line gradient demonstrates a rise of 16% Nav1.8 protein per decade of ageing. When organised into groups of oldest and youngest in our cohort, $Na_v1.8$ protein expression was significantly increased by 32% in the older group (t-test, P=<0.05).

iii. **When matched on age, patients in AF had significantly reduced expression of $Na_v1.5$.** For the first time, human subjects in AF were found to possess significantly reduced expression of the $Na_v1.5$ cardiac isoform at 52% less when compared with their age-matched, comorbidity matched counterparts in sinus rhythm (t-test, P=<0.05).

iv. **Total JNK expression in significantly increased in elderly patients.** We demonstrated a 56 % increase in total JNK protein expression a compared within tissue samples from the oldest patients to the youngest patients (n=9, t-test P=<0.05), however, no significance difference was found in the same patient comparisons for P-JNK protein expression.

v. **Expression of $Na_v1.8$ and $Na_v1.5$ can be modulated through drug manipulation of the JNK pathway.** Unfortunately, the drug manipulation arm of our study was severely disrupted due to the covid-19 pandemic. However, following the development of a protocol for cardiac slicing of human right atrial appendage and drug manipulation, we found that SP600125 seemed to significantly

decrease the expression of this isoform compared to the control. New data from our laboratory has since been released which has much more convincingly supported this notion that both $Na_v1.5$ and $Na_v1.8$ expression is influenced through the activation and inhibition of JNK.

vi. **JNK activation through Anisomycin significantly reduces the expression of $Na_v1.5$.** This is a particularly novel result through new data from our lab suggesting that as total JNK increases expression of $Na_v1.5$ decreases with a 46% reduction in expression of $Na_v1.5$ in comparison to the control P=0.04.

vii. **JNK inhibition through SP600125 significantly reduces the expression of $Na_v1.8$.** Again, extremely novel data which suggests that through the inhibition of JNK expression, the potentially pathological expression of $Na_v1.8$ is significantly reduced by 40% when compared to control P=0.048.

6.2 General discussion

In recent decades, the literature has frequently alluded to age being a determinant factor in VGSC remodelling, and consequent arrhythmia, in animal studies (Baba et al., 2006; Cooper & Jones, 2015; Huang et al., 2015; Henry et al., 2016; Ahmad et al., 2019c). For the first time, we have elucidated the nature of this correlation of ageing and sodium channel expression within the human heart. The ageing process fundamentally reshapes the cellular landscape of the cardiomyocyte. The key protein required for adequate depolarisation within the heart is gradually lost, and instead there is an upregulation of a channel (that primarily operates in neuronal tissue) a sodium current which has been

demonstrated by others to be pathological (Yang et al., 2012b; Bezzina et al., 2013; Savio-Galimberti et al., 2014; Chen et al., 2016; Dybkova et al., 2018; Macri et al., 2018a). Our observation that tissue donated form older patients demonstrated increased expression of $Na_v1.8$ coupled with a reduced of $Na_v1.5$ now offers a novel explanation to the development of AF in the elderly population: There are an increased number of sodium channels exhibiting the late sodium current, thus priming the cardiomyocyte into a longer duration of action potential, whilst a loss of the native channel leads to poor availability of sodium ions at the critical depolarisation phase, ultimately contributing to a susceptibly to arrhythmogenesis. The proarrhythmic nature of the $Na_v1.8$ channel has been previously documented in the literature and as such has become the target of novel approaches in treating AF (Makielski & Valdivia, 2006; Savio-Galimberti et al., 2014; Chen et al., 2016; Macri et al., 2018b; Rivaud et al., 2018a; Ahmad et al., 2019a).

Our novel data demonstrates that expression of $Na_v1.5$ is more than halved in humans diagnosed with AF compared with those patients in sinus rhythm (we removed age as a factor due to age-matched patients). The precise biomechanics of VGSC remodelling is still unclear, though studies have suggested that JNK plays a regulatory role in the expression of channel proteins, with examples already in the literature of Cx43 (Petrich et al., 2002; Yan et al., 2013; Yan et al., 2018). Our data supports this through the demonstration of significant increases in JNK expression in older patients, thus strongly implies a potential cellular mechanism linking the remodelling of sodium channels with JNK. We have observed through newly released data from our labs that JNK expression does indeed have a role to play in the modulation of VGSC expression in the human heart. This data begins to fill in the gaps in the molecular physiology underpinning the

ionic remodelling observed with age, offering a deeper insight into the modulation of VGSC and the susceptibility of the ageing heart to arrhythmia.

6.2.1 Recommendations for future research

The use of human right atrial appendage is a massively underutilised approach. Commonly discarded as clinical waste during cardiac surgery, this tissue is invaluable for basic science research. If more resources were allocated to sampling and freezing of this tissue, the possibilities for unravelling human disease mechanisms are limitless. Generating a bank of human tissue would allow for more detailed study and ultimately produce more robust generalisable data. It would also allow for more time of the researcher to be spent in the laboratory conducting the experiments; as the process of finding appropriate patients, consenting them, collecting and transporting the samples has been a significantly time costly endeavour in these studies. Integrating the practice of collecting right atrial appendage in cardiac surgery-where safe, would supercharge the field of basic science cardiovascular research. This could produce large scale studies spanning across both clinical and basic science domains, building powerful alliances proving fruitful for both parties. The capability to rapidly uncover new knowledge of disease, and ultimately novel treatment approaches would of course be of innumerable value to the patients whom we ultimately serve.

In terms of direction of research, functional studies measuring and blocking sodium currents in human tissue of patients with AF would be the next logical step. Researchers in Germany have done this with patients with left ventricular hypertrophy as well as heart failure (Dybkova et al., 2018; Ahmad et al., 2019a). Demonstrating the structural

remodelling of human cardiomyocytes is only part of the story, illustrating the functional consequences provides a much richer perspective of these channels and their role in the disease process. The pharmacological manipulation of sodium channel expression is a tremendously exciting concept, and the relationship of modulatory proteins such as JNK needs to be investigated fully. Currently, there is much focus in blocking pathological currents produced by the $Na_v1.8$ channel. To inhibit the upregulation of this channel in the first place and be able to prevent the diminishment of the native cardiac isoform could be the next revolutionary step in this field of research.

6.3 Conclusion

In conclusion this study has provided novel data, affirming the relationships of VGSCs $Na_v1.5$ and $Na_v1.8$ expression with age in human subjects. The downregulation of $Na_v1.5$ protein expression has been demonstrated for the first-time in humans in AF, whilst the exhibiting a. We have offered early suggestions that the expression of VGSCs may be modulated through pharmacological manipulation of JNK-offering a novel link in the biomechanics of ionic remodelling in the ageing human heart.

As research in this field continues to gain the attention of academics and clinicians alike, pressing forward in unravelling the apparatus underlying arrhythmia will be paramount, as prevalence of AF continues to pose significant challenges across healthcare systems worldwide. Novel therapeutic approaches in targeting sodium currents are proving promising through multiple large scale clinical studies. And the ongoing collaboration of the basic sciences with clinical practitioners in the field of cardiac electrophysiology is a tremendously exciting prospect, offering the potential for significant and applicable patient orientated research.

Bibliography

Ahmad, S., Tirilomis, P., Pabel, S., Dybkova, N., Hartmann, N., Molina, C. E., Tirilomis, T., Kutschka, I., Frey, N., Maier, L. S., Hasenfuss, G., Streckfuss-Bomeke, K. & Sossalla, S. (2019a) The functional consequences of sodium channel NaV 1.8 in human left ventricular hypertrophy. *ESC Heart Failure*, 6(1), 154-163.

Ahmad, S., Valli, H., Smyth, R., Jiang, A. Y., Jeevaratnam, K., Matthews, H. R. & Huang, C. L. H. (2019c) Reduced cardiomyocyte Na+ current in the age-dependent murine Pgc-1(-/-) model of ventricular arrhythmia. *Journal of Cellular Physiology*, 234(4), 3921-3932.

Akopian, A. N., Sivilotti, L. & Wood, J. N. (1996) A tetrodotoxin-resistant voltage-gated sodium channel expressed by sensory neurons. *Nature*, 379(6562), 257-62.

Alpert, J. S., Petersen, P. & Godtfredsen, J. (1988) Atrial fibrillation: natural history, complications, and management. *Annual Review of Medicine*, 39, 41-52.

Antzelevitch, C., Belardinelli, L., Zygmunt, A. C., Burashnikov, A., Di Diego, J. M., Fish, J. M., Cordeiro, J. M. & Thomas, G. (2004) Electrophysiological effects of ranolazine, a novel antianginal agent with antiarrhythmic properties. *Circulation*, 110(8), 904-10.

Anyukhovsky, E. P., Sosunov, E. A., Chandra, P., Rosen, T. S., Boyden, P. A., Danilo, P., Jr. & Rosen, M. R. (2005) Age-associated changes in electrophysiologic remodeling: a potential contributor to initiation of atrial fibrillation. *Cardiovascular Research*, 66(2), 353-363.

Archer, M. D. (1989) Genesis of the Nernst Equation, *Electrochemistry, Past and Present*. ACS Symposium SeriesAmerican Chemical Society, 115-126.

Ariyarajah, V., Fernandes, J., Kranis, M., Apiyasawat, S., Mercado, K. & Spodick, D. H. (2007) Prospective evaluation of atrial tachyarrhythmias in patients with interatrial block. *International Journal of Cardiology*, 118(3), 332-7.

Baba, S., Dun, W., Hirose, M. & Boyden, P. A. (2006) Sodium current function in adult and aged canine atrial cells. *American Journal of Physiology-Heart and Circulatory Physiology*, 291(2), H756-H761.

Bachmann, G. (1916) The Inter-Auricular Time Interval. *American Journal of Physiology*, 41(3), 309-320.

Begg, G. A., Holden, A. V., Lip, G. Y., Plein, S. & Tayebjee, M. H. (2016) Assessment of atrial fibrosis for the rhythm control of atrial fibrillation. *International Journal of Cardiology*, 220, 155-61.

Belardinelli, L., Shryock, J. C. & Fraser, H. (2006) Inhibition of the late sodium current as a potential cardioprotective principle: effects of the late sodium current inhibitor ranolazine. *Heart*, 92 Suppl 4, iv6-iv14.

Benjamin, E. J., Wolf, P. A., D'Agostino, R. B., Silbershatz, H., Kannel, W. B. & Levy, D. (1998) Impact of atrial fibrillation on the risk of death: the Framingham Heart Study. *Circulation*, 98(10), 946-52.

Bennett, B. L., Sasaki, D. T., Murray, B. W., O'Leary, E. C., Sakata, S. T., Xu, W., Leisten, J. C., Motiwala, A., Pierce, S., Satoh, Y., Bhagwat, S. S., Manning, A. M. & Anderson, D. W. (2001) SP600125, an anthrapyrazolone inhibitor of Jun N-terminal kinase. *Procceedings of the National Acadamy of Sciences USA*, 98(24), 13681-6.

Bers, D. M. (2002) Cardiac excitation-contraction coupling. *Nature*, 415(6868), 198-205.

Bezzina, C. R., Barc, J., Mizusawa, Y., Remme, C. A., Gourraud, J.-B., Simonet, F., Verkerk, A. O., Schwartz, P. J., Crotti, L., Dagradi, F., Guicheney, P., Fressart, V., Leenhardt, A., Antzelevitch, C., Bartkowiak, S., Borggrefe, M., Schimpf, R., Schulze-Bahr, E., Zumhagen, S., Behr, E. R., Bastiaenen, R., Tfelt-Hansen, J., Olesen, M. S., Kääb, S., Beckmann, B. M., Weeke, P., Watanabe, H., Endo, N., Minamino, T., Horie, M., Ohno, S., Hasegawa, K., Makita, N., Nogami, A., Shimizu, W., Aiba, T., Froguel, P., Balkau, B., Lantieri, O., Torchio, M., Wiese, C., Weber, D., Wolswinkel, R., Coronel, R., Boukens, B. J., Bézieau, S., Charpentier, E., Chatel, S., Despres, A., Gros, F., Kyndt, F., Lecointe, S., Lindenbaum, P., Portero, V., Violleau, J., Gessler, M., Tan, H. L., Roden, D. M., Christoffels, V. M., Le Marec, H., Wilde, A. A., Probst, V., Schott, J.-J., Dina, C. & Redon, R. (2013) Common variants at SCN5A-SCN10A and HEY2 are associated with Brugada syndrome, a rare disease with high risk of sudden cardiac death. *Nature Genetics*, 45(9), 1044-1049.

Biernacka, A. & Frangogiannis, N. G. (2011) Aging and Cardiac Fibrosis. *Aging and Disease*, 2(2), 158-173.

Biet, M., Barajas-Martinez, H., Ton, A. T., Delabre, J. F., Morin, N. & Dumaine, R. (2012) About half of the late sodium current in cardiac myocytes from dog ventricle is due to

non-cardiac-type Na(+) channels. *Journal of Molecular and Cellular Cardiology*, 53(5), 593-8.

Bogoyevitch, M. A., Ngoei, K. R., Zhao, T. T., Yeap, Y. Y. & Ng, D. C. (2010) c-Jun N-terminal kinase (JNK) signaling: recent advances and challenges. *Biochimica et Biophysica Acta*, 1804(3), 463-75.

Bootman, M. D., Smyrnias, I., Thul, R., Coombes, S. & Roderick, H. L. (2011) Atrial cardiomyocyte calcium signalling. *Biochimica et Biophysica Acta*, 1813(5), 922-34.

Brandenburg, S., Arakel, E. C., Schwappach, B. & Lehnart, S. E. (2016) The molecular and functional identities of atrial cardiomyocytes in health and disease. *Biochimica et Biophysica Acta*, 1863(7 Pt B), 1882-93.

Brundel, B. J., Van Gelder , I. C., Henning, R. H., Tieleman, R. G., Tuinenburg, A. E., Wietses, M., Grandjean, J. G., Van Gilst , W. H. & Crijns, H. J. (2001) Ion channel remodeling is related to intraoperative atrial effective refractory periods in patients with paroxysmal and persistent atrial fibrillation. *Circulation*, 103(5), 684-90.

Burashnikov, A. & Antzelevitch, C. (2013) Role of late sodium channel current block in the management of atrial fibrillation. *Cardiovascular Drugs and Therapy*, 27(1), 79-89.

Burashnikov, A., Di Diego, J. M., Barajas-Martinez, H., Hu, D., Cordeiro, J. M., Moise, N. S., Kornreich, B. G., Belardinelli, L. & Antzelevitch, C. (2014) Ranolazine effectively

suppresses atrial fibrillation in the setting of heart failure. *Circulation Heart Failure*, 7(4), 627-33.

Burashnikov, A., Di Diego, J. M., Zygmunt, A. C., Belardinelli, L. & Antzelevitch, C. (2007) Atrium-selective sodium channel block as a strategy for suppression of atrial fibrillation: differences in sodium channel inactivation between atria and ventricles and the role of ranolazine. *Circulation*, 116(13), 1449-57.

Burstein, B., Comtois, P., Michael, G., Nishida, K., Villeneuve, L., Yeh, Y. H. & Nattel, S. (2009) Changes in connexin expression and the atrial fibrillation substrate in congestive heart failure. *Circulation Research*, 105(12), 1213-22.

Burstein, B., Qi, X. Y., Yeh, Y. H., Calderone, A. & Nattel, S. (2007) Atrial cardiomyocyte tachycardia alters cardiac fibroblast function: a novel consideration in atrial remodeling. *Cardiovascular Research*, 76(3), 442-52.

Carstensen, H., Hesselkilde, E. Z., Haugaard, M. M., Flethøj, M., Carlson, J., Pehrson, S., Jespersen, T., Platonov, P. G. & Buhl, R. (2019) Effects of dofetilide and ranolazine on atrial fibrillatory rate in a horse model of acutely induced atrial fibrillation. *Journal of Cardiovascular Electrophysiology*, 30(4), 596-606.

Catterall, W. A., Goldin, A. L. & Waxman, S. G. (2005) International Union of Pharmacology. XLVII. Nomenclature and structure-function relationships of voltage-gated sodium channels. *Pharmacology Review*, 57(4), 397-409.

Caves, R. E., Cheng, H. W., Choisy, S. C., Gadeberg, H. C., Bryant, S. M., Hancox, J. C. & James, A. F. (2017) Atrial-ventricular differences in rabbit cardiac voltage-gated Na+ currents: Basis for atrial-selective block by ranolazine. *Heart Rhythm*, 14(11), 1657-1664.

Chambers, J. W. & LoGrasso, P. V. (2011) Mitochondrial c-Jun N-terminal kinase (JNK) signaling initiates physiological changes resulting in amplification of reactive oxygen species generation. *Journal of Biological Chemistry*, 286(18), 16052-62.

Chen, X. M., Yu, L. L., Shi, S. B., Jiang, H., Huang, C. X., Desai, M., Li, Y. G., Barajas-Martinez, H. & Hu, D. (2016) Neuronal Na(v)1.8 Channels as a Novel Therapeutic Target of Acute Atrial Fibrillation Prevention. *Journal of the American Heart Association*, 5(11).

Chugh, S. S., Havmoeller, R., Narayanan, K., Singh, D., Rienstra, M., Benjamin, E. J., Gillum, R. F., Kim, Y. H., McAnulty, J. H., Jr., Zheng, Z. J., Forouzanfar, M. H., Naghavi, M., Mensah, G. A., Ezzati, M. & Murray, C. J. (2014) Worldwide epidemiology of atrial fibrillation: a Global Burden of Disease 2010 Study. *Circulation*, 129(8), 837-47.

Clarke, J. D., Piccini, J. P. & Friedman, D. J. (2021) The role of posterior wall isolation in catheter ablation of persistent atrial fibrillation. *Journal of Cardiovascular Electrophysiology*, 32(9), 2567-2576.

Colombo, A., Bastone, A., Ploia, C., Sclip, A., Salmona, M., Forloni, G. & Borsello, T. (2009) JNK regulates APP cleavage and degradation in a model of Alzheimer's disease. *Neurobiology of Disease*, 33(3), 518-25.

Cooper, S. & Jones, S. (2015) 201 Age-Associated Decline in $Na_v1.4$ and $Na_v.5$ Isoforms of the Sodium Channel in Rat Heart. *Heart*, 101(Suppl 4), A111-A111.

Curran, J. & Mohler, P. J. (2015) Alternative paradigms for ion channelopathies: disorders of ion channel membrane trafficking and posttranslational modification. *Annual Review of Physiology*, 77, 505-24.

Darbar, D., Kannankeril, P. J., Donahue, B. S., Kucera, G., Stubblefield, T., Haines, J. L., George, A. L. & Roden, D. M. (2008) Cardiac sodium channel (SCN5A) variants associated with atrial fibrillation. *Circulation*, 117(15), 1927-1935.

Davidson (2010) *Davidson's Principles and Practice of Medicine*, 21 edition.Elsevier.

De Ferrari, G. M., Maier, L. S., Mont, L., Schwartz, P. J., Simonis, G., Leschke, M., Gronda, E., Boriani, G., Darius, H., Guillamon Toran, L., Savelieva, I., Dusi, V., Marchionni, N., Quintana Rendon, M., Schumacher, K., Tonini, G., Melani, L., Giannelli, S., Alberto Maggi, C. & Camm, A. J. (2015) Ranolazine in the treatment of atrial fibrillation: Results of the dose-ranging RAFFAELLO (Ranolazine in Atrial Fibrillation Following An ELectricaL CardiOversion) study. *Heart Rhythm*, 12(5), 872-8.

DeMarco, K. R. & Clancy, C. E. (2016) Cardiac Na Channels: Structure to Function. *Current Topics In Membranes*, 78, 287-311.

Drake, R. (2014) Grey's Anatomy for Students. 3rd edition edition.: Churchil Livingstone.

Dubois, J. M. & Bergman, C. (1975) Late sodium current in the node of Ranvier. *Pflugers Archives*, 357(1-2), 145-8.

Dun, W. & Boyden, P. A. (2009) Aged atria: electrical remodeling conducive to atrial fibrillation. *Journal of Interventional Cardiac Electrophysiology*, 25(1), 9-18.

Dybkova, N., Ahmad, S., Pabel, S., Tirilomis, P., Hartmann, N., Fischer, T. H., Bengel, P., Tirilomis, T., Ljubojevic, S., Renner, A., Gummert, J., Ellenberger, D., Wagner, S., Frey, N., Maier, L. S., Streckfuss-Bomeke, K., Hasenfuss, G. & Sossalla, S. (2018) Differential regulation of sodium channels as a novel proarrhythmic mechanism in the human failing heart. *Cardiovascular Research*, 114(13), 1728-1737.

Eisner, D. A., Caldwell, J. L., Kistamás, K. & Trafford, A. W. (2017) Calcium and Excitation-Contraction Coupling in the Heart. *Circulation Research*, 121(2), 181-195.

Ellermann, C., Kohnke, A., Dechering, D. G., Kochhäuser, S., Reinke, F., Fehr, M., Eckardt, L. & Frommeyer, G. (2018) Ranolazine Prevents Levosimendan-Induced Atrial Fibrillation. *Pharmacology*, 102(3-4), 138-141.

Ellinor, P. T., Nam, E. G., Shea, M. A., Milan, D. J., Ruskin, J. N. & MacRae, C. A. (2008) Cardiac sodium channel mutation in atrial fibrillation. *Heart Rhythm*, 5(1), 99-105.

England, P. H. (2017) *Atrial fibrillation prevalence estimatesin England.* (2014778). https://www.gov.uk/government/publications/atrial-fibrillation-prevalence-estimates-for-local-populations: Available online:

https://assets.publishing.service.gov.uk/government/uploads/system/uploads/attachment_data/file/644869/atrial_fibrillation_AF_briefing.pdf [Accessed 27/11/2018].

Enyedi, P. & Czirják, G. (2010) Molecular background of leak K+ currents: two-pore domain potassium channels. *Physiology Review*, 90(2), 559-605.

Fang, Z., Jiang, Y., Wang, Y. F., Lin, Y., Liu, Y. W., Zhao, L. Y., Xu, Y., Toorabally, M. B., He, S. H. & Zhang, F. X. (2016) The rs6771157 C/G polymorphism in SCN10A is associated with the risk of atrial fibrillation in a Chinese Han population. *Scientific Reports*, 6.

Freeman, J. V., Wang, Y., Akar, J., Desai, N. & Krumholz, H. (2017) National Trends in Atrial Fibrillation Hospitalization, Readmission, and Mortality for Medicare Beneficiaries, 1999-2013. *Circulation*, 135(13), 1227-1239.

Frustaci, A., Chimenti, C., Bellocci, F., Morgante, E., Russo, M. A. & Maseri, A. (1997) Histological substrate of atrial biopsies in patients with lone atrial fibrillation. *Circulation*, 96(4), 1180-4.

Fuster, V., Rydén, L. E., Cannom, D. S., Crijns, H. J., Curtis, A. B., Ellenbogen, K. A., Halperin, J. L., Le Heuzey, J. Y., Kay, G. N., Lowe, J. E., Olsson, S. B., Prystowsky, E. N., Tamargo, J. L., Wann, S., Smith, S. C., Jacobs, A. K., Adams, C. D., Anderson, J. L., Antman, E. M., Hunt, S. A., Nishimura, R., Ornato, J. P., Page, R. L., Riegel, B., Priori, S. G., Blanc, J. J., Budaj, A., Camm, A. J., Dean, V., Deckers, J. W., Despres, C., Dickstein, K., Lekakis, J., McGregor, K., Metra, M., Morais, J., Osterspey, A., Zamorano, J. L., Cardiology, A. C. o.,

Force, A. H. A. T., Guidelines, E. S. o. C. C. f. P., Association, E. H. R. & Society, H. R. (2006) ACC/AHA/ESC 2006 guidelines for the management of patients with atrial fibrillation: full text: a report of the American College of Cardiology/American Heart Association Task Force on practice guidelines and the European Society of Cardiology Committee for Practice Guidelines (Writing Committee to Revise the 2001 guidelines for the management of patients with atrial fibrillation) developed in collaboration with the European Heart Rhythm Association and the Heart Rhythm Society. *Europace*, 8(9), 651-745.

Gillet, L., Shy, D. & Abriel, H. (2014) Elucidating sodium channel NaV1.5 clustering in cardiac myocytes using super-resolution techniques, *Cardiovascular Research*. Translated from eng by. England, 231-3.

Glukhov, A. V., Balycheva, M., Sanchez-Alonso, J. L., Ilkan, Z., Alvarez-Laviada, A., Bhogal, N., Diakonov, I., Schobesberger, S., Sikkel, M. B., Bhargava, A., Faggian, G., Punjabi, P. P., Houser, S. R. & Gorelik, J. (2015) Direct Evidence for Microdomain-Specific Localization and Remodeling of Functional L-Type Calcium Channels in Rat and Human Atrial Myocytes. *Circulation*, 132(25), 2372-84.

Go, A. S., Hylek, E. M., Phillips, K. A., Chang, Y., Henault, L. E., Selby, J. V. & Singer, D. E. (2001) Prevalence of diagnosed atrial fibrillation in adults: national implications for rhythm management and stroke prevention: the AnTicoagulation and Risk Factors in Atrial Fibrillation (ATRIA) Study. *Journal of the American Medical Association*, 285(18), 2370-5.

Goldin, A. L. (2003) Mechanisms of sodium channel inactivation. *Current Opinion in Neurobiology*, 13(3), 284-90.

Goldin, A. L., Barchi, R. L., Caldwell, J. H., Hofmann, F., Howe, J. R., Hunter, J. C., Kallen, R. G., Mandel, G., Meisler, M. H., Netter, Y. B., Noda, M., Tamkun, M. M., Waxman, S. G., Wood, J. N. & Catterall, W. A. (2000) Nomenclature of Voltage-Gated Sodium Channels. *Neuron*, 28(2), 365-368.

Grandi, E., Pandit, S. V., Voigt, N., Workman, A. J., Dobrev, D., Jalife, J. & Bers, D. M. (2011) Human atrial action potential and Ca2+ model: sinus rhythm and chronic atrial fibrillation. *Circulation Research*, 109(9), 1055-66.

Grubb, N. R., Elder, D., Broadhurst, P., Reoch, A., Tassie, E. & Neilson, A. (2019) Atrial fibrillation case finding in over 65 s with cardiovascular risk factors - Results of initial Scottish clinical experience. *International Journal of Cardiology*, 288, 94-99.

Guzadhur, L., Pearcey, S. M., Duehmke, R. M., Jeevaratnam, K., Hohmann, A. F., Zhang, Y., Grace, A. A., Lei, M. & Huang, C. L. H. (2010) Atrial arrhythmogenicity in aged Scn5a+/ΔKPQ mice modeling long QT type 3 syndrome and its relationship to Na+channel expression and cardiac conduction. *Pflugers Archive; European Journal of Physiology*, 460(3), 593-601.

Han, M., Zhang, Y., Sun, S., Wang, Z., Wang, J., Xie, X., Gao, M., Yin, X. & Hou, Y. (2013) Renin-angiotensin system inhibitors prevent the recurrence of atrial fibrillation: a meta-

analysis of randomized controlled trials. *Journal of Cardiovascular Pharmacology*, 62(4), 405-15.

Hao, X., Zhang, Y., Zhang, X., Nirmalan, M., Davies, L., Konstantinou, D., Yin, F., Dobrzynski, H., Wang, X., Grace, A., Zhang, H., Boyett, M., Huang, C. L. & Lei, M. (2011) TGF-β1-mediated fibrosis and ion channel remodeling are key mechanisms in producing the sinus node dysfunction associated with SCN5A deficiency and aging. *Circulation Arrhythmia and Electrophysiology*, 4(3), 397-406.

Haïssaguerre, M., Jaïs, P., Shah, D. C., Takahashi, A., Hocini, M., Quiniou, G., Garrigue, S., Le Mouroux, A., Le Métayer, P. & Clémenty, J. (1998) Spontaneous initiation of atrial fibrillation by ectopic beats originating in the pulmonary veins. *New England Journal of Medicine*, 339(10), 659-66.

Henry, B. L., Gabris, B., Li, Q., Martin, B., Giannini, M., Parikh, A., Patel, D., Haney, J., Schwartzman, D. S., Shroff, S. G. & Salama, G. (2016) Relaxin suppresses atrial fibrillation in aged rats by reversing fibrosis and upregulating Na+ channels. *Heart Rhythm*, 13(4), 983-991.

Herruzo-Rojas, M. S., Martín-Toro, M. A. & Carrillo-Bailén, M. (2019) Ranolazine in chronic ischaemic heart disease: a protective factor against de novo atrial fibrillation. *Revista Colombiana de Cardiologia 27(5), 400-404*.

Ho, S. Y. & Sánchez-Quintana, D. (2009) The importance of atrial structure and fibers. *Clinical Anatomy*, 22(1), 52-63.

Horvath, B., Banyasz, T., Jian, Z., Hegyi, B., Kistamas, K., Nanasi, P. P., Izu, L. T. & Chen-Izu, Y. (2013) Dynamics of the late Na(+) current during cardiac action potential and its contribution to afterdepolarizations. *Journal of Molecular and Cellular Cardiology*, 64, 59-68.

Huang, X., Du, Y., Yang, P., Lin, S. F., Xi, Y. T., Yang, Z. & Ma, A. Q. (2015) Age-dependent alterations of voltage-gated Na+ channel isoforms in rat sinoatrial node. *Mechanisms of Ageing and Development*, 152, 80-90.

Israel, C. W., Grönefeld, G., Ehrlich, J. R., Li, Y. G. & Hohnloser, S. H. (2004) Long-term risk of recurrent atrial fibrillation as documented by an implantable monitoring device: implications for optimal patient care. *Journal of American Collective of Cardiology*, 43(1), 47-52.

Iwasaki, Y. K., Nishida, K., Kato, T. & Nattel, S. (2011) Atrial fibrillation pathophysiology: implications for management. *Circulation*, 124(20), 2264-74.

Johnson, J. N., Tester, D. J., Perry, J., Salisbury, B. A., Reed, C. R. & Ackerman, M. J. (2008) Prevalence of early-onset atrial fibrillation in congenital long QT syndrome. *Heart Rhythm*, 5(5), 704-9.

Jones, S., Steer, E., Haqzad, Y., Tahir, Z. & Loubani, M. (2018) Total JNK Protein Eexpression Is Elevated In Patients Diagnosed With Hypertension Or

Hypercholesterolaemia, Wheras Activated-JNK Is Raised In Patients Recieving Pharmacological Treatment. *Heart*, 104, A110-A110.

Kamkin, A. G. & Kiseleva, I. S. (1998) Heart fibroblasts, the mechanism of the appearance of their potentials and their possible role in regulating cardiac work. *Uspekhi Fiziologicheskikh Nauk*, 29(1), 72-102.

Kataoka, N., Nishida, K., Kinoshita, K., Sakamoto, T., Nakatani, Y., Tsujino, Y., Mizumaki, K., Inoue, H. & Kinugawa, K. (2016) Effect of irbesartan on development of atrial fibrosis and atrial fibrillation in a canine atrial tachycardia model with left ventricular dysfunction, association with p53. *Heart Vessels*, 31(12), 2053-2060.

Kato, T., Yamashita, T., Sagara, K., Iinuma, H. & Fu, L. T. (2004) Progressive nature of paroxysmal atrial fibrillation. Observations from a 14-year follow-up study. *Circulation*, 68(6), 568-72.

Kaufmann, S. G., Westenbroek, R. E., Maass, A. H., Lange, V., Renner, A., Wischmeyer, E., Bonz, A., Muck, J., Ertl, G., Catterall, W. A., Scheuer, T. & Maier, S. K. G. (2013) Distribution and function of sodium channel subtypes in human atrial myocardium. *Journal of Molecular and Cellular Cardiology*, 61, 133-141.

Kerr, C. R., Humphries, K. H., Talajic, M., Klein, G. J., Connolly, S. J., Green, M., Boone, J., Sheldon, R., Dorian, P. & Newman, D. (2005) Progression to chronic atrial fibrillation after the initial diagnosis of paroxysmal atrial fibrillation: results from the Canadian Registry of Atrial Fibrillation. *American Heart Journal*, 149(3), 489-96.

Kistler, P. M., Sanders, P., Fynn, S. P., Stevenson, I. H., Spence, S. J., Vohra, J. K., Sparks, P. B. & Kalman, J. M. (2004) Electrophysiologic and electroanatomic changes in the human atrium associated with age. *Journal of the American College of Cardiology*, 44(1), 109-116.

Kohl, P., Kamkin, A. G., Kiseleva, I. S. & Noble, D. (1994) Mechanosensitive fibroblasts in the sino-atrial node region of rat heart: interaction with cardiomyocytes and possible role. *Experimental Physiology*, 79(6), 943-56.

Krijthe, B. P., Kunst, A., Benjamin, E. J., Lip, G. Y., Franco, O. H., Hofman, A., Witteman, J. C., Stricker, B. H. & Heeringa, J. (2013) Projections on the number of individuals with atrial fibrillation in the European Union, from 2000 to 2060. *European Heart Journal*, 34(35), 2746-51.

Larson, E. D., St Clair, J. R., Sumner, W. A., Bannister, R. A. & Proenza, C. (2013) Depressed pacemaker activity of sinoatrial node myocytes contributes to the age-dependent decline in maximum heart rate. *Proceedings of the National Academy of Sciences USA*, 110(44), 18011-6.

Legato, M. J. (1973) Ultrastructure of the atrial, ventricular, and Purkinje cell, with special reference to the genesis of arrhythmias. *Circulation*, 47(1), 178-89.

Li, Q., Huang, H., Liu, G., Lam, K., Rutberg, J., Green, M. S., Birnie, D. H., Lemery, R., Chahine, M. & Gollob, M. H. (2009) Gain-of-function mutation of Nav1.5 in atrial

fibrillation enhances cellular excitability and lowers the threshold for action potential firing. *Biochemical and Biophysical Research Communications*, 380(1), 132-7.

Liu, Y., Song, Z., Jiang, W., Wu, S., Liu, X. & Qin, M. (2022) Right atrial appendage: an important structure to drive atrial fibrillation. *Journal of Interventional Cardiac Electrophysiology*.

Lévy, S. (1998) Epidemiology and classification of atrial fibrillation. *Journal of Cardiovascular Electrophysiology*, 9(8 Suppl), S78-82.

Macri, V., Brody, J. A., Arking, D. E., Hucker, W. J., Yin, X., Lin, H., Mills, R. W., Sinner, M. F., Lubitz, S. A., Liu, C. T., Morrison, A. C., Alonso, A., Li, N., Fedorov, V. V., Janssen, P. M., Bis, J. C., Heckbert, S. R., Dolmatova, E. V., Lumley, T., Sitlani, C. M., Cupples, L. A., Pulit, S. L., Newton-Cheh, C., Barnard, J., Smith, J. D., Van Wagoner, D. R., Chung, M. K., Vlahakes, G. J., O'Donnell, C. J., Rotter, J. I., Margulies, K. B., Morley, M. P., Cappola, T. P., Benjamin, E. J., Muzny, D., Gibbs, R. A., Jackson, R. D., Magnani, J. W., Herndon, C. N., Rich, S. S., Psaty, B. M., Milan, D. J., Boerwinkle, E., Mohler, P. J., Sotoodehnia, N. & Ellinor, P. T. (2018a) Common Coding Variants in SCN10A Are Associated With the Nav1.8 Late Current and Cardiac Conduction. *Circulation Genomic and Precision Medicine*, 11(5), e001663.

Makielski, J. C. & Valdivia, C. R. (2006) Ranolazine and late cardiac sodium current--a therapeutic target for angina, arrhythmia and more? *British journal of pharmacology*, 148(1), 4-6.

Makiyama, T., Akao, M., Shizuta, S., Doi, T., Nishiyama, K., Oka, Y., Ohno, S., Nishio, Y., Tsuji, K., Itoh, H., Kimura, T., Kita, T. & Horie, M. (2008) A novel SCN5A gain-of-function mutation M1875T associated with familial atrial fibrillation. *Journal of the American College of Cardiology*, 52(16), 1326-34.

Maltsev, V. A., Kyle, J. W., Mishra, S. & Undrovinas, A. (2008) Molecular identity of the late sodium current in adult dog cardiomyocytes identified by Nav1.5 antisense inhibition. *American journal of physiology. Heart and circulatory physiology*, 295(2), H667-H676.

Manning, W. J., Silverman, D. I., Katz, S. E., Riley, M. F., Come, P. C., Doherty, R. M., Munson, J. T. & Douglas, P. S. (1994) Impaired left atrial mechanical function after cardioversion: relation to the duration of atrial fibrillation. *Journal of the American College of Cardiology*, 23(7), 1535-40.

Mao, W., You, T., Ye, B., Li, X., Dong, H. H., Hill, J. A., Li, F. & Xu, H. (2012) Reactive oxygen species suppress cardiac NaV1.5 expression through Foxo1. *Public Library of Science One*, 7(2), e32738.

McNair, W. P., Ku, L., Taylor, M. R., Fain, P. R., Dao, D., Wolfel, E. & Mestroni, L. (2004) SCN5A mutation associated with dilated cardiomyopathy, conduction disorder, and arrhythmia. *Circulation*, 110(15), 2163-7.

Molina, D. K. & DiMaio, V. J. M. (2015) Normal Organ Weights in Women: Part I—The Heart. *The American Journal of Forensic Medicine and Pathology*, 36(3).

Morrow, D. A., Scirica, B. M., Karwatowska-Prokopczuk, E., Murphy, S. A., Budaj, A., Varshavsky, S., Wolff, A. A., Skene, A., McCabe, C. H. & Braunwald, E. (2007) Effects of ranolazine on recurrent cardiovascular events in patients with non-ST-elevation acute coronary syndromes: the MERLIN-TIMI 36 randomized trial. *Journal of the American Medical Association*, 297(16), 1775-83.

Murphy, N. F., Simpson, C. R., Jhund, P. S., Stewart, S., Kirkpatrick, M., Chalmers, J., MacIntyre, K. & McMurray, J. J. (2007) A national survey of the prevalence, incidence, primary care burden and treatment of atrial fibrillation in Scotland. *Heart*, 93(5), 606-12.

Nabauer, M., Gerth, A., Limbourg, T., Schneider, S., Oeff, M., Kirchhof, P., Goette, A., Lewalter, T., Ravens, U., Meinertz, T., Breithardt, G. & Steinbeck, G. (2009) The Registry of the German Competence NETwork on Atrial Fibrillation: patient characteristics and initial management. *Europace*, 11(4), 423-34.

Naish, J., Revest, P. & Court Syndercombe, D. (2009) *Medical Sciences*, *1*, 1 vols, 1st edition. London, United Kingdom: Elsevier.

Nattel, S., Burstein, B. & Dobrev, D. (2008) Atrial remodeling and atrial fibrillation: mechanisms and implications. *Circulation Arrhythmia and Electrophysiology*, 1(1), 62-73.

Nerbonne, J. M. & Kass, R. S. (2005) Molecular physiology of cardiac repolarization. *Physiology Review*, 85(4), 1205-53.

NICE (2016) *Stable Angina Management.* Available online: https://www.nice.org.uk/guidance/cg126/chapter/1-Guidance#anti-anginal-drug-treatment [Accessed 01/06/2019].

Nieuwlaat, R., Capucci, A., Camm, A. J., Olsson, S. B., Andresen, D., Davies, D. W., Cobbe, S., Breithardt, G., Le Heuzey, J. Y., Prins, M. H., Lévy, S., Crijns, H. J. & Investigators, E. H. S. (2005) Atrial fibrillation management: a prospective survey in ESC member countries: the Euro Heart Survey on Atrial Fibrillation. *European Heart Journal*, 26(22), 2422-34.

Ogawa, T., Hayashi, T., Kyoizumi, S., Kusunoki, Y., Nakachi, K., MacPhee, D. G., Trosko, J. E., Kataoka, K. & Yorioka, N. (2004) Anisomycin downregulates gap-junctional intercellular communication via the p38 MAP-kinase pathway. *Journal of Cellular Sciences*, 117(Pt 10), 2087-96.

Pandit, S. V., Berenfeld, O., Anumonwo, J. M., Zaritski, R. M., Kneller, J., Nattel, S. & Jalife, J. (2005) Ionic determinants of functional reentry in a 2-D model of human atrial cells during simulated chronic atrial fibrillation. *Biophysics Journal*, 88(6), 3806-21.

Pathak, R., Lau, D. H., Mahajan, R. & Sanders, P. (2013) Structural and Functional Remodeling of the Left Atrium: Clinical and Therapeutic Implications for Atrial Fibrillation. *Journal of atrial fibrillation*, 6(4), 986-986.

Petrich, B. G., Gong, X., Lerner, D. L., Wang, X., Brown, J. H., Saffitz, J. E. & Wang, Y. (2002) c-Jun N-terminal kinase activation mediates downregulation of connexin43 in cardiomyocytes. *Circulation Research*, 91(7), 640-7.

Platonov, P. G. (2017) Atrial fibrosis: an obligatory component of arrhythmia mechanisms in atrial fibrillation? *Journal of Geriatrics Cardiology*, 14(3), 174-178.

Ragbaoui, Y., Chehbouni, C., Hammiri, A. E. & Habbal, R. (2017) Epidemiology of the relationship between atrial fibrillation and heart failure. *Pan African Medical Journal*, 26, 116.

Reiffel, J. A., Camm, A. J., Belardinelli, L., Zeng, D., Karwatowska-Prokopczuk, E., Olmsted, A., Zareba, W., Rosero, S. & Kowey, P. (2015) The HARMONY Trial: Combined Ranolazine and Dronedarone in the Management of Paroxysmal Atrial Fibrillation: Mechanistic and Therapeutic Synergism. *Circ Arrhythm Electrophysiol*, 8(5), 1048-56.

Richards, M. A., Clarke, J. D., Saravanan, P., Voigt, N., Dobrev, D., Eisner, D. A., Trafford, A. W. & Dibb, K. M. (2011) Transverse tubules are a common feature in large mammalian atrial myocytes including human. *American Journal of Physiology Heart Circulation Physiology*, 301(5), H1996-2005.

Ritchie, J. M. (1988) Sodium-channel turnover in rabbit cultured Schwann cells. *Proceedings of the Royal Society*, 233(1273), 423-30.

Rivaud, M. R., Baartscheer, A., Verkerk, A. O., Beekman, L., Rajamani, S., Belardinelli, L., Bezzina, C. R. & Remme, C. A. (2018b) Enhanced late sodium current underlies pro-

arrhythmic intracellular sodium and calcium dysregulation in murine sodium channelopathy. *International Journal of Cardiology*, 263, 54-62.

Rodriguez, C. J., Soliman, E. Z., Alonso, A., Swett, K., Okin, P. M., Goff, D. C., Jr. & Heckbert, S. R. (2015) Atrial fibrillation incidence and risk factors in relation to race-ethnicity and the population attributable fraction of atrial fibrillation risk factors: the Multi-Ethnic Study of Atherosclerosis. *Annals of Epidemiology*, 25(2), 71-6, 76.e1.

Ruddox, V., Sandven, I., Munkhaugen, J., Skattebu, J., Edvardsen, T. & Otterstad, J. E. (2017) Atrial fibrillation and the risk for myocardial infarction, all-cause mortality and heart failure: A systematic review and meta-analysis. *European Journal of Preventative Cardiology*, 24(14), 1555-1566.

Salih, M., Abdel-Hafez, O., Ibrahim, R. & Nair, R. (2021) Atrial fibrillation in the elderly population: Challenges and management considerations. *Journal of Arrhythmia*, 37(4), 912-921.

Savio-Galimberti, E., Weeke, P., Muhammad, R., Blair, M., Ansari, S., Short, L., Atack, T. C., Kor, K., Vanoye, C. G., Olesen, M. S., LuCamp, Yang, T., George, A. L., Jr., Roden, D. M. & Darbar, D. (2014) SCN10A/Nav1.8 modulation of peak and late sodium currents in patients with early onset atrial fibrillation. *Cardiovascular Research*, 104(2), 355-63.

Schnabel, R. B., Yin, X., Gona, P., Larson, M. G., Beiser, A. S., McManus, D. D., Newton-Cheh, C., Lubitz, S. A., Magnani, J. W., Ellinor, P. T., Seshadri, S., Wolf, P. A., Vasan, R. S., Benjamin, E. J. & Levy, D. (2015) 50 year trends in atrial fibrillation prevalence,

incidence, risk factors, and mortality in the Framingham Heart Study: a cohort study. *Lancet*, 386(9989), 154-62.

Schotten, U., Verheule, S., Kirchhof, P. & Goette, A. (2011) Pathophysiological mechanisms of atrial fibrillation: a translational appraisal. *Physiology Review*, 91(1), 265-325.

Simopoulos, V., Hevas, A., Hatziefthimiou, A., Dipla, K., Skoularigis, I., Tsilimingas, N. & Aidonidis, I. (2018) Amiodarone plus Ranolazine for Conversion of Post-Cardiac Surgery Atrial Fibrillation: Enhanced Effectiveness in Reduced Versus Preserved Ejection Fraction Patients. *Cardiovascular Drugs and Therapy*, 32(6), 559-565.

Song, Y., Shryock, J. C., Wu, L. & Belardinelli, L. (2004) Antagonism by ranolazine of the pro-arrhythmic effects of increasing late INa in guinea pig ventricular myocytes. *J Cardiovascular Pharmacology*, 44(2), 192-9.

Splawski, I., Timothy, K. W., Tateyama, M., Clancy, C. E., Malhotra, A., Beggs, A. H., Cappuccio, F. P., Sagnella, G. A., Kass, R. S. & Keating, M. T. (2002) Variant of SCN5A sodium channel implicated in risk of cardiac arrhythmia. *Science (New York, N.Y.)*, 297(5585), 1333-1336.

Stadtman, E. R. (1992) Protein oxidation and aging. *Science*, 257(5074), 1220-4.

Stadtman, E. R. (2004) Role of oxidant species in aging. *Current Medicinal Chemistry*, 11(9), 1105-12.

Stewart, S., Murphy, N., Walker, A., McGuire, A. & McMurray, J. J. V. (2007) Cost of an emerging epidemic: an economic analysis of atrial fibrillation in the UK (vol 90, pg 282, 2004). *Heart*, 93(11), 1472-1472.

Stillitano, F., Lonardo, G., Zicha, S., Varro, A., Cerbai, E., Mugelli, A. & Nattel, S. (2008) Molecular basis of funny current (If) in normal and failing human heart. *Journal of Molecular and Cellular Cardiology*, 45(2), 289-99.

Stride, N., Larsen, S., Hey-Mogensen, M., Sander, K., Lund, J. T., Gustafsson, F., Køber, L. & Dela, F. (2013) Decreased mitochondrial oxidative phosphorylation capacity in the human heart with left ventricular systolic dysfunction. *European Journal of Heart Failure*, 15(2), 150-7.

Söhl, G. & Willecke, K. (2004) Gap junctions and the connexin protein family. *Cardiovascular Research*, 62(2), 228-32.

Tsuji, H., Larson, M. G., Venditti, F. J., Jr., Manders, E. S., Evans, J. C., Feldman, C. L. & Levy, D. (1996) Impact of reduced heart rate variability on risk for cardiac events. The Framingham Heart Study. *Circulation*, 94(11), 2850-5.

Vadnais, D. S. & Wenger, N. K. (2010) Emerging clinical role of ranolazine in the management of angina. *Theruptics and Clinical Risk Management*, 6, 517-30.

Voigt, N., Li, N., Wang, Q., Wang, W., Trafford, A. W., Abu-Taha, I., Sun, Q., Wieland, T., Ravens, U., Nattel, S., Wehrens, X. H. & Dobrev, D. (2012) Enhanced sarcoplasmic

reticulum Ca2+ leak and increased Na+-Ca2+ exchanger function underlie delayed afterdepolarizations in patients with chronic atrial fibrillation. *Circulation*, 125(17), 2059-70.

Wakili, R., Voigt, N., Kääb, S., Dobrev, D. & Nattel, S. (2011) Recent advances in the molecular pathophysiology of atrial fibrillation. *Journal of Clinical Investigation*, 121(8), 2955-2968.

Walker, K. E., Lakatta, E. G. & Houser, S. R. (1993) Age associated changes in membrane currents in rat ventricular myocytes. *Cardiovascular Research*, 27(11), 1968-77.

Wang, K., Ho, S. Y., Gibson, D. G. & Anderson, R. H. (1995) Architecture of atrial musculature in humans. *British Heart Journal*, 73(6), 559-65.

Wang, X. & Li, G. (2018) Irbesartan prevents sodium channel remodeling in a canine model of atrial fibrillation. *Journal of Renin Angiotensin Aldosterone System*, 19(1), 1470320318755269.

Wang, Z., Fermini, B. & Nattel, S. (1993) Delayed rectifier outward current and repolarization in human atrial myocytes. *Circulation Research*, 73(2), 276-85.

Wannenburg, T., Heijne, G. H., Geerdink, J. H., Van Den Dool, H. W., Janssen, P. M. & De Tombe, P. P. (2000) Cross-bridge kinetics in rat myocardium: effect of sarcomere length and calcium activation. *American Journal of Physiology Heart Circulation Physiology*, 279(2), H779-90.

Weng, L. C., Lunetta, K. L., Muller-Nurasyid, M., Smith, A. V., Theriault, S., Weeke, P. E., Barnard, J., Bis, J. C., Lyytikainen, L. P., Kleber, M. E., Martinsson, A., Lin, H. J., Rienstra, M., Trompet, S., Krijthe, B. P., Dorr, M., Klarin, D., Chasman, D. I., Sinner, M. F., Waldenberger, M., Launer, L. J., Harris, T. B., Soliman, E. Z., Alonso, A., Pare, G., Teixeira, P. L., Denny, J. C., Shoemaker, M. B., Van Wagoner, D. R., Smith, J. D., Psaty, B. M., Sotoodehnia, N., Taylor, K. D., Kahonen, M., Nikus, K., Delgado, G. E., Melander, O., Engstrom, G., Yao, J., Guo, X. Q., Christophersen, I. E., Ellinor, P. T., Geelhoed, B., Verweij, N., Macfarlane, P., Ford, I., Heeringa, J., Franco, O. H., Uitterlinden, A. G., Volker, U., Teumer, A., Rose, L. M., Kaab, S., Gudnason, V., Arking, D. E., Conen, D., Roden, D. M., Chung, M. K., Heckbert, S. R., Benjamin, E. J., Lehtimaki, T., Marz, W., Smith, J. G., Rotter, J. I., van der Harst, P., Jukema, J. W., Stricker, B. H., Felix, S. B., Albert, C. M. & Lubitz, S. A. (2017) Genetic Interactions with Age, Sex, Body Mass Index, and Hypertension in Relation to Atrial Fibrillation: The AFGen Consortium. *Scientific Reports*, 7, 11303

Wilde, A. A. M. & Amin, A. S. (2018) Clinical Spectrum of SCN5A Mutations: Long QT Syndrome, Brugada Syndrome, and Cardiomyopathy. *JACC Clinical Electrophysiology*, 4(5), 569-579.

Wolf, P. A., Abbott, R. D. & Kannel, W. B. (1991) ATRIAL-FIBRILLATION AS AN INDEPENDENT RISK FACTOR FOR STROKE - THE FRAMINGHAM-STUDY. *Stroke*, 22(8), 983-988.

Wu, C. C., Su, M. J., Chi, J. F., Wu, M. H. & Lee, Y. T. (1997) Comparison of aging and hypercholesterolemic effects on the sodium inward currents in cardiac myocytes. *Life Sciences*, 61(16), 1539-51.

Yan, J., Kong, W., Zhang, Q., Beyer, E. C., Walcott, G., Fast, V. G. & Ai, X. (2013) c-Jun N-terminal kinase activation contributes to reduced connexin43 and development of atrial arrhythmias. *Cardiovascular Research*, 97(3), 589-97.

Yan, J., Thomson, J. K., Zhao, W., Wu, X., Gao, X., DeMarco, D., Kong, W., Tong, M., Sun, J., Bakhos, M., Fast, V. G., Liang, Q., Prabhu, S. D. & Ai, X. (2018) The stress kinase JNK regulates gap junction Cx43 gene expression and promotes atrial fibrillation in the aged heart. *Journal Molecular and Cellular Cardiology*, 114, 105-115.

Yang, T., Atack, T. C., Stroud, D. M., Zhang, W., Hall, L. & Roden, D. M. (2012b) Blocking Scn10a channels in heart reduces late sodium current and is antiarrhythmic. *Circulation Research*, 111(3), 322-32.

Yu, L., Wang, M., Hu, D., Huang, B., Zhou, L., Zhou, X., Wang, Z., Wang, S. & Jiang, H. (2017) Blocking the Nav1.8 channel in the left stellate ganglion suppresses ventricular arrhythmia induced by acute ischemia in a canine model. *Scientific Reports*, 7(1), 534.

Yue, L., Feng, J., Gaspo, R., Li, G. R., Wang, Z. & Nattel, S. (1997) Ionic remodeling underlying action potential changes in a canine model of atrial fibrillation. *Circulation Research*, 81(4), 512-25.

Yue, L., Xie, J. & Nattel, S. (2011) Molecular determinants of cardiac fibroblast electrical function and therapeutic implications for atrial fibrillation. *Cardiovascular Research*, 89(4), 744-53.

Zeng, Z., Zhou, J., Hou, Y., Liang, X., Zhang, Z., Xu, X., Xie, Q., Li, W. & Huang, Z. (2013) Electrophysiological characteristics of a SCN5A voltage sensors mutation R1629Q associated with Brugada syndrome. *PLoS One*, 8(10).

Zimmer, T., Haufe, V. & Blechschmidt, S. (2014) Voltage-gated sodium channels in the mammalian heart. *Global Cardiology Science and Practice*, 2014(4), 449-63.

Zipes, D. P. & Knope, R. F. (1972) Electrical properties of the thoracic veins. *American Journal of Cardiology*, 29(3), 372-6.